ESI

for

Competing photochemical reactions of bis-naphthols and their photoinduced antiproliferative activity

by

Matija Sambol,[a,b] Katja Ester,*[c] Stephan Landgraf,[d] Branka Mihaljević,[e] Mario Cindrić,[c] Marijeta Kralj,[c] Nikola Basarić[a]*

[a] Department of Organic Chemistry and Biochemistry, Ruđer Bošković Institute, Bijenička cesta 54, 10 000 Zagreb, Croatia. Fax: +385 1 4680 195; Tel: +385 12 4561 141; E-mail: nbasaric@irb.hr

[b] Current address: Fidelta Ltd., Prilaz baruna Filipovića 29, 10000 Zagreb, Croatia

[c] Division of Molecular Medicine, Ruđer Bošković Institute, Bijenička cesta 54, 10 000 Zagreb, Croatia. Fax: +385 1 4561 010; E-mail: kester@irb.hr

[d] Institute of Physical and Theoretical Chemistry, Graz University of Technology, Stremayrgasse 9, A-8010 Graz, Austria

[e] Division of Materials Chemistry, Ruđer Bošković Institute, Zagreb, Croatia

Content

1. Synthetic procedures for the preparation of intermediates S2
2. Quantum yields for photomethanolysis S5
3. UV-vis and fluorescence spectra, time-resolved fluorescence (Figs S1-S15) S6
4. Laser Flash Photolysis (LFP) (Figs S16-S38) S13
5. Noncovalent and covalent binding to BSA protein (Figs S39-S43) S23
6. MALDI-TOF/TOF Mass Spectra after the Irradiation of **4a** in the presence of HSA and BSA (Tables S1 and S2) S26
7. DNA cross-linking experiments with naphthols (Fig S44) S43
8. Antiproliferative activity (Fig S45) S45
9. NMR spectra S47
10. References S97

1. Synthetic procedures for the preparation of intermediates

Synthesis of hydroxy carbaldehydes - general procedure

In a two-necked round bottomed flask (100 mL), equipped with a dropping funnel and septum, naphthol or anthrol bromide (1.0 mmol) was dissolved in dry Et_2O (4 mL) under Ar atmosphere. The solution was cooled to -10 °C (ice/methanol bath) and 2.5 M *n*-BuLi in hexanes (4.3 mmol) was added dropwise. The stirring was continued at -10 °C for the next 20 min. To the reaction mixture dry DMF (8.0 mmol) was added dropwise. The stirring was continued at -10 °C for the next 20 min and then the reaction mixture was allowed to heat to rt over 60 min. The reaction was quenched by a careful addition of water (1 mL), followed by the addition of 2 M HCl (8 mL). The reaction mixture was stirred at rt for 16 h, and then the mixture was transferred to a separation funnel. The organic layer was separated and the aqueous layer was extracted with EtOAc. The combined organic extracts were dried over anhydrous $MgSO_4$, filtered and the solvent was removed on a rotary evaporator. The crude residue was chromatographed on a column of silica gel using gradient method from 0 to 50 % of CH_2Cl_2/cyclohexane as eluent.

3-Hydroxynaphthalene-2-carbaldehyde[1]

According to the general procedure, formylation reaction was performed on 3-bromo-2-naphthol (2.02 g, 9.9 mmol). The carbaldehyde product (1.10 g, 70 %) was obtained in the form of intense yellow solid.

mp 92-95 °C; ^{1}H NMR ($CDCl_3$, 600 MHz) δ/ppm: 10.30 (s, 1H), 10.08 (s, 1H), 8.14 (s, 1H), 7.86 (d, 1H, *J* = 8.4 Hz), 7.70 (d, 1H, *J* = 8.4 Hz), 7.56 (dd, 1H, *J* = 7.5 Hz, *J* = 8.4 Hz), 7.37 (dd, 1H, *J* = 7.5 Hz, *J* = 8.4 Hz), 7.28 (s, 1H); ^{13}C NMR ($CDCl_3$, 150 MHz) δ/ppm: 196.5, 155.8, 138.2, 137.7, 130.2, 129.3, 127.4, 126.6, 124.3, 122.3, 111.9.

3-Hydroxyanthracene-2-carbaldehyde[2,3]

According to the general procedure, formylation reaction was performed on 3-bromo-2-anthrol (1.40 g, 5.1 mmol). The carbaldehyde product (0.62 g, 54 %) was obtained in the form of intense orange solid.

mp = 222-224 °C; ^{1}H NMR ($CDCl_3$, 300 MHz) δ/ppm: 10.13 (s, 1H), 10.07 (s, 1H), 8.53 (s, 1H), 8.40 (s, 1H), 8.25 (s, 1H), 7.96 (d, 1H, *J* = 8.5 Hz), 7.93 (d, 1H, *J* = 8.5 Hz), 7.52 (ddd, 1H, *J* = 1.0 Hz, *J* = 6.8 Hz, *J* = 8.5 Hz), 7.43 (ddd, 1H, *J* = 1.0 Hz, *J* = 6.8 Hz, *J* = 8.5 Hz), 7.39 (s, 1H); ^{13}C NMR ($CDCl_3$, 75 MHz) δ/ppm: 196.5, 153.8, 153.3, 140.7, 134.6, 134.4, 130.6, 129.5, 128.7, 127.7, 127.5, 125.2, 124.2, 123.7, 110.0.

Synthesis of TBDMS-*O*-protected carbaldehydes – general procedure[4]

In a two neck flask (250 mL), equipped with a dropping funnel and a $CaCl_2$ tube, hydroxy-aldehyde (1 mmol), triethylamine (1.5 mmol), 4-(*N*,*N*-dimethylamino)pyridine (0.03 mmol) and dichloromethane (2 mL) were added. The reaction mixture was cooled to 0°C, and a solution of *tert*-butyldimethylsilyl chloride (1.5 mmol) in dichloromethane (1.5 mL) was added dropwise over 20 min. The reaction mixture was stirred at rt for 20 h, transferred to a separation funnel, and washed with a saturated aqueous solution of $NaHCO_3$. The organic layer was separated and the aqueous extracted with dichloromethane. The combined organic extracts were washed with brine and dried over anhydrous $MgSO_4$. After filtration, the solvent was removed on a rotary evaporator and the residue chromatographed on a column of silica gel using gradient method from 0 to 30 % of EtOAc/cyclohexane or 0 to 50 % of CH_2Cl_2/cyclohexane as eluent.

3-(*Tert*-butyldimethylisilyloxy)naphthtalene-2-carbaldehyde (6)

According to the general procedure, the protection of OH group was performed on naphthol carbaldehyde (0.31 g, 1.8 mmol). The desired product **6** (0.41 g, 80 %) was isolated in a form of pale-yellow solid.

mp 61-63 °C; ^{1}H NMR ($CDCl_3$, 300 MHz) δ/ppm: 10.59 (s, 1H), 8.37 (s, 1H), 7.88 (d, 1H, J = 8.2 Hz), 7.69 (d, 1H, J = 8.2 Hz), 7.52 (dd, 1H, J = 7.5 Hz, J = 8.2 Hz), 7.38 (dd, 1H, J = 7.5 Hz, J = 8.2 Hz), 7.19 (s, 1H), 1.06 (s, 9H), 0.34 (s, 6H); ^{13}C NMR ($CDCl_3$, 150 MHz) δ/ppm: 190.6, 154.1, 137.5, 130.6, 129.9, 129.0, 128.3, 127.7, 126.5, 124.8, 115.1, 25.7, 18.4, – 4.3.

3-(*tert*-butyldimethylisilyloxy)anthracene-2-carbaldehyde (8)

According to the general procedure, the protection of OH group was performed on anthrol carbaldehyde (0.60 g, 2.7 mmol). The desired product **8** (0.72 g, 79 %) was isolated in a form of intense yellow solid.

mp 61-63 °C; ^{1}H NMR ($CDCl_3$, 400 MHz) δ/ppm: 10.61 (s, 1H), 8.59 (s, 1H), 8.51 (s, 1H), 8.23 (s, 1H), 7.97 (d, 1H, J = 8.3 Hz), 7.92 (d, 1H, J = 8.3 Hz), 7.49 (dd, 1H, J = 7.5 Hz, J = 8.2 Hz), 7.43 (dd, 1H, J = 7.5 Hz, J = 8.2 Hz), 7.30 (s, 1H), 1.08 (s, 9H), 0.38 (s, 6H); ^{13}C NMR ($CDCl_3$, 100 MHz) δ/ppm: 190.6, 152.4, 134.2, 133.7, 132.4, 130.9, 129.7, 128.6, 128.4 (s), 127.7, 127.0, 125.1, 124.1, 113.2, 25.7, 18.4, – 4.2.

2. Quantum yields for photomethanolysis

The **number of absorbed photons for the KIO_3/KI** was calculated from:

$$n(\text{absorbed photons}) = \frac{\Delta A_{352} \times V_{irr}}{\varepsilon_{352} \times \ell \times \Phi_{\text{lit.}}} \qquad \text{(S1)}$$

where:

ΔA_{352}	absorbance difference at 352 nm for the irradiated and non-irradiated sample
V_{irr}	volume of the solution which was irradiated
ε_{352}	molar absorption coefficient for I_3^- in solution which contains iodides and iodates, 27600 M^{-1} cm^{-1}
l	length of the optical path (1 cm in all experiments)
$\Phi_{\text{lit.}}$	quantum yield (Φ_{254} = 0.74), the precise value was calculated from:

$$c(I^-) = A_{300} / 1.061 \quad [M] \qquad \text{(S2)}$$

$$\Phi = 0.75 \times [1 + 0.02(T - 20.7)] \times [1+0.23(c(I^-) - 0.577)] \qquad \text{(S3)}$$

For the absorbances in the range 0.4-0.8 the number of absorbed photons was calculated according to:

$$n(\text{absorbed photons}) = n(\text{total photons}) \times (1-T) \qquad \text{(S4)}$$

The quantum yield of the photohydrolysis was calculated according to:

$$\Phi = \frac{A_{254} \cdot V_{\text{irr}} \cdot x(\text{photoproduct})_{\text{HPLC}}}{\varepsilon_{254} \cdot \ell \cdot n(\text{total photons}) \cdot (1 - T_{254})} \qquad \text{(S5)}$$

3. UV-vis and fluorescence spectra, time-resolved fluorescence

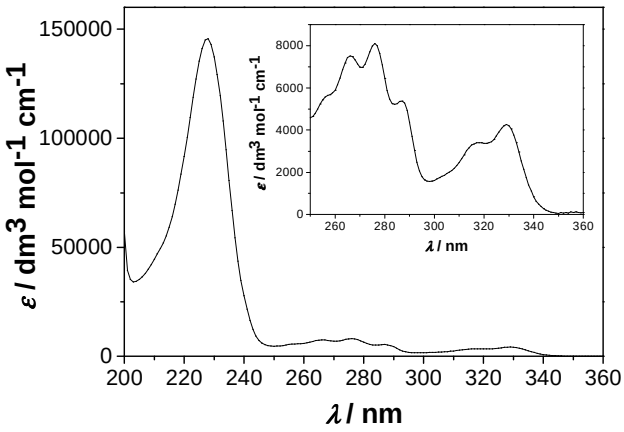

Fig S1. Absorption spectrum of **4a** in CH_3OH-H_2O (4:1).

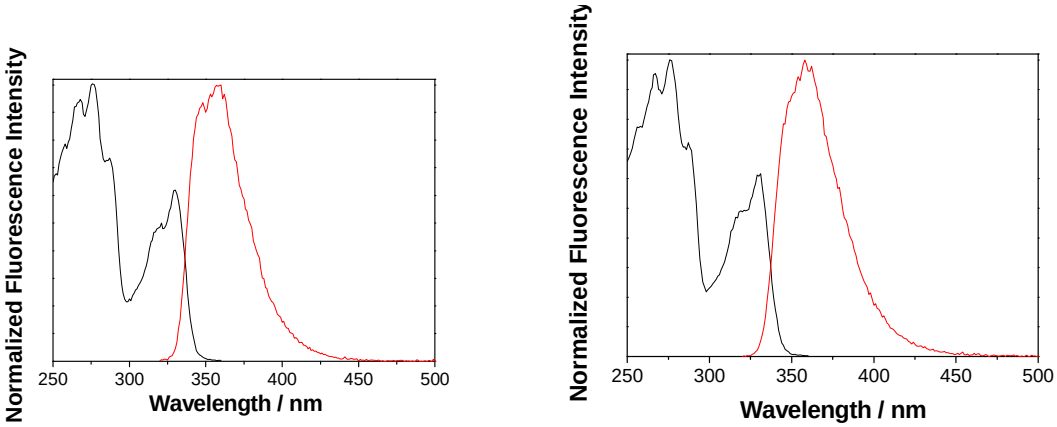

Fig S2. Normalized excitation (λ_{em} = 370 nm) and emission (λ_{ex} = 310 nm) spectra of **4a** in CH_3CN (left) and CH_3CN-H_2O (3:1, right)

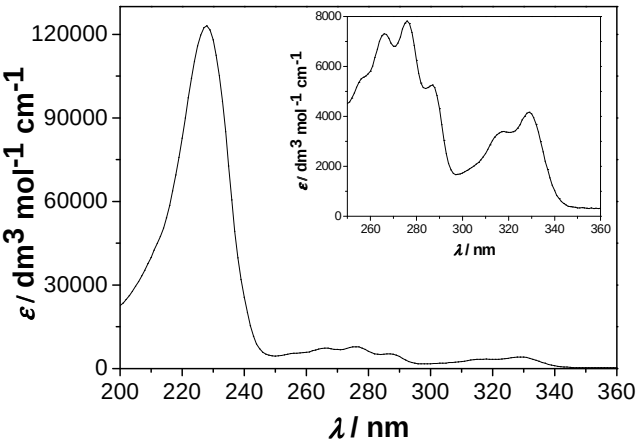

Fig S3. Absorption spectrum of **4b** in CH_3OH-H_2O (4:1).

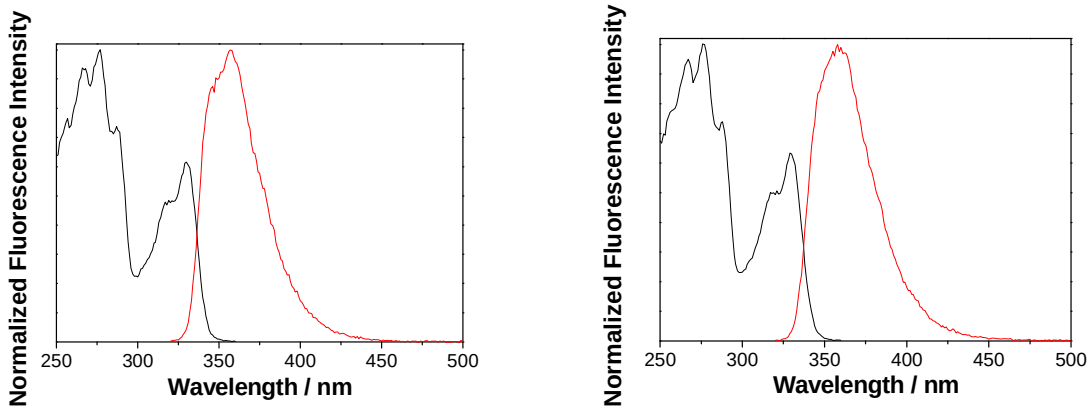

Fig S4. Normalized excitation (λ_{em} = 370 nm) and emission (λ_{ex} = 310 nm) spectra of **4b** in CH_3CN (left) and CH_3CN-H_2O (3:1, right)

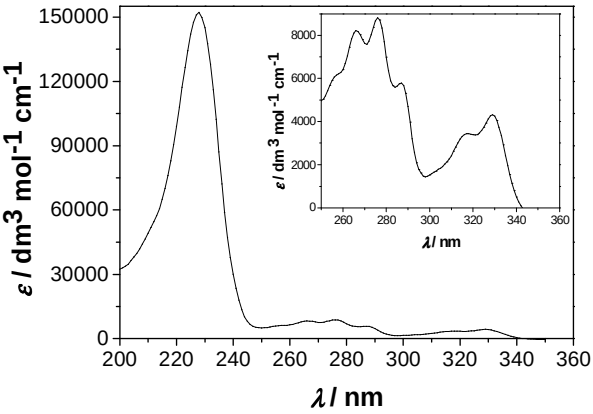

Fig S5. Absorption spectrum of **4c** in CH_3OH-H_2O (4:1).

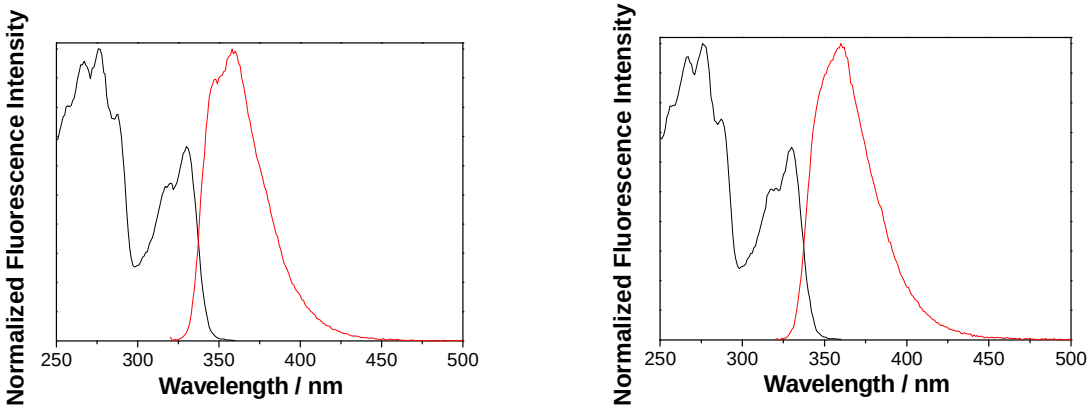

Fig S6. Normalized excitation (λ_{em} = 370 nm) and emission (λ_{ex} = 310 nm) spectra of **4c** in CH_3CN (left) and CH_3CN-H_2O (3:1, right)

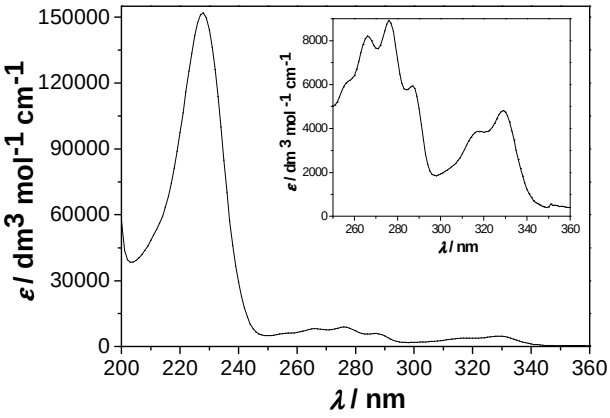

Fig S7. Absorption spectrum of **4d** in CH_3OH-H_2O (4:1).

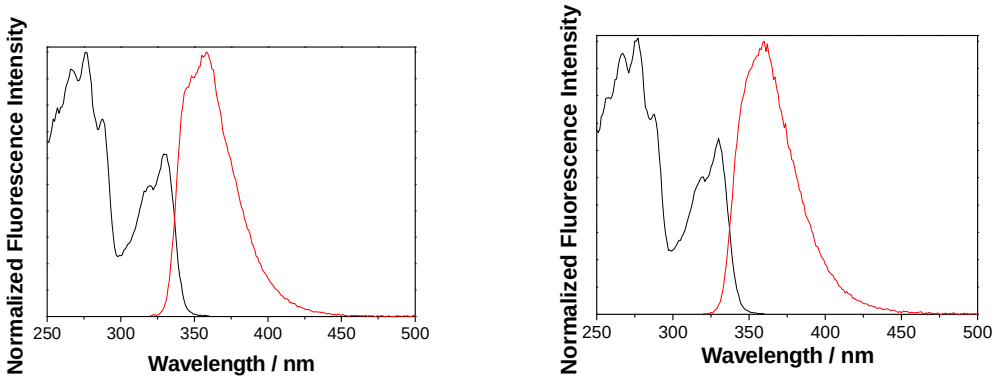

Fig S8. Normalized excitation (λ_{em} = 370 nm) and emission (λ_{ex} = 310 nm) spectra of **4d** in CH_3CN (left) and CH_3CN-H_2O (3:1, right)

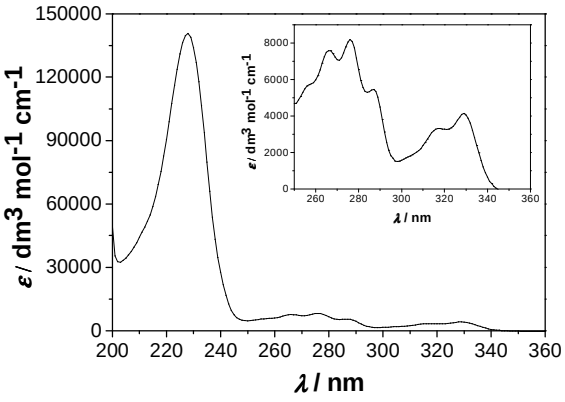

Fig S9. Absorption spectrum of **4e** in CH_3OH-H_2O (3:1).

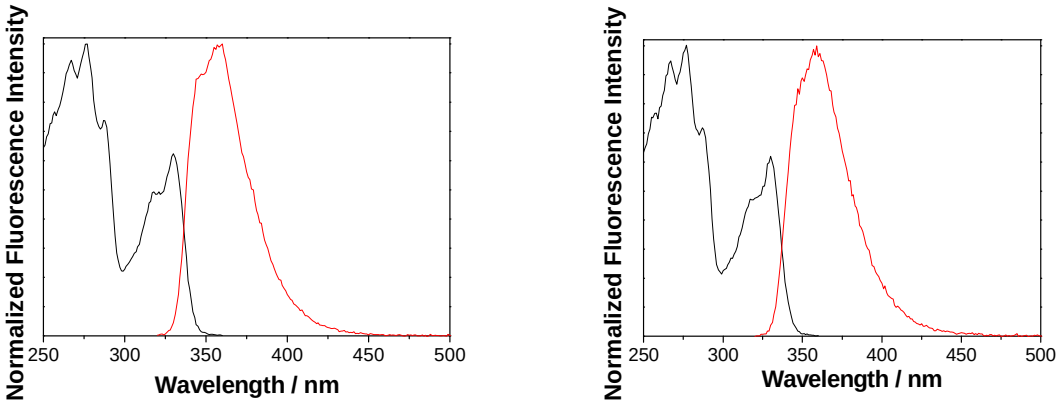

Fig S10. Normalized excitation (λ_{em} = 370 nm) and emission (λ_{ex} = 310 nm) spectra of **4e** in CH_3CN (left) and CH_3CN-H_2O (3:1, right)

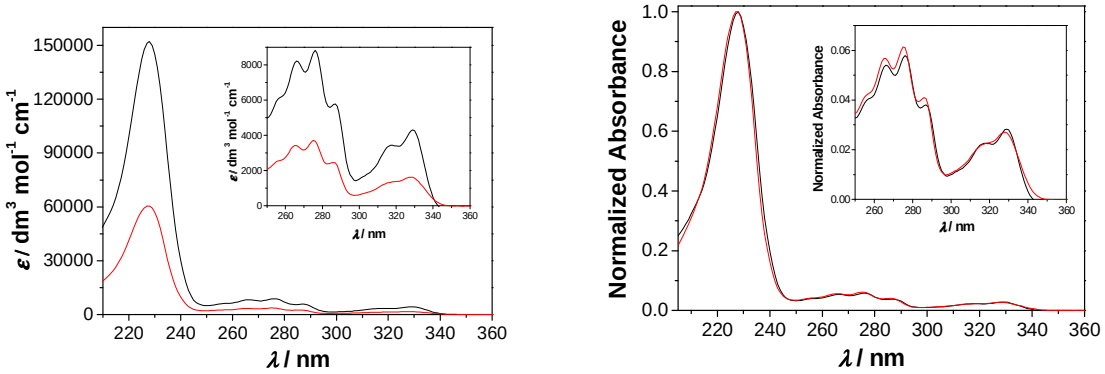

Fig S11. Absorption spectra (left) and normalized absorption spectra (right) of **4a** (black line) and 3-hydroxymethyl-2-naphthol (**3**, red line) in CH_3OH-H_2O (4:1).

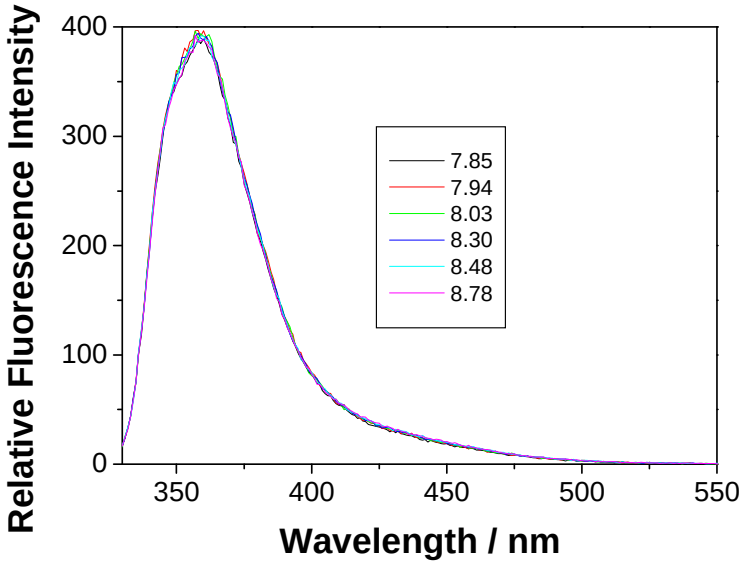

Fig S12. Fluorescence spectra (λ_{ex} = 320 nm) of **4a** in CH_3CN-H_2O (1:1) in the presence of phosphate buffer (c = 0.05 M) at different pH values.

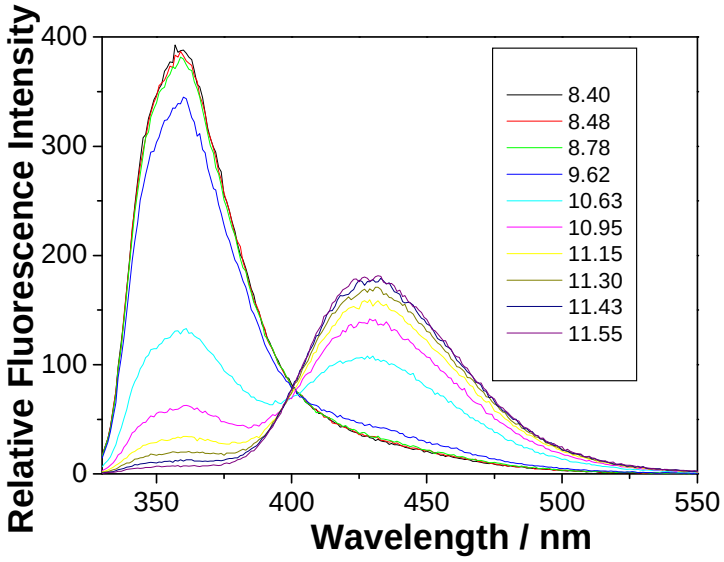

Fig S13. Fluorescence spectra (λ_{ex} = 320 nm) of **4a** in CH_3CN-H_2O (1:1) in the presence of phosphate buffer (c = 0.05 M) at different pH values.

The following equation was used for the determination of fluorescence quantum yields:

$$\Phi = \Phi_R \frac{I}{I_R} \frac{A_R}{A} \left(\frac{n_D}{n_D^R}\right)^2 \quad \text{(S6)}$$

wherein

Φ - quantum yield of fluorescence

Φ_R - quantum yield of fluorescence of reference compound, Fluorescence quantum yields were measured by use of quinine sulfate in aqueous 1.0 N H_2SO_4 (Φ = 0.55)[5]

I - intensity of fluorescence (integral of the corrected emission spectrum)

I_R - intensity of fluorescence (integral of the corrected emission spectrum) for the reference compound

A - absorbance of the solution at the excitation wavelength

A_R - absorbance of the solution of the reference compound at the excitation wavelength

n_D - refractive index of the solvent

n_D^R - refractive index of the solvent used to dissolve the reference compound (H_2O)

Fluorescence decays, were fit as sums of exponentials using Gaussian-weighted non-linear least-squares fitting based on Marquardt-Levenberg minimization implemented in the PicoQuant FluoFit (Version 4.6.6) software

Fluorescence decays were fit to a sum of exponentials using the following expression:

$$F(t) = \alpha_1 \exp\left(-\frac{t}{\tau_1}\right) + \alpha_2 \exp\left(-\frac{t}{\tau_2}\right) + \alpha_3 \exp\left(-\frac{t}{\tau_3}\right) + \ldots \quad \text{(S7)}$$

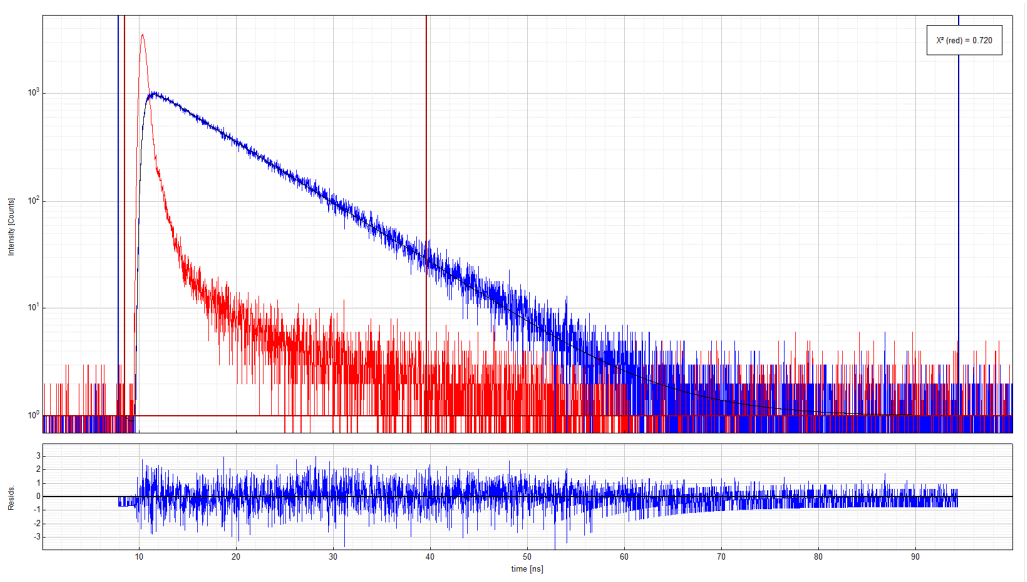

Fig S14. Fluorescence decay for **4a** in CH_3CN measured by use of a long pass absorbing glass filter (WG325, Schott, Mainz, Germany)

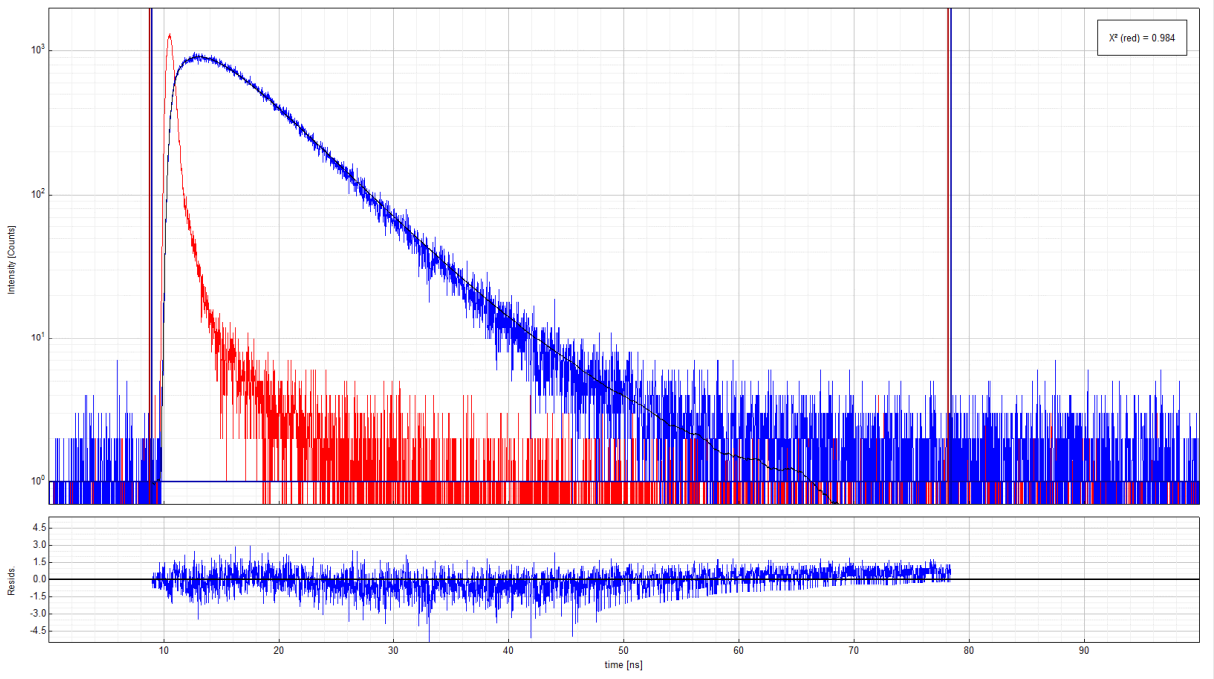

Fig S15. Fluorescence decay for **4a** in CH_3CN-H_2O in the presence of phosphate buffer (c = 0.05 M, pH = 7.0) measured by use of an optical dichroic filter, centered at 412 nm, width 22 nm (Omega Optical, Brattleboro, VT 05301, USA).

4. Laser Flash Photolysis (LFP)

Prepared stock solution of **4a** in CH_3CN, $c = 5.05 \times 10^{-4}$ M by dissolving 2.03 mg in 10 mL CH_3CN.

For the LFP measurement, the stock was diluted ten times, $c = 5.05 \times 10^{-5}$ M, $A_{266} = 0.41$.

LFP measurements were performed on a Edinburgh Instruments spectrometer. For the excitation, a Quantel YAG laser fourth harmonic (λ_{exc} = 266 nm) was used. The energy of the laser pulse was set to 20 mJ. Prior to the measurements, the solution was purged with a stream of Ar or O_2 for 15 min. Static cells were used for the measurements, and the solution was replaced frequently to assure that the transients are not formed from photoproducts.

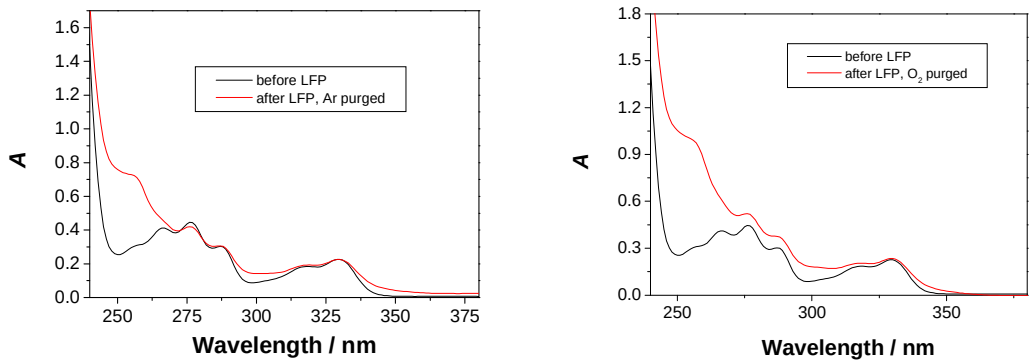

Fig S16. UV-vis spectra of **4a** in Ar-purged (left) and O_2-purged CH_3CN solution before and after the LFP measurements.

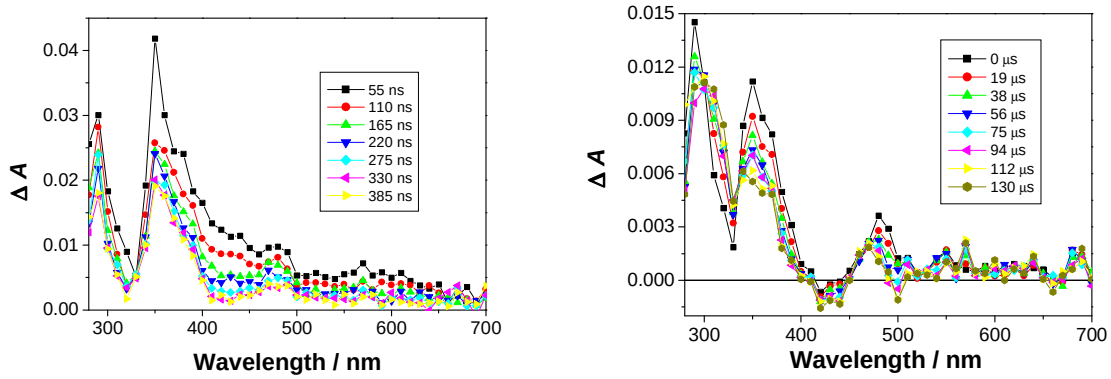

Fig S17. Transient absorption spectra of **4a** in Ar-purged CH_3CN solution collected at two different time-scales.

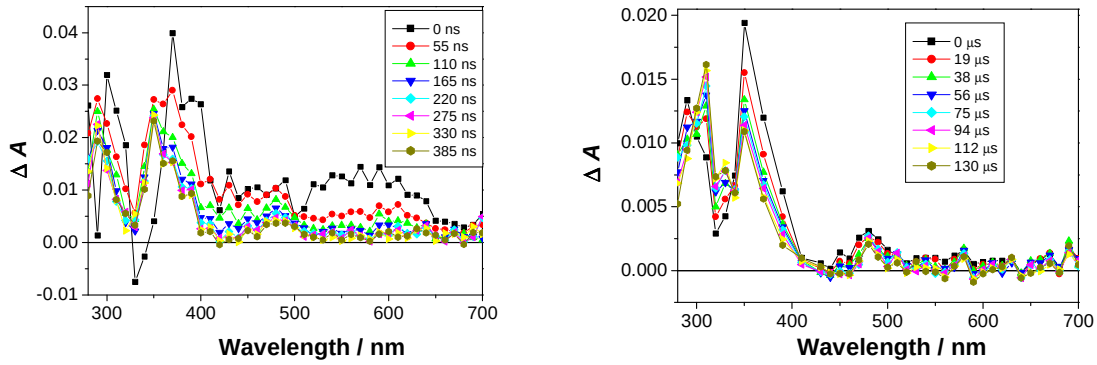

Fig S18. Transient absorption spectra of **4a** in O_2-purged CH_3CN solution collected at two different time-scales.

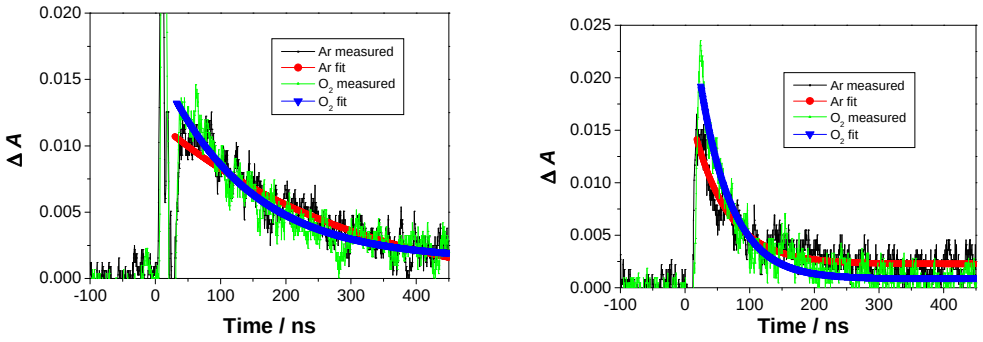

Fig S19. Decay of transient absorption for Ar- and O_2-purged solution of **4a** in CH_3CN at 450 nm (left) and 550 nm (right). The fitting revealed the following lifetimes: 450 nm τ_{Ar} = 320 ± 20 ns and τ_{O2} = 130 ± 10 ns; 550 nm: τ_{Ar} = 54 ± 1 ns and τ_{O2} = 48 ± 1 ns.

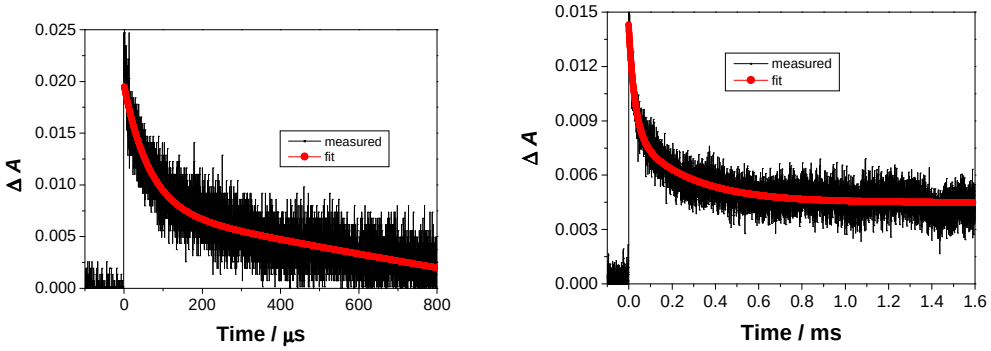

Fig S20. Decay of transient absorbance at 350 nm for Ar-purged (left) and O_2-purged CH_3CN solution (right) of **4a**. Fiting revailed two decay times τ_{Ar} = 26 ± 2 µs and 280 ± 10 µs; and τ_{O2} = 60 ± 2 µs and 720 ± 70 µs.

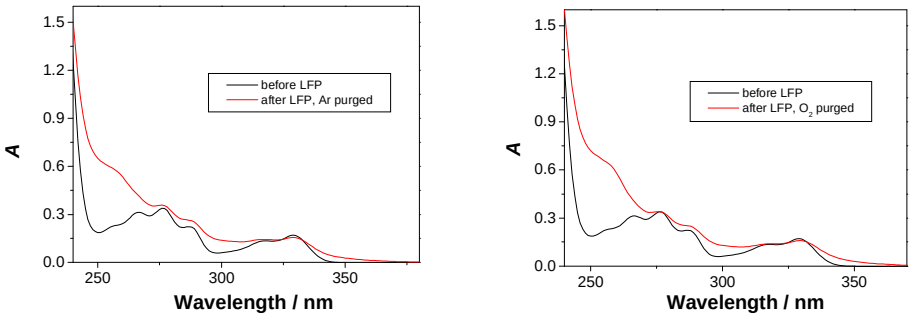

Fig S21. UV-vis spectra of **4a** in Ar-purged (left) and O_2-purged CH_3CN-H_2O (1:1) in the presence of phosphate buffer (pH = 7.0, *c* = 0.05 M) solution before and after the LFP measurements.

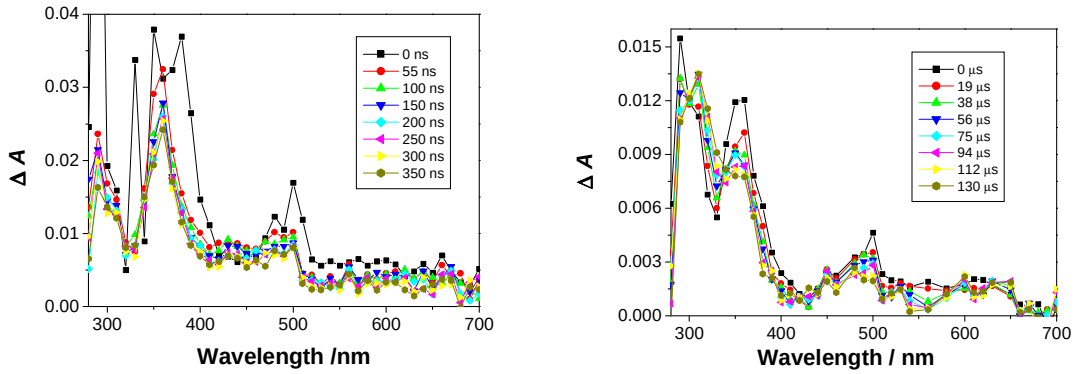

Fig S22. Transient absorption spectra of **4a** in Ar-purged purged CH_3CN-H_2O (1:1) in the presence of phosphate buffer (pH = 7, *c* = 0.05 M) solution, collected at two different time-scales.

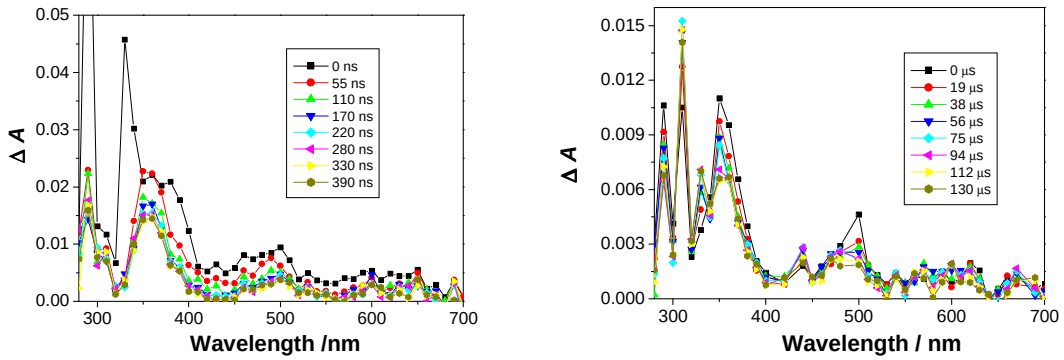

Fig S23. Transient absorption spectra of **4a** in O_2-purged purged CH_3CN-H_2O (1:1) in the presence of phosphate buffer (pH = 7, *c* = 0.05 M) solution, collected at two different time-scales.

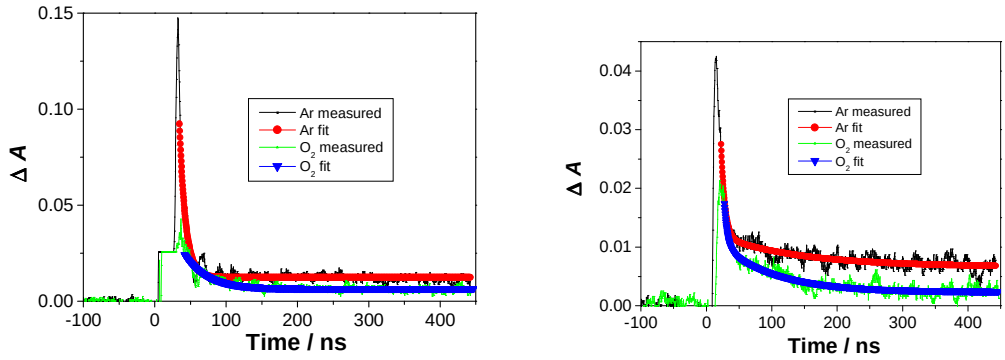

Fig S24. Decay of transient absorption for Ar- and O_2-purged CH_3CN-H_2O (1:1) solution of **4a**, in the presence of phosphate buffer (pH = 7, *c* = 0.05 M), at 380 nm (left) and 480 nm (right). The fitting revealed the following lifetimes: 380 nm $\tau_{Ar} \approx 10$ ns and $\tau_{O2} \approx 32 \pm 1$ ns; 480 nm: $\tau_{Ar} = 5$ and 120 ± 10 ns and $\tau_{O2} = 5$ and 83 ± 3 ns.

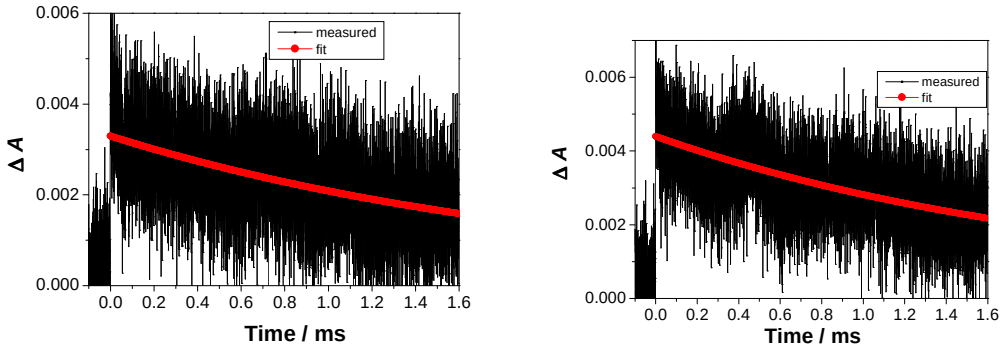

Fig S25. Decay of transient absorbance at 350 nm for Ar-purged (left) and O_2-purged (right) CH_3CN-H_2O (1:1) solution of **4a**, in the presence of phosphate buffer (pH = 7, *c* = 0.05 M). Fiting revailed decay times $\tau_{Ar} = 2.1 \pm 0.6$ ms; and $\tau_{O2} = 2.8 \pm 0.8$ ms.

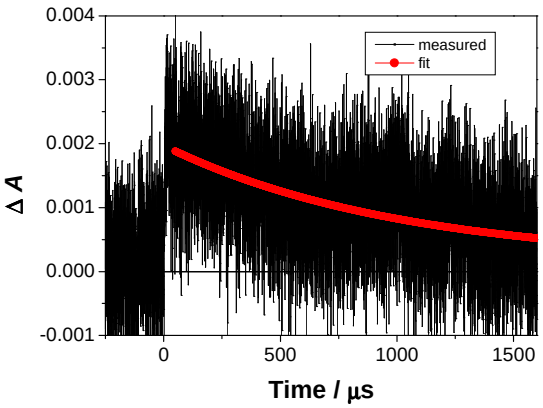

Fig S26. Decay of transient absorbance at 350 nm for non-purged CH_3CN-H_2O (1:1) solution of **4a** (c = 5.8 ×10^{-5} M) in the presence of phosphate buffer (pH = 7, c = 0.05 M) and NaN_3 (c = 0.010 M) Fiting revailed decay times τ = 230 ± 80 μs. From two decay times, the estimated quenching constant is ≈ 4 × 10^5 M^{-1} s^{-1}.

Prepared stock solution of **4e** in CH_3CN, $c = 4.99 \times 10^{-4}$ M by dissolving 2.29 mg in 10 mL CH_3CN.

For the LFP measurement, the stock was diluted (2.4 mL to 25 mL), $c = 4.79 \times 10^{-5}$ M, $A_{266} = 0.33$.

LFP measurements were performed on a Edinburgh Instruments spectrometer. For the excitation, a Quantel YAG laser fourth harmonic (λ_{exc} = 266 nm) was used. The energy of the laser pulse was set to 20 mJ. Prior to the measurements, the solution was purged with a stream of Ar or O_2 for 15 min. Static cells were used for the measurements, and the solution was replaced frequently to assure that the transients are not formed from photoproducts.

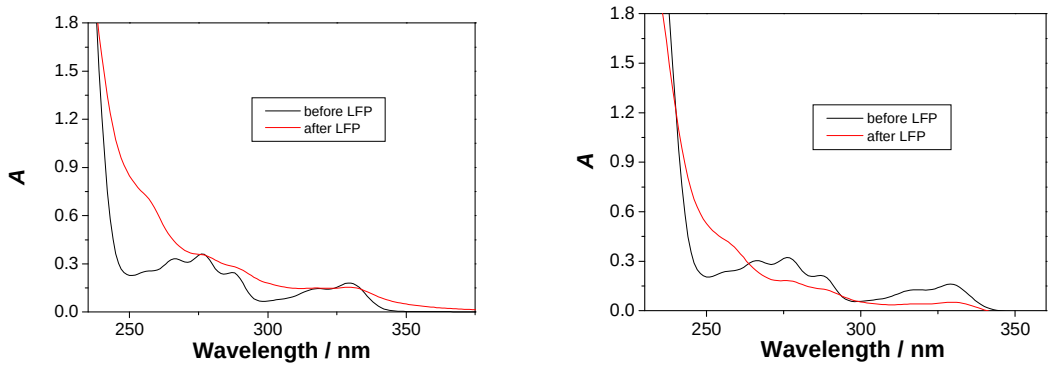

Fig S27. UV-vis spectra of **4e** in O_2-purged CH_3CN solution before and after the LFP measurements (left), and O_2-purged CH_3CN-H_2O (1:1) in the presence of phosphate buffer (pH = 7.0, c = 0.05 M) solution before and after the LFP measurements.

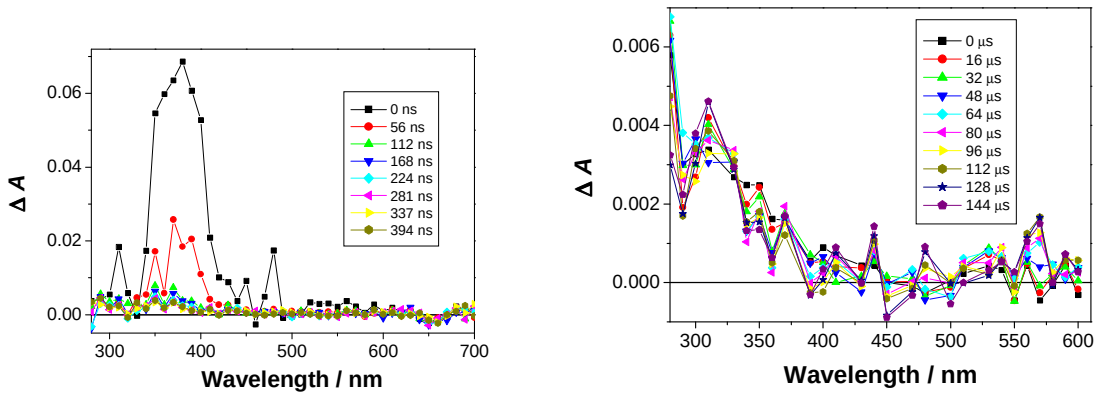

Fig S28. Transient absorption spectra of **4e** in Ar-purged CH_3CN solution collected at two different time-scales.

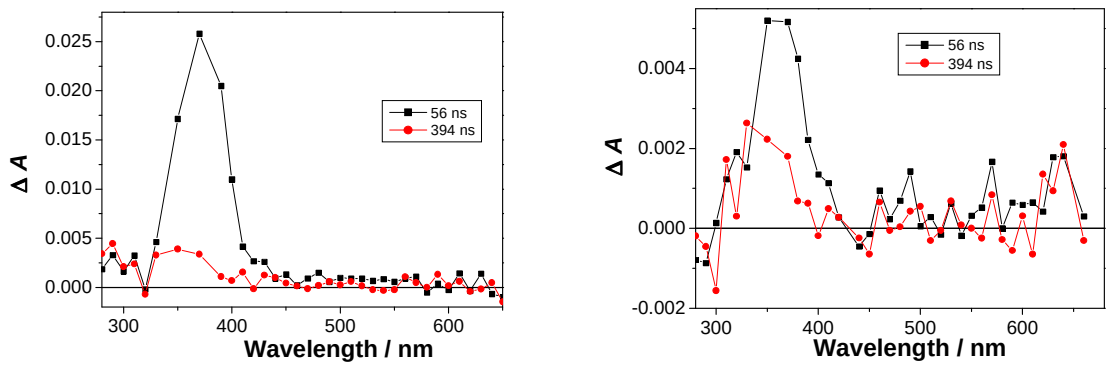

Fig S29. Transient absorption spectra of **4e** in Ar-purged (left) and O_2-purged CH_3CN solution detected at 56 and 494 ns after the laser pulse.

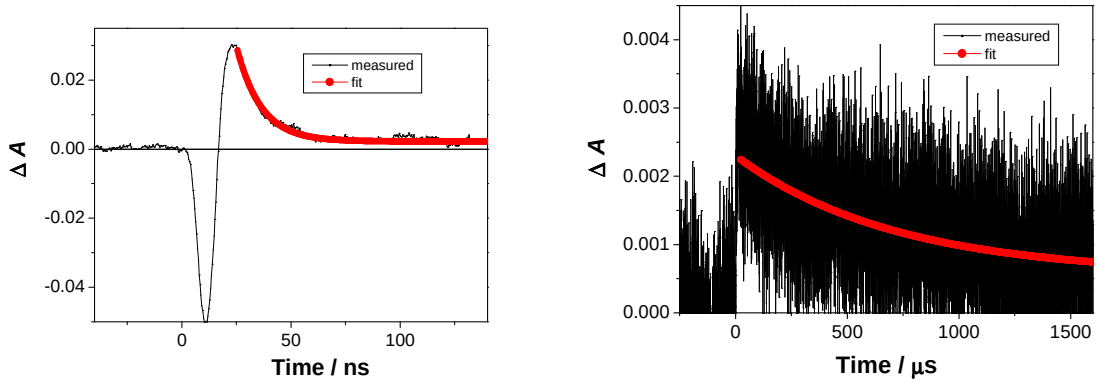

Fig S30. Decay of transient absorbance at 470 nm in Ar-purged CH_3CN solution of **4e**, $\tau_{O2} \approx 11 \pm 1$ ns (left); and decay of transient absorbance at 350 nm in Ar-purged CH_3CN solution of **4e**, $\tau_{O2} \approx 900 \pm 100$ μs (right).

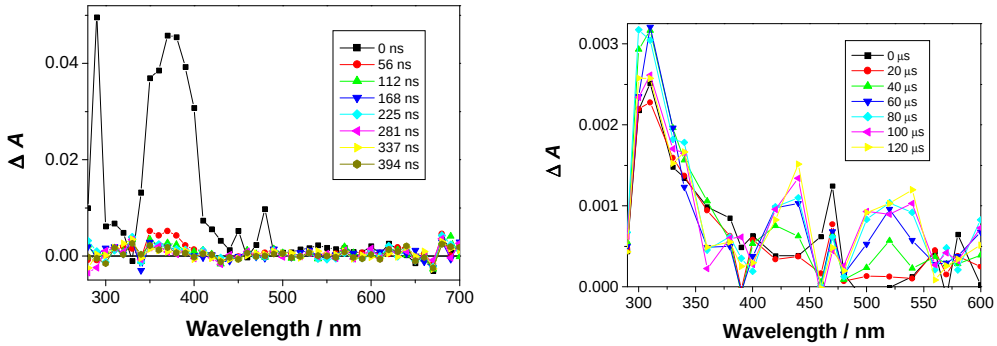

Fig S31. Transient absorption spectra of O_2-purged CH_3CN solution of **4e** collected at two different time-scales.

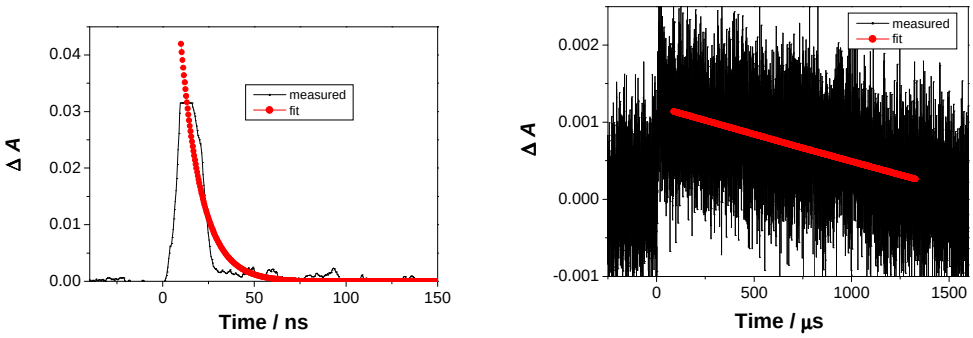

Fig S32. Decay of transient absorbance at 480 nm in O_2-purged CH_3CN solution of **4e**, $\tau_{O2} \approx 10 \pm 1$ ns (left); and decay of transient absorbance at 350 nm in O_2-purged CH_3CN solution of **4e**, $\tau_{O2} \approx 8 \pm 2$ ms (right).

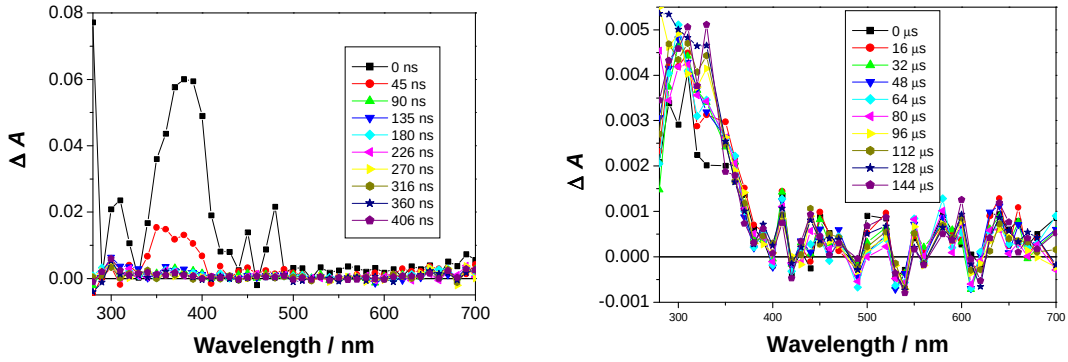

Fig S33. Transient absorption spectra of **4e** in Ar-purged purged CH_3CN-H_2O (1:1) in the presence of phosphate buffer (pH = 7, c = 0.05 M) solution, collected at two different time-scales.

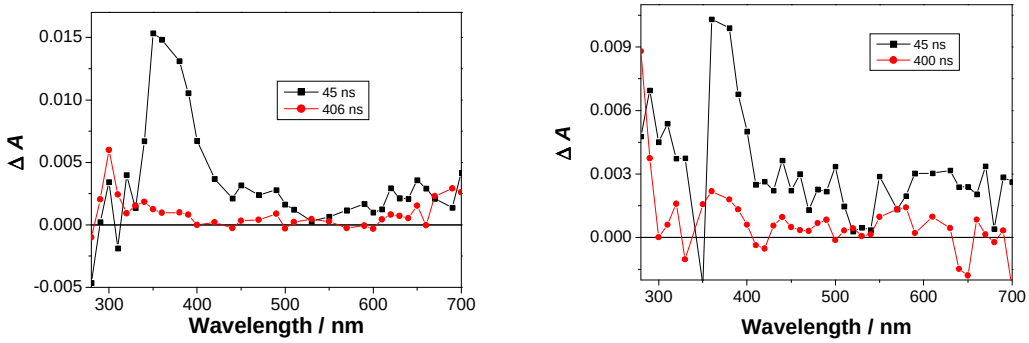

Fig S34. Transient absorption spectra of **4e** in Ar-purged (left) and O_2-purged CH_3CN-H_2O (1:1) solution, in the presence of phosphate buffer (pH = 7, c = 0.05 M), detected at 45 and 400 ns after the laser pulse.

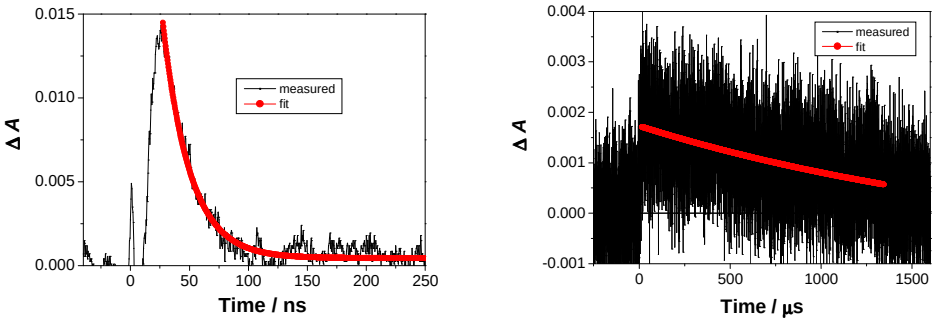

Fig S35. Decay of transient absorbance at 470 nm (left) in Ar-purged CH_3CN-H_2O (1:1) solution of **4e**, in the presence of phosphate buffer (pH = 7, c = 0.05 M), $\tau_{Ar} \approx 23 \pm 1$ ns, and at 350 nm (right), $\tau_{O2} \approx 2.2 \pm 0.7$ ms.

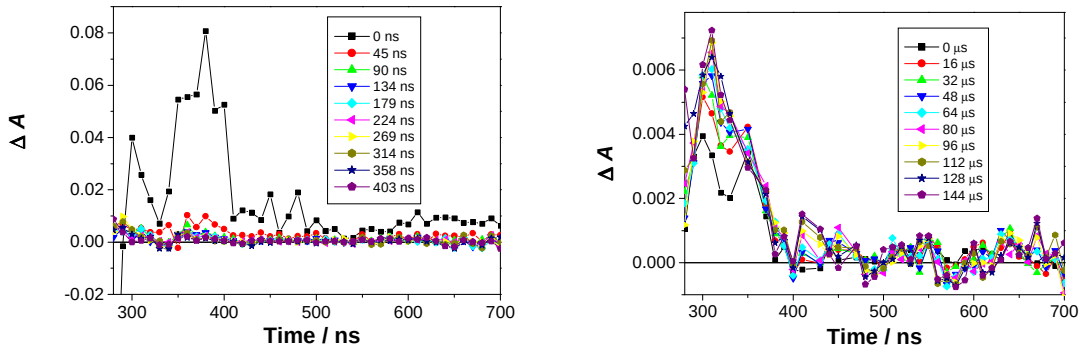

Fig S36. Transient absorption spectra of **4e** in O_2-purged purged CH_3CN-H_2O (1:1) in the presence of phosphate buffer (pH = 7, c = 0.05 M) solution, collected at two different time-scales.

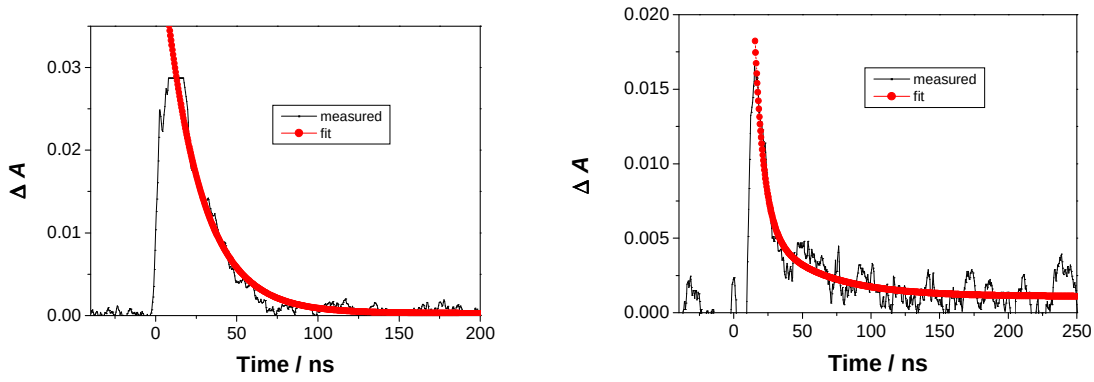

Fig S37. Decay of transient absorbance at 470 nm (left) and 550 nm (right) in O_2-purged CH_3CN-H_2O (1:1) solution of **4e**, in the presence of phosphate buffer (pH = 7, c = 0.05 M), $\tau_{450} \approx 24 \pm 1$ ns; $\tau_{550} \approx 6 \pm 1$ ns and 43 ± 1 ns.

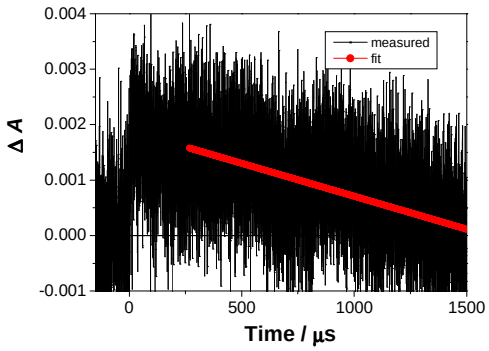

Fig S38. Decay of transient absorbance at 350 nm in O_2-purged CH_3CN-H_2O (1:1) solution of **4e**, in the presence of phosphate buffer (pH = 7, c = 0.05 M), $\tau_{02} \approx 1.0 \pm 0.1$ ms.

5. Noncovalent and covalent binding to BSA protein

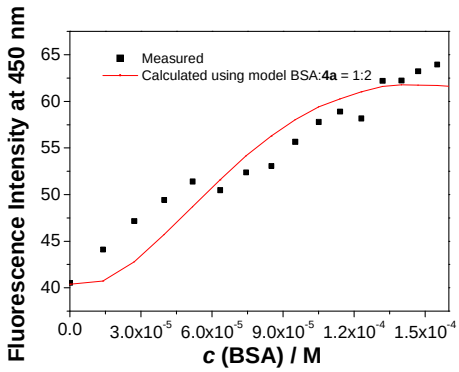

Fig S39. Dependence of the fluorescence intensity at 450 nm on the BSA concentration for the fluorescence spectra (λ_{ex} = 320 nm) of **4a** (c = 1.49×10^{-5} M) in aqueous sodium phosphate buffer (c = 0.05 M, pH = 7.0) : CH_3CN 1:1, in the presence of increasing concentration of BSA (c = 0 - 1.63×10^{-4} M); the dots correspond to the experimental values, whereas the red line is calculated fluorescence intensity by using Specfit program and complex stoichiometry model 1:2 (protein:**4a**).

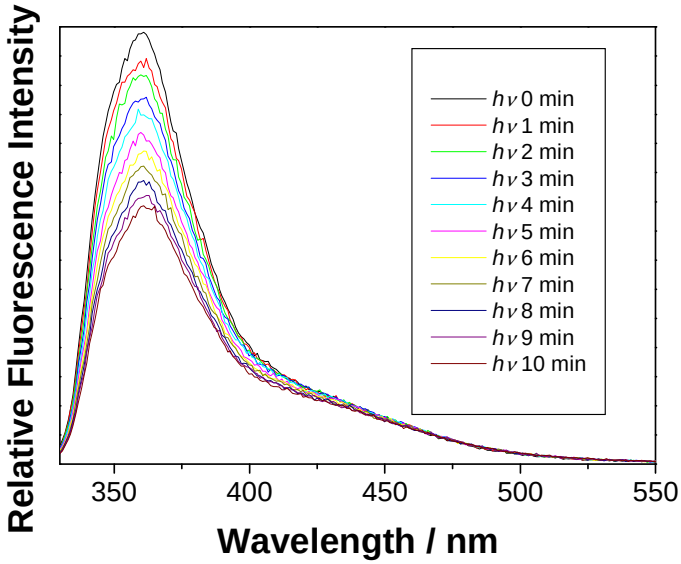

Fig S40. Fluorescence spectra of **4a** (c = 5.60×10^{-5} M) and BSA (c = 1.20×10^{-4} M) in aqueous sodium phosphate buffer (c = 0.05 M, pH 0 7.0) : CH_3CN 1:1, after irradiation in a Luzchem reactor (8 lamps, 350 nm, 1 lamp 8W; the irradiance from the Luzchem LZC-UVA lamps is available on line at: https://www.luzchem.com/files/pdfs/Exposure%20standards%20pdf/LZC-UVA-016.pdf).

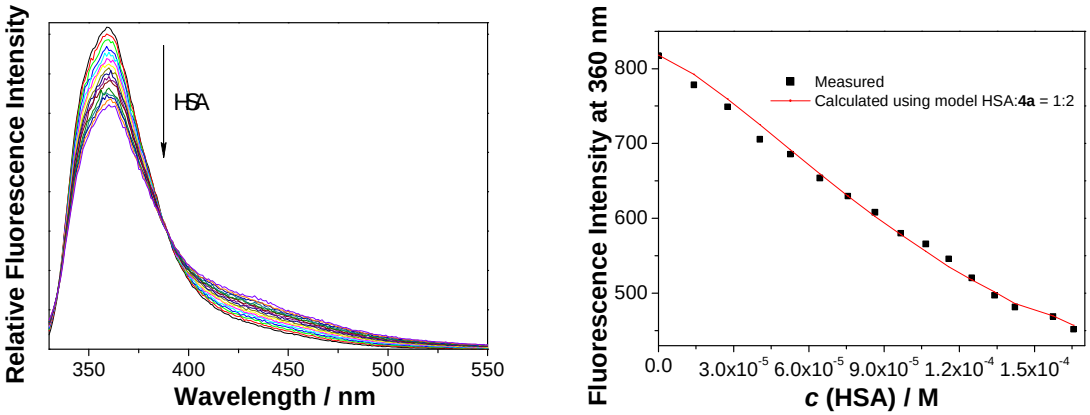

Fig S41. Fluorescence spectra (λ_{ex} = 320 nm) of **4a** (c = 1.49×10^{-5} M) in aqueous sodium phosphate buffer (c = 0.05 M, pH = 7.0) : CH_3CN 1:1, in the presence of increasing concentration of HSA (c = 0 - 1.65×10^{-4} M) (left); and dependence of the fluorescence intensity at 360 nm on the BSA concentration (right); the dots correspond to the experimental values, whereas the red line is calculated fluorescence intensity by using Specfit program and complex stoichiometry model 1:2 (protein:**4a**).

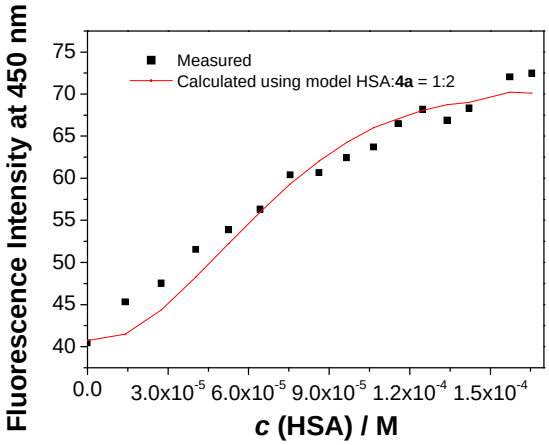

Fig S42. Dependence of the fluorescence intensity at 450 nm on the HSA concentration for the fluorescence spectra (λ_{ex} = 320 nm) of **4a** (c = 1.49×10^{-5} M) in aqueous sodium phosphate buffer (c = 0.05 M, pH = 7.0) : CH_3CN 1:1, in the presence of increasing concentration of HSA (c = 0 - 1.65×10^{-4} M); the dots correspond to the experimental values, whereas the red line is calculated fluorescence intensity by using Specfit program and complex stoichiometry model 1:2 (protein:**4a**).

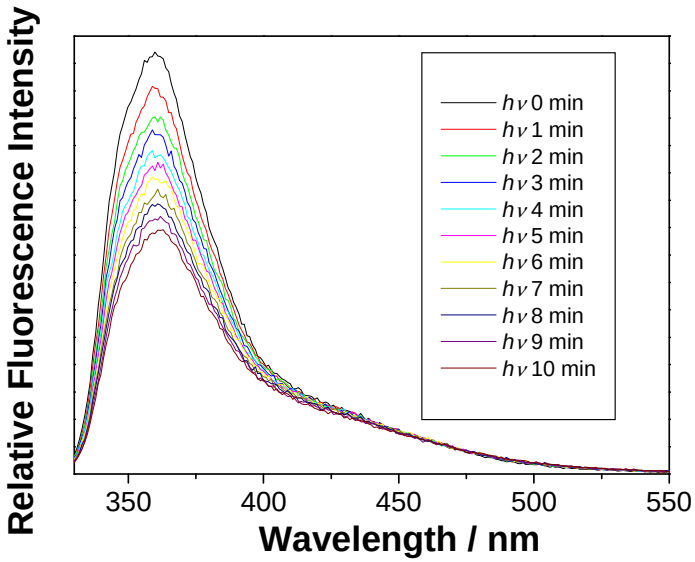

Fig S43. Fluorescence spectra of **4a** (c = 5.60×10^{-5} M) and HSA (c = 1.42×10^{-4} M) in aqueous sodium phosphate buffer (c = 0.05 M, pH 0 7.0) : CH_3CN 1:1, after irradiation in a Luzchem reactor (8 lamps, 350 nm, 1 lamp 8W).

6. MALDI-TOF/TOF mass spectra after the irradiation of 4a with HSA and BSA

HSA

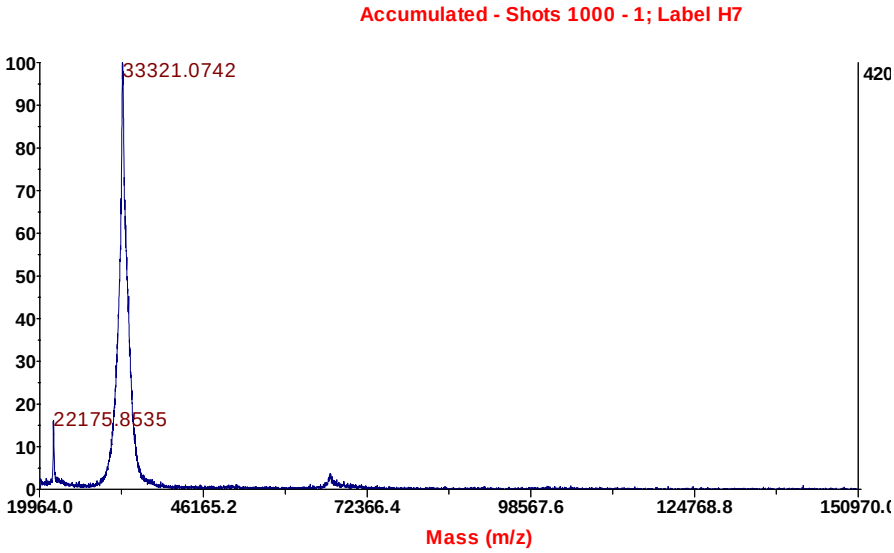

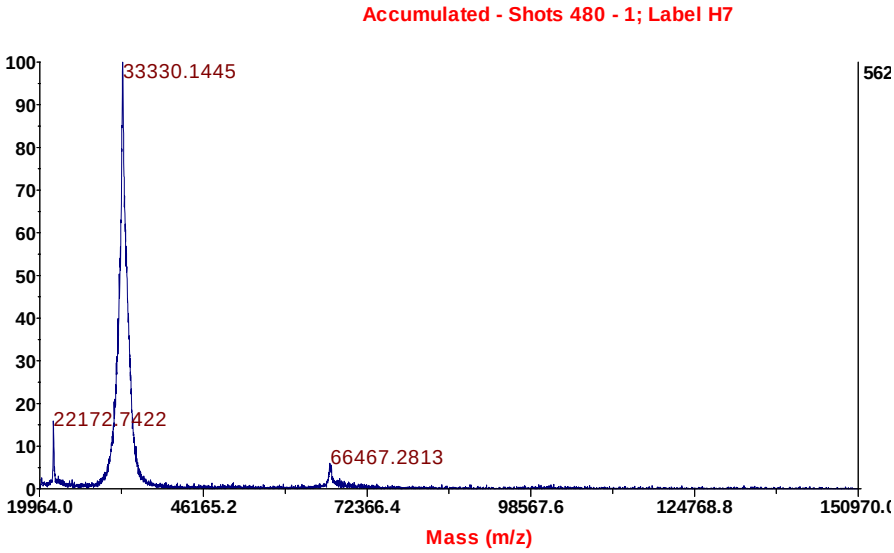

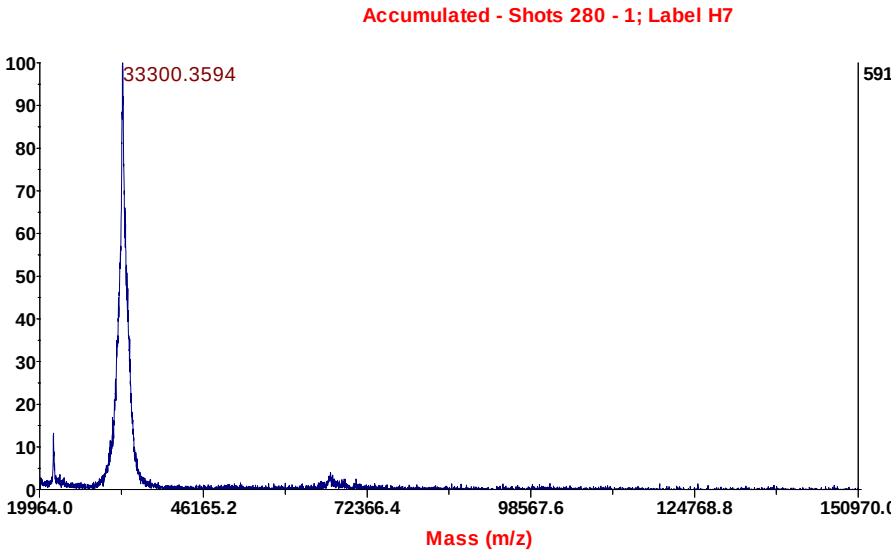
Accumulated - Shots 280 - 1; Label H7
33300.3594
591
100
90
80
70
60
50
40
30
20
10
0
19964.0
46165.2
72366.4
98567.6
124768.8
150970.(
Mass (m/z)

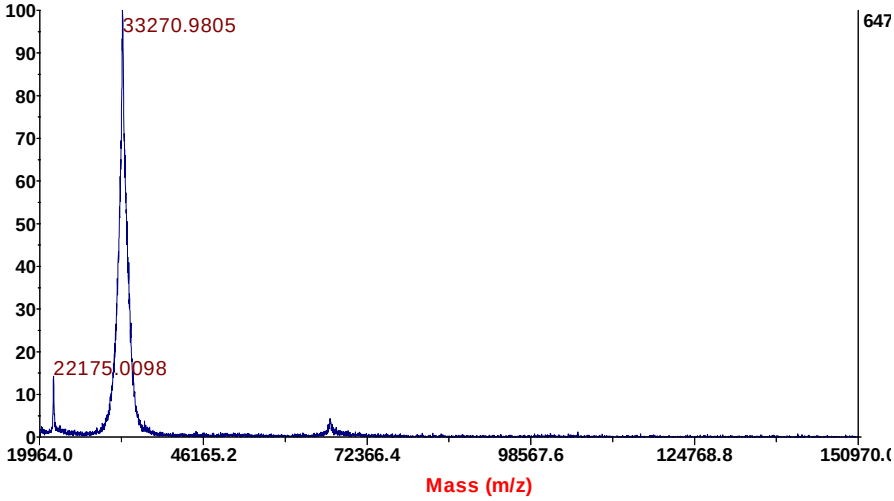
Accumulated - Shots 440 - 1; Label H7
33270.9805
647
22175.0098
100
90
80
70
60
50
40
30
20
10
0
19964.0
46165.2
72366.4
98567.6
124768.8
150970.(
Mass (m/z)

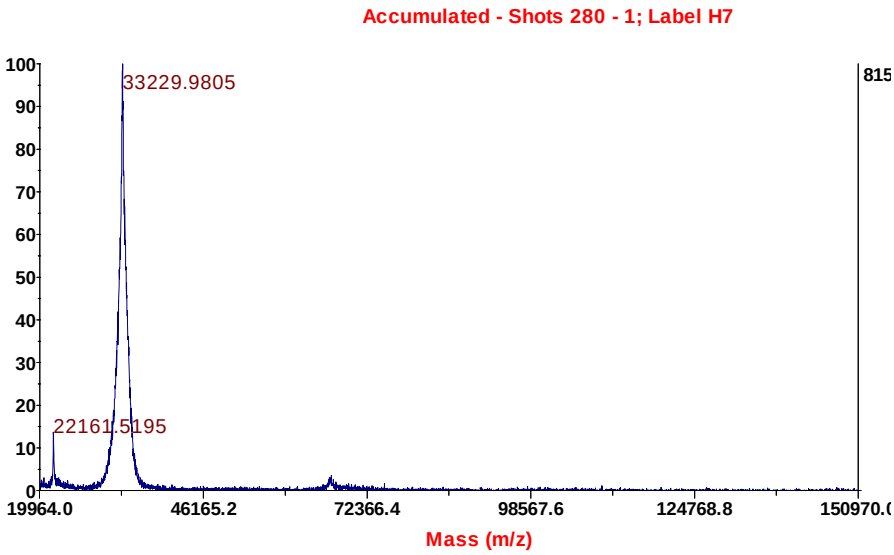
Accumulated - Shots 280 - 1; Label H7
33229.9805
815
22161.5195
100
90
80
70
60
50
40
30
20
10
0
19964.0
46165.2
72366.4
98567.6
124768.8
150970.(
Mass (m/z)

Accumulated - Shots 280 - 1; Label H7

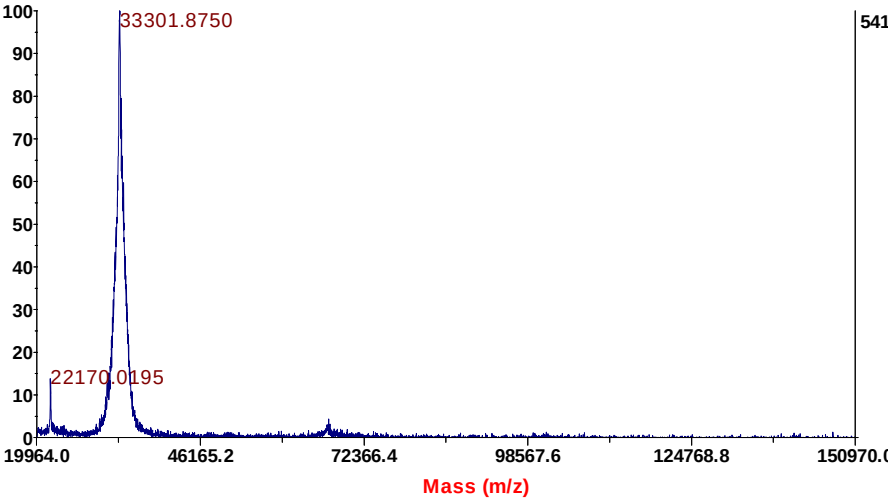

Accumulated - Shots 160 - 1; Label H7

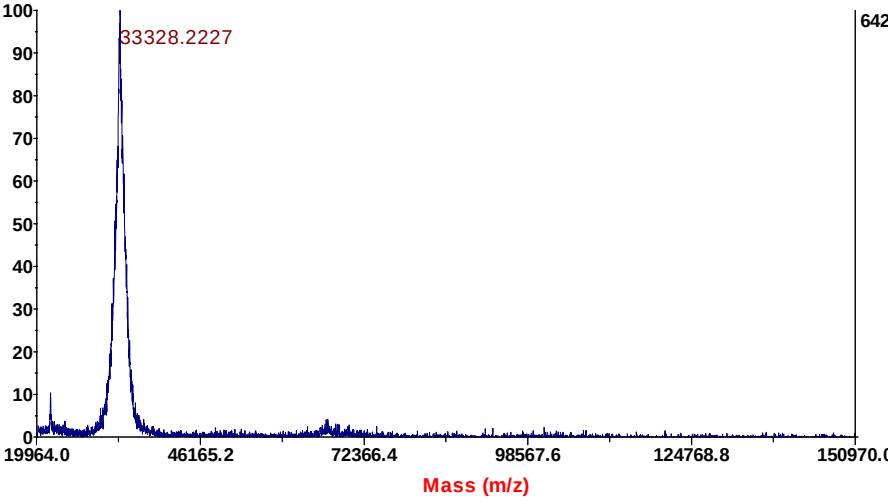

Accumulated - Shots 480 - 1; Label H7

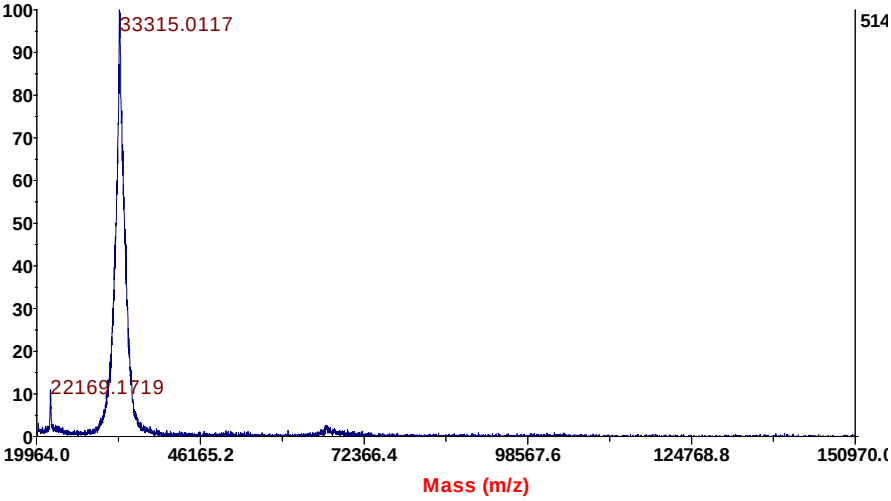

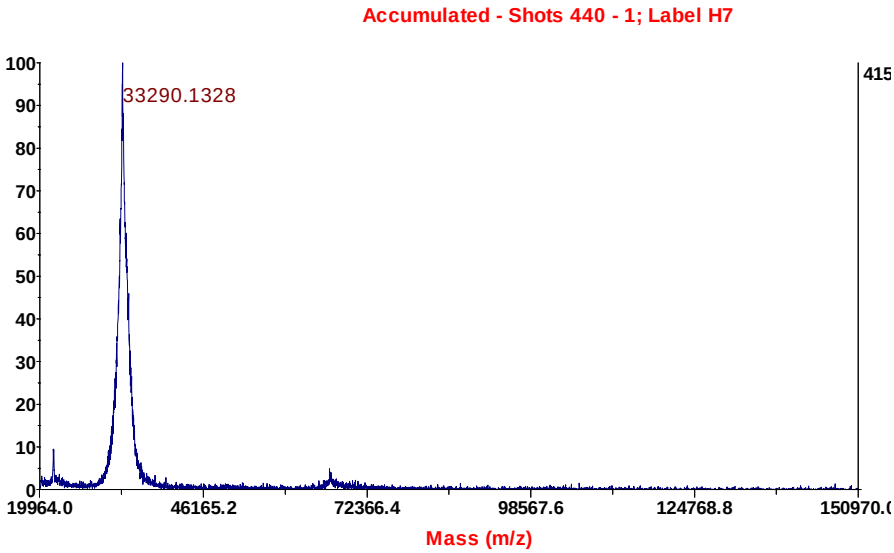
Accumulated - Shots 440 - 1; Label H7
33290.1328
100
90
80
70
60
50
40
30
20
10
0
19964.0
46165.2
72366.4
98567.6
124768.8
Mass (m/z)

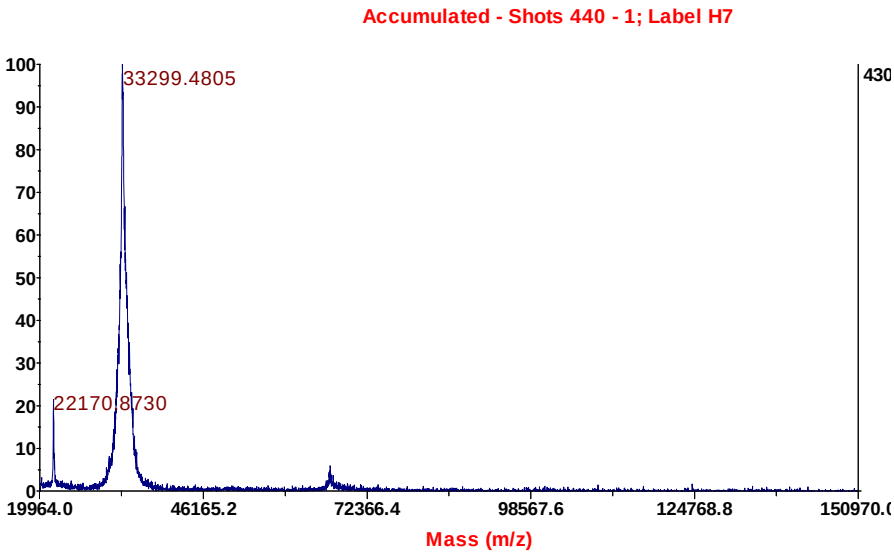
Accumulated - Shots 440 - 1; Label H7
33299.4805
22170.8730
100
90
80
70
60
50
40
30
20
10
0
19964.0
46165.2
72366.4
98567.6
124768.8
Mass (m/z)

HSA+ **4a**

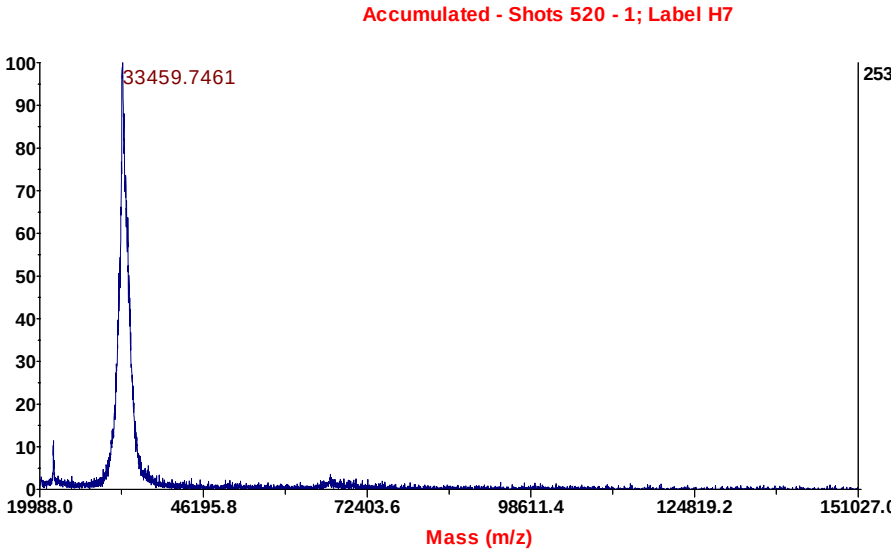
Accumulated - Shots 520 - 1; Label H7
33459.7461
100
90
80
70
60
50
40
30
20
10
0
19988.0
46195.8
72403.6
98611.4
124819.2
Mass (m/z)

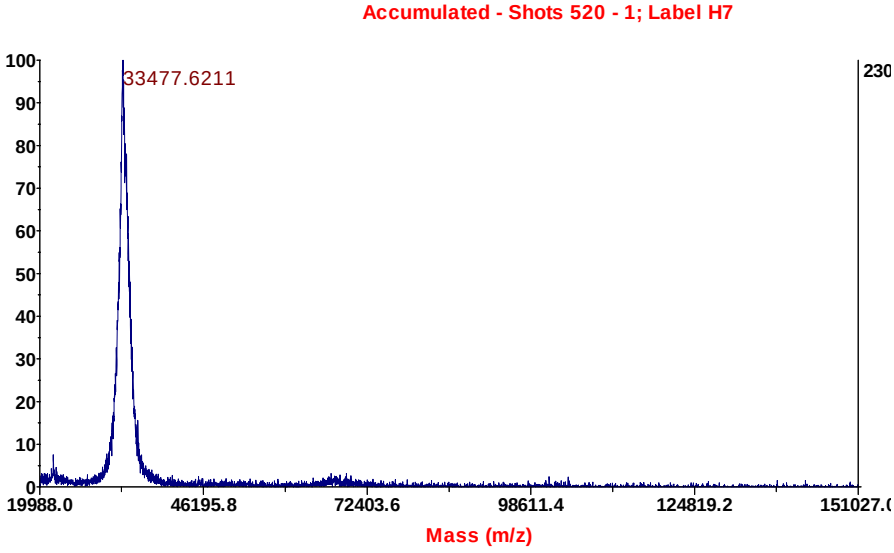
Accumulated - Shots 520 - 1; Label H7
33477.6211
100
90
80
70
60
50
40
30
20
10
0
19988.0
46195.8
72403.6
98611.4
124819.2
Mass (m/z)

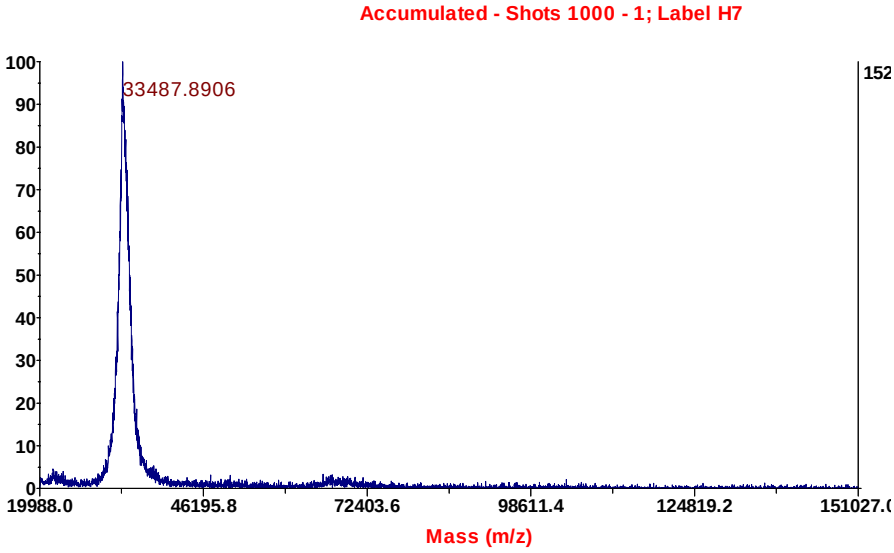
Accumulated - Shots 1000 - 1; Label H7
33487.8906
100
90
80
70
60
50
40
30
20
10
0
19988.0
46195.8
72403.6
98611.4
124819.2
Mass (m/z)

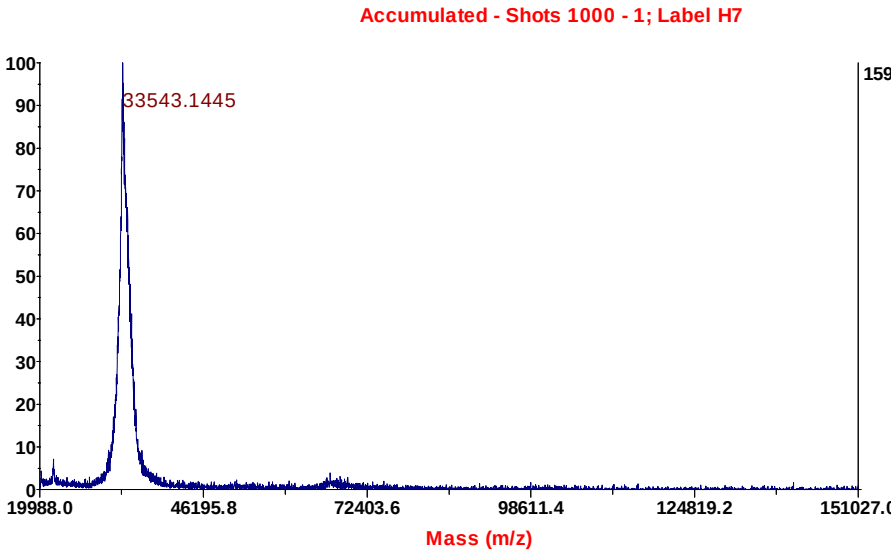
Accumulated - Shots 1000 - 1; Label H7
33543.1445
100
90
80
70
60
50
40
30
20
10
0
19988.0
46195.8
72403.6
98611.4
124819.2
Mass (m/z)

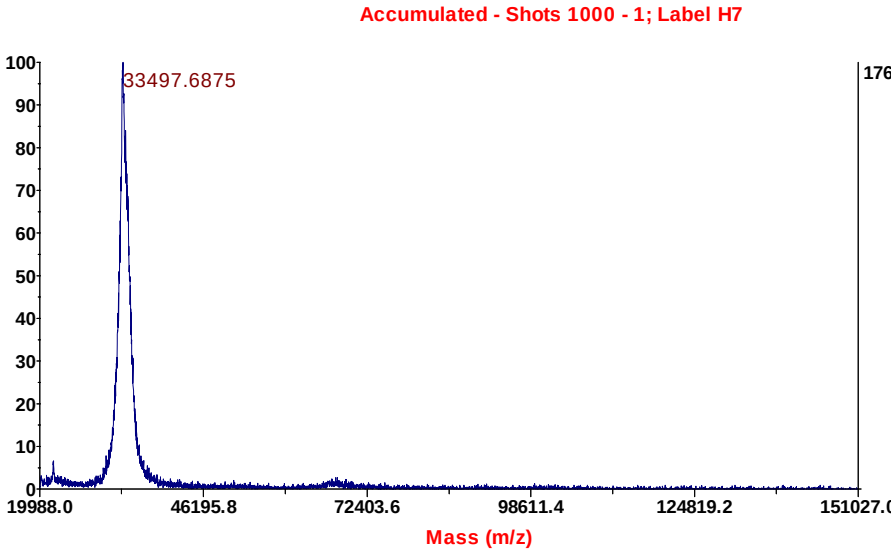
Accumulated - Shots 1000 - 1; Label H7
33497.6875
100
90
80
70
60
50
40
30
20
10
0
19988.0
46195.8
72403.6
98611.4
124819.2
Mass (m/z)

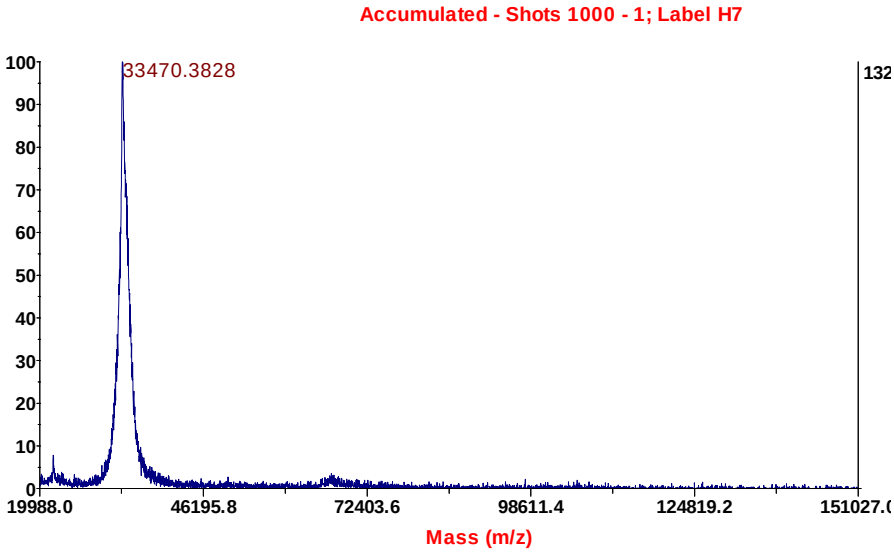
Accumulated - Shots 1000 - 1; Label H7
33470.3828
100
90
80
70
60
50
40
30
20
10
0
19988.0
46195.8
72403.6
98611.4
124819.2
Mass (m/z)

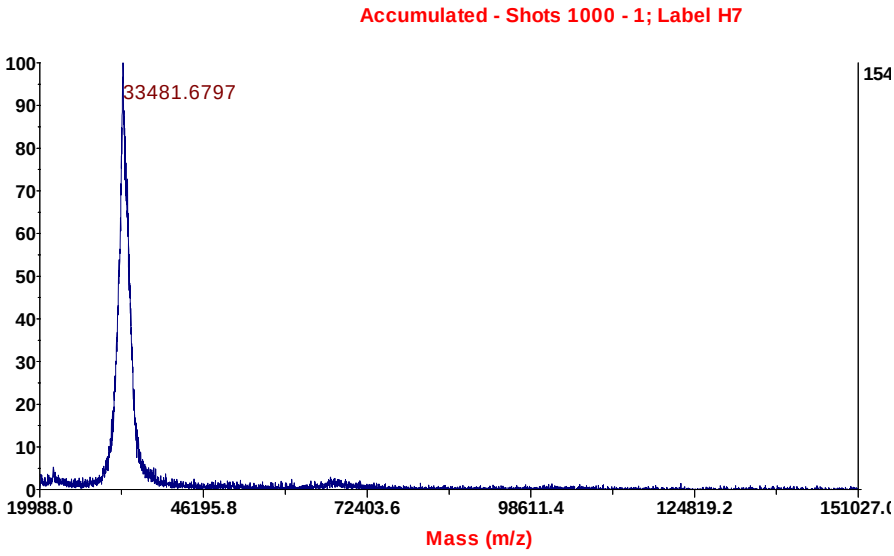
Accumulated - Shots 1000 - 1; Label H7
33481.6797
100
90
80
70
60
50
40
30
20
10
0
19988.0
46195.8
72403.6
98611.4
124819.2
Mass (m/z)

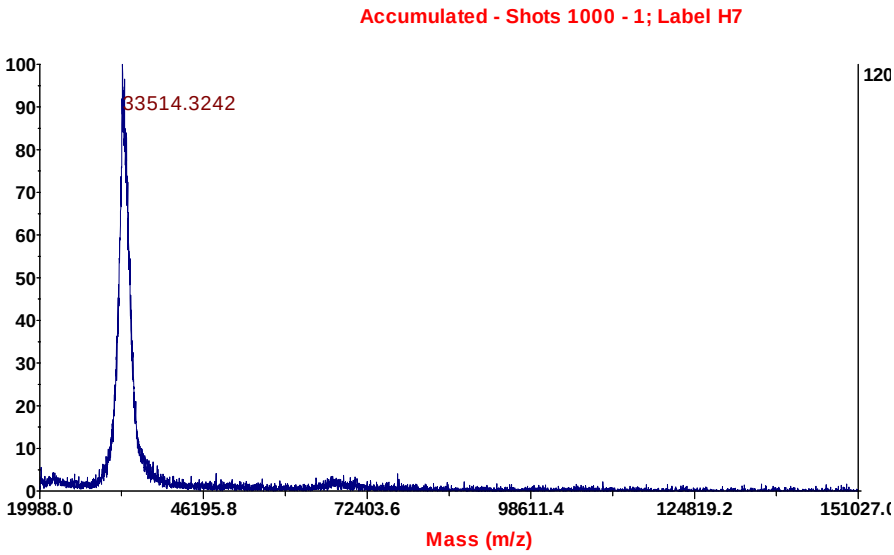
Accumulated - Shots 1000 - 1; Label H7
33514.3242
100
90
80
70
60
50
40
30
20
10
0
19988.0
46195.8
72403.6
98611.4
124819.2
Mass (m/z)

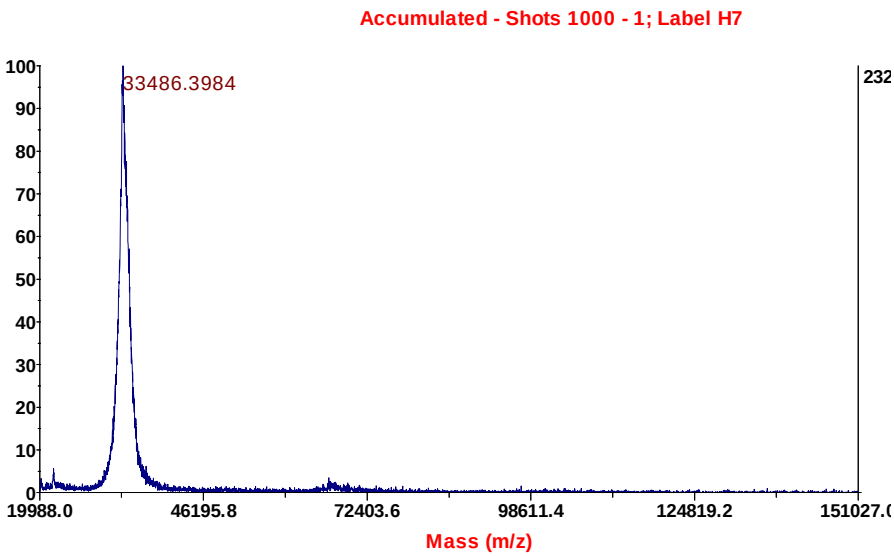
Accumulated - Shots 1000 - 1; Label H7
33486.3984
100
90
80
70
60
50
40
30
20
10
0
19988.0
46195.8
72403.6
98611.4
124819.2
Mass (m/z)

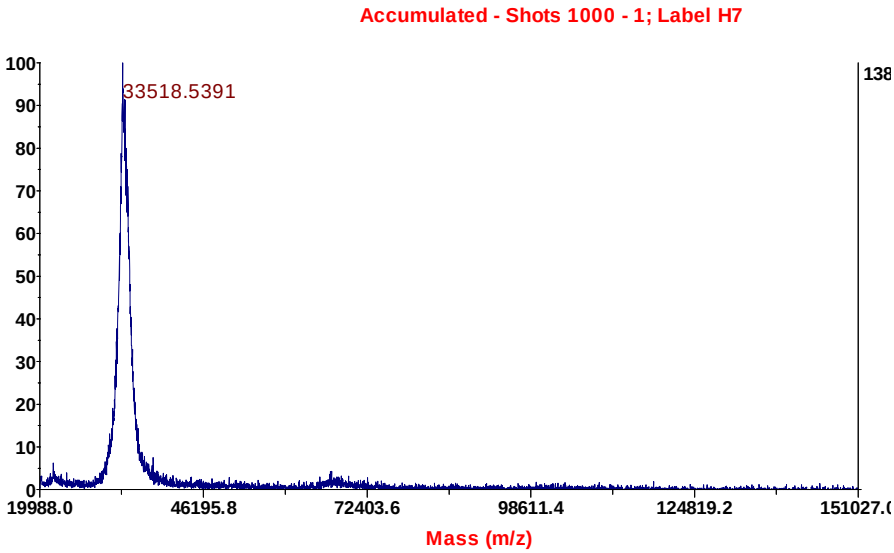
Accumulated - Shots 1000 - 1; Label H7
33518.5391
100
90
80
70
60
50
40
30
20
10
0
19988.0
46195.8
72403.6
98611.4
124819.2
Mass (m/z)

BSA

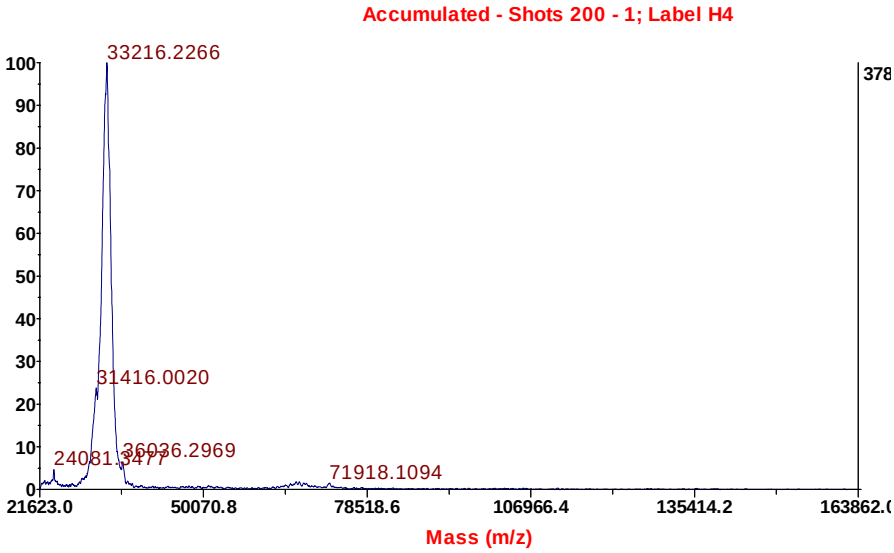
Accumulated - Shots 200 - 1; Label H4
33216.2266
31416.0020
36036.2969
24081.3477
71918.1094
Mass (m/z)

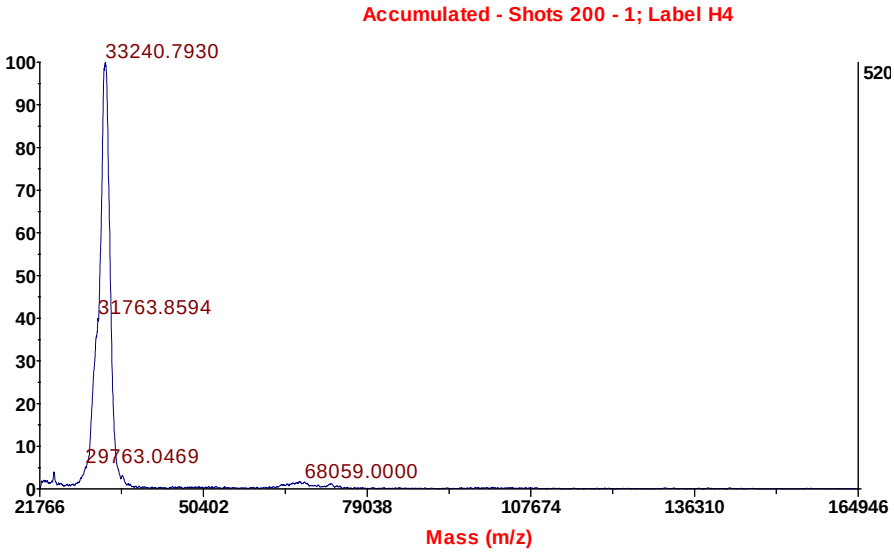
Accumulated - Shots 200 - 1; Label H4
33240.7930
31763.8594
29763.0469
68059.0000
Mass (m/z)

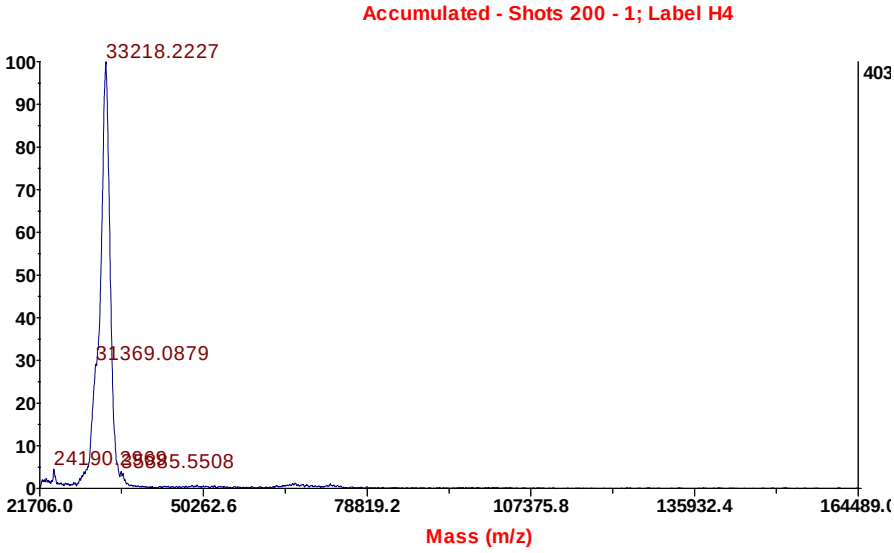
Accumulated - Shots 200 - 1; Label H4
33218.2227
31369.0879
24190.3669
35885.5508
Mass (m/z)

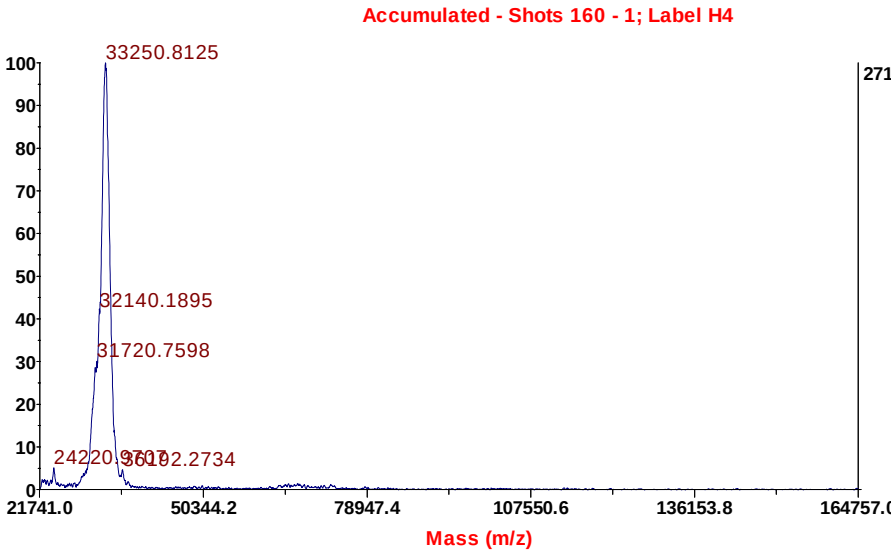
Accumulated - Shots 160 - 1; Label H4
33250.8125
32140.1895
31720.7598
24220.9707
36192.2734
100
90
80
70
60
50
40
30
20
10
0
21741.0
50344.2
78947.4
107550.6
136153.8
164757.(
271
Mass (m/z)

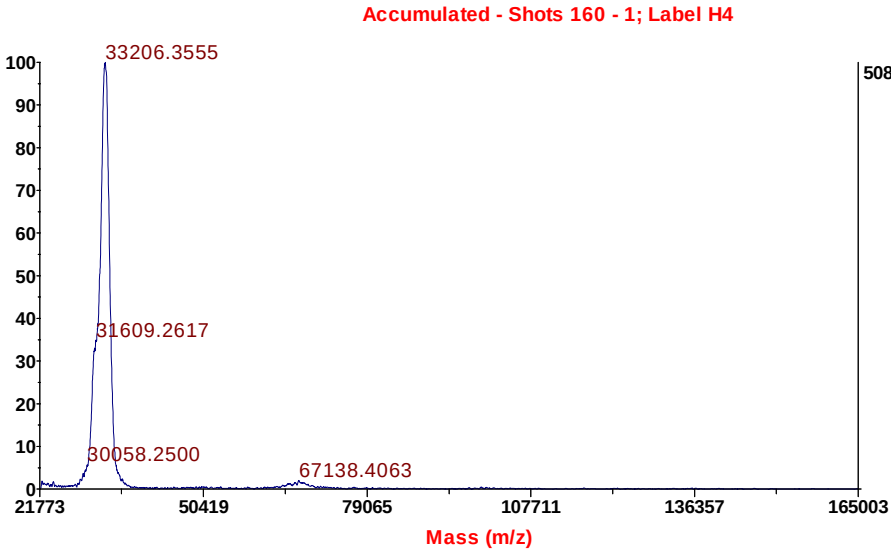
Accumulated - Shots 160 - 1; Label H4
33206.3555
31609.2617
30058.2500
67138.4063
100
90
80
70
60
50
40
30
20
10
0
21773
50419
79065
107711
136357
165003
508
Mass (m/z)

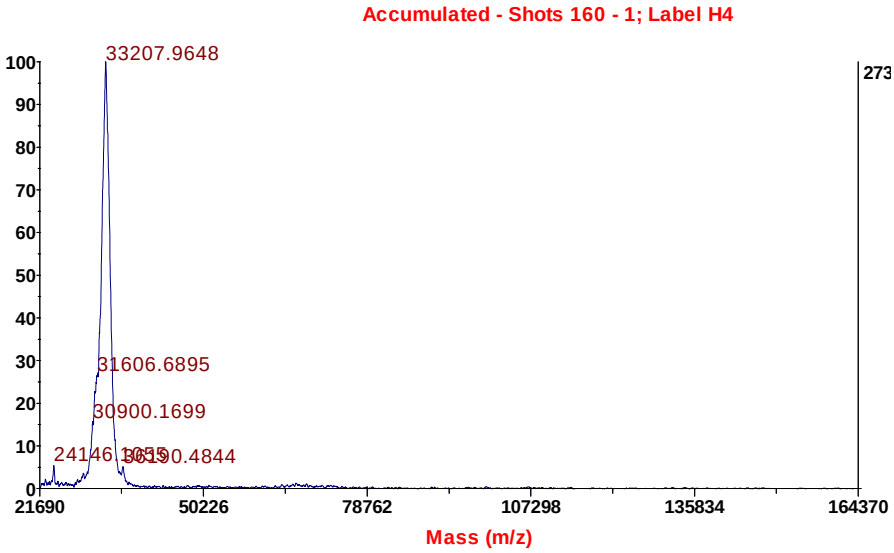
Accumulated - Shots 160 - 1; Label H4
33207.9648
31606.6895
30900.1699
24146.3555
36190.4844
100
90
80
70
60
50
40
30
20
10
0
21690
50226
78762
107298
135834
164370
273
Mass (m/z)

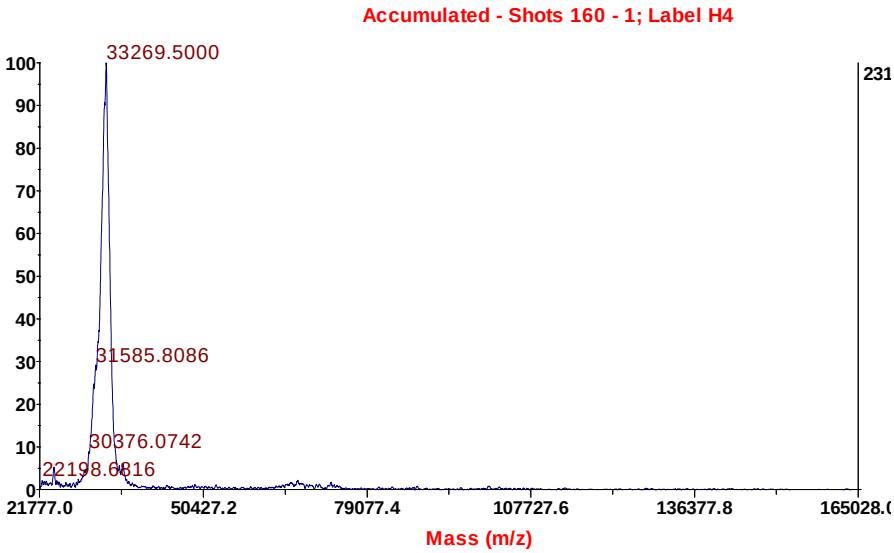
Accumulated - Shots 160 - 1; Label H4
33269.5000
31585.8086
30376.0742
22198.6816
100
90
80
70
60
50
40
30
20
10
0
21777.0
50427.2
79077.4
107727.6
136377.8
231
Mass (m/z)

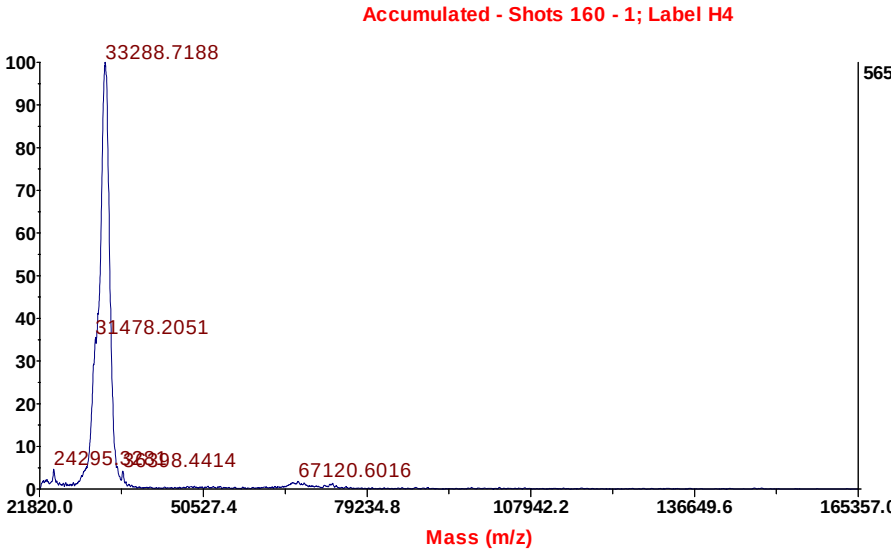
Accumulated - Shots 160 - 1; Label H4
33288.7188
31478.2051
67120.6016
100
90
80
70
60
50
40
30
20
10
0
21820.0
50527.4
79234.8
107942.2
136649.6
565
Mass (m/z)

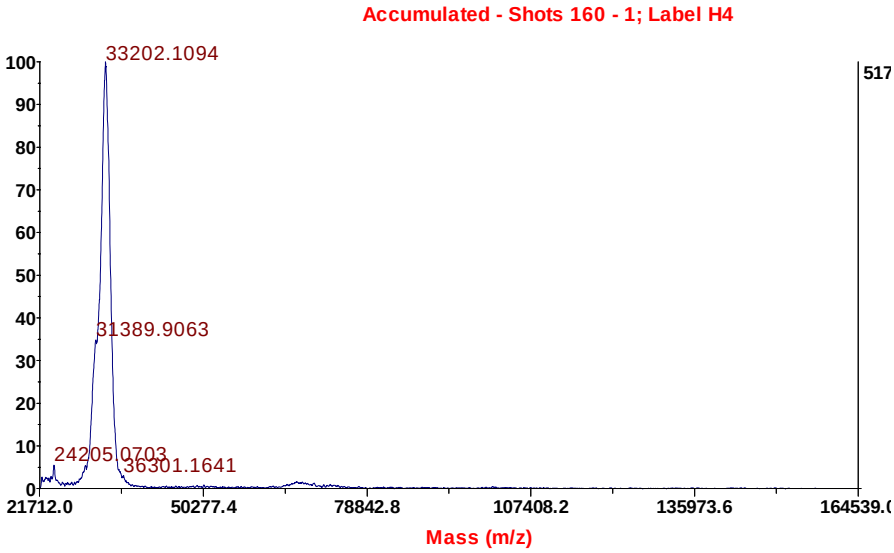
Accumulated - Shots 160 - 1; Label H4
33202.1094
31389.9063
24205.0703
36301.1641
100
90
80
70
60
50
40
30
20
10
0
21712.0
50277.4
78842.8
107408.2
135973.6
517
Mass (m/z)

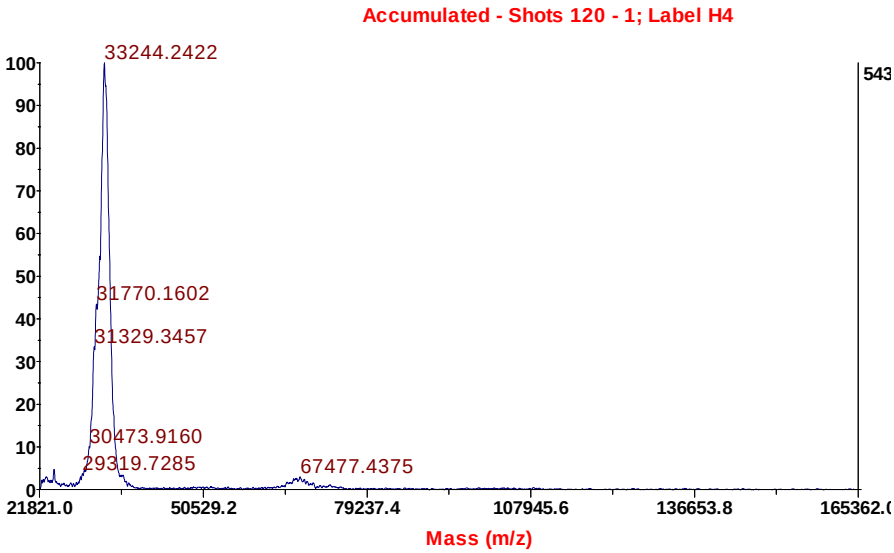
Accumulated - Shots 120 - 1; Label H4
33244.2422
31770.1602
31329.3457
30473.9160
29319.7285
67477.4375
100
90
80
70
60
50
40
30
20
10
0
21821.0
50529.2
79237.4
107945.6
136653.8
Mass (m/z)

BSA + **4a**

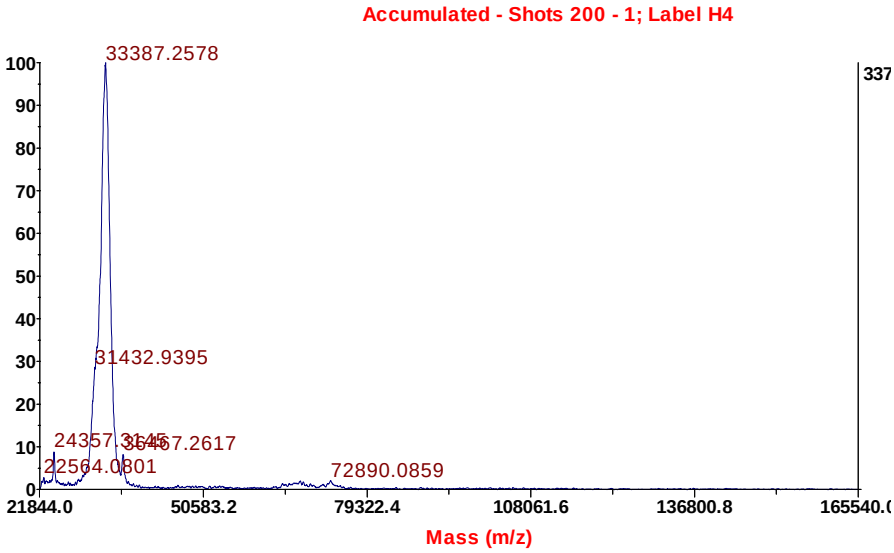
Accumulated - Shots 200 - 1; Label H4
33387.2578
31432.9395
24357.3145
22564.0801
36467.2617
72890.0859
21844.0
50583.2
79322.4
108061.6
136800.8
Mass (m/z)

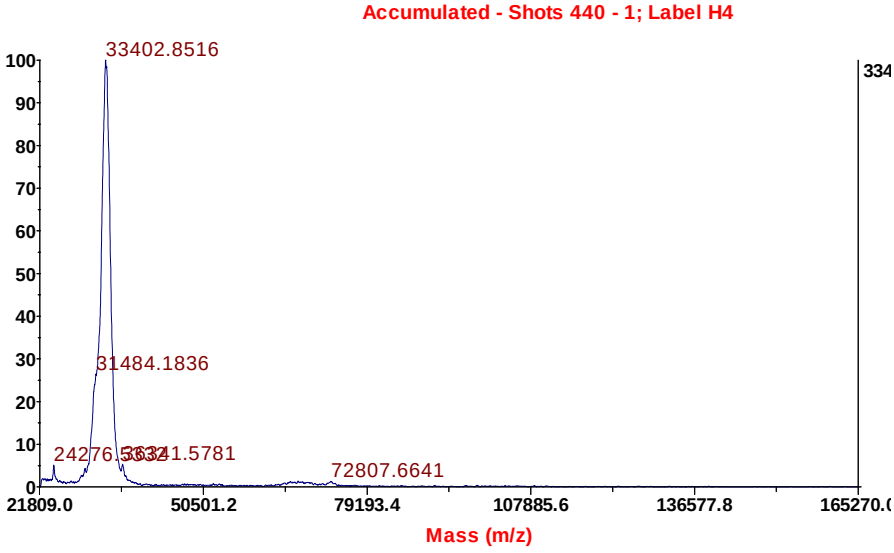
Accumulated - Shots 440 - 1; Label H4
33402.8516
31484.1836
72807.6641
21809.0
50501.2
79193.4
107885.6
136577.8
Mass (m/z)

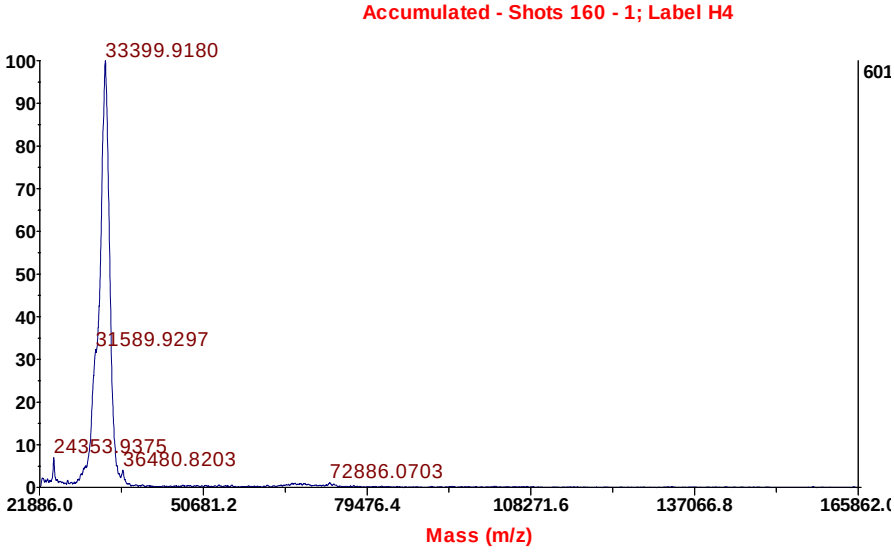
Accumulated - Shots 160 - 1; Label H4
33399.9180
31589.9297
24353.9375
36480.8203
72886.0703
21886.0
50681.2
79476.4
108271.6
137066.8
Mass (m/z)

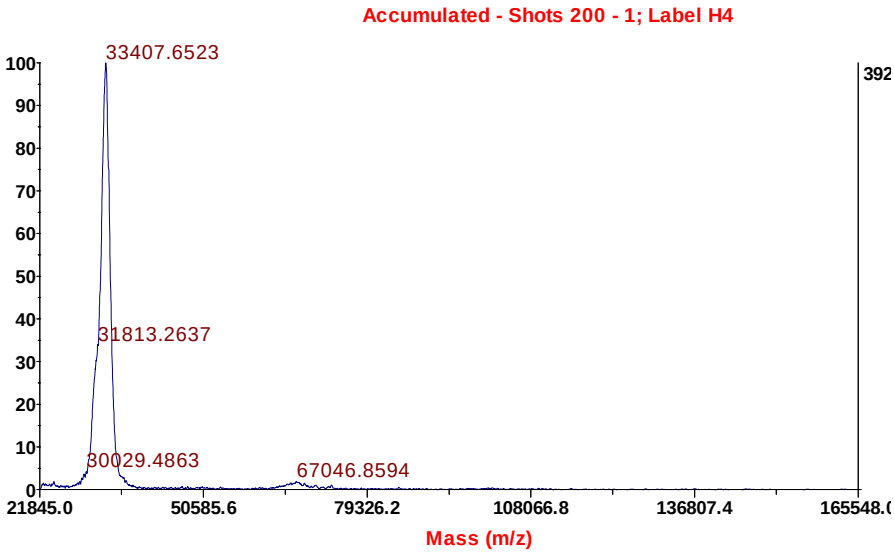
Accumulated - Shots 200 - 1; Label H4
33407.6523
31813.2637
30029.4863
67046.8594
Mass (m/z)

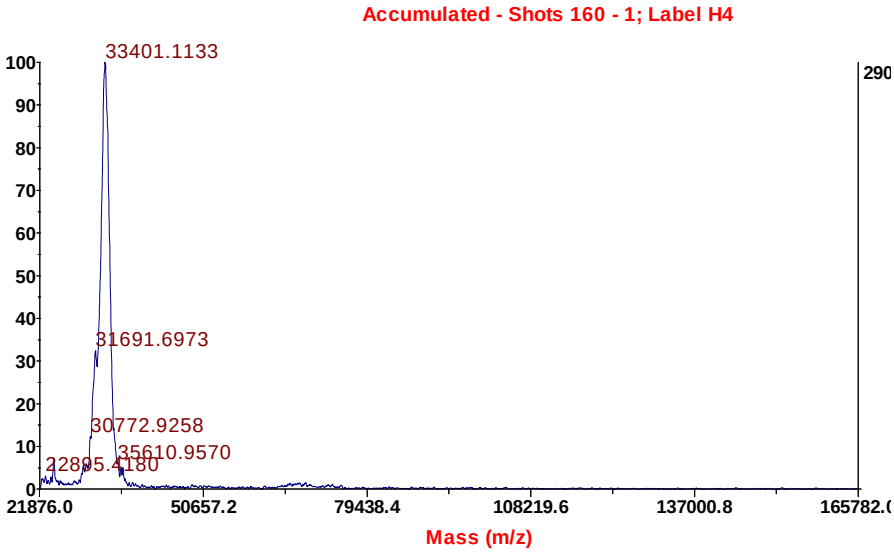
Accumulated - Shots 160 - 1; Label H4
33401.1133
31691.6973
30772.9258
35610.9570
Mass (m/z)

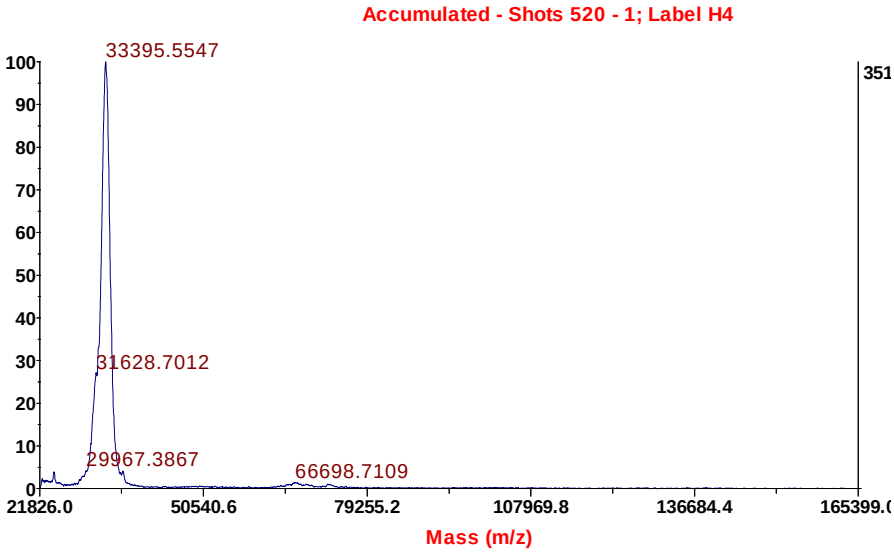
Accumulated - Shots 520 - 1; Label H4
33395.5547
31628.7012
29967.3867
66698.7109
Mass (m/z)

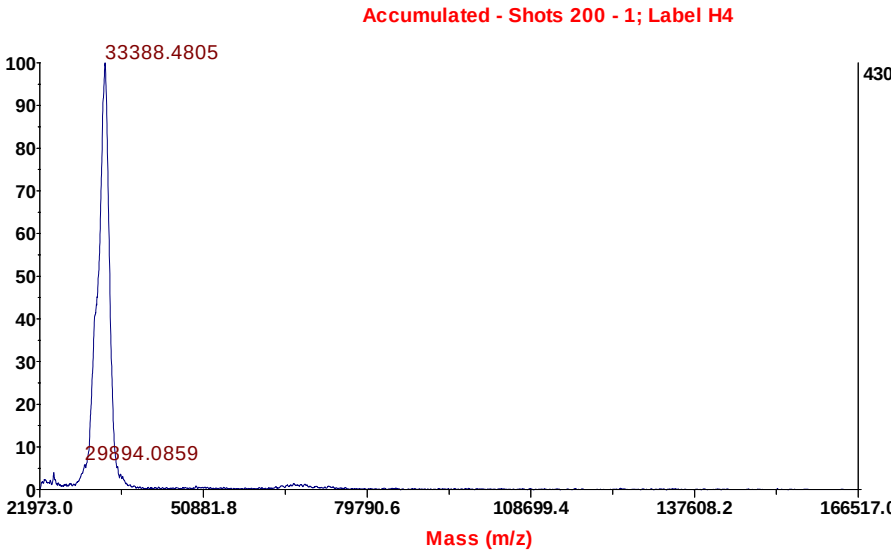
Accumulated - Shots 200 - 1; Label H4
33388.4805
29894.0859
100
90
80
70
60
50
40
30
20
10
0
21973.0
50881.8
79790.6
108699.4
137608.2
166517.(
Mass (m/z)

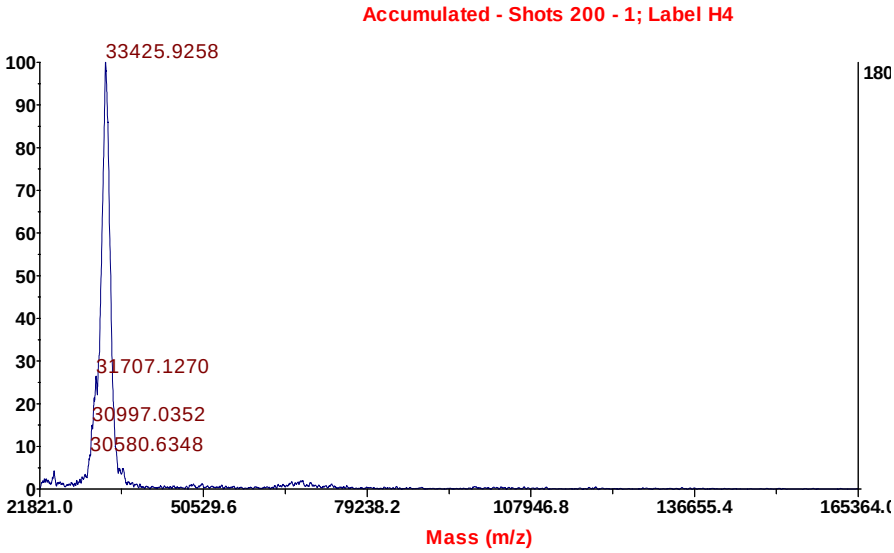
Accumulated - Shots 200 - 1; Label H4
33425.9258
31707.1270
30997.0352
30580.6348
100
90
80
70
60
50
40
30
20
10
0
21821.0
50529.6
79238.2
107946.8
136655.4
165364.(
Mass (m/z)

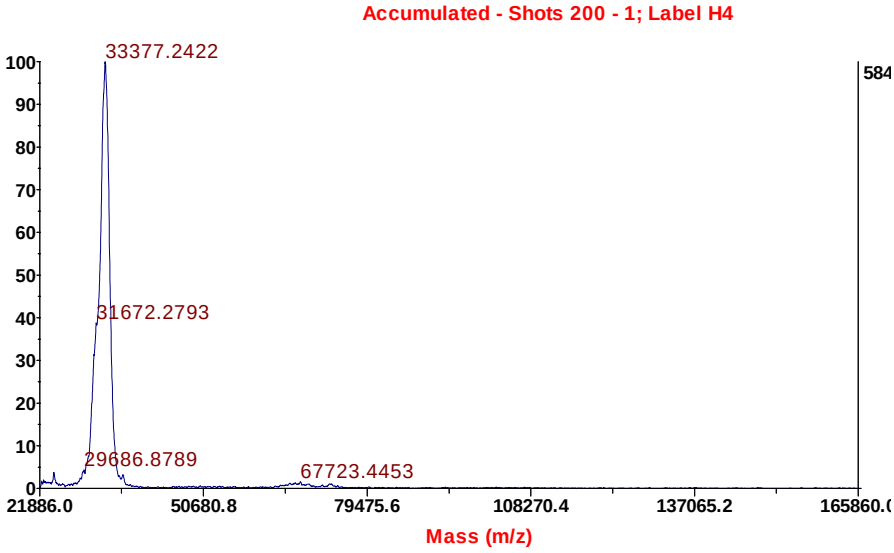
Accumulated - Shots 200 - 1; Label H4
33377.2422
31672.2793
29686.8789
67723.4453
100
90
80
70
60
50
40
30
20
10
0
21886.0
50680.8
79475.6
108270.4
137065.2
165860.(
Mass (m/z)

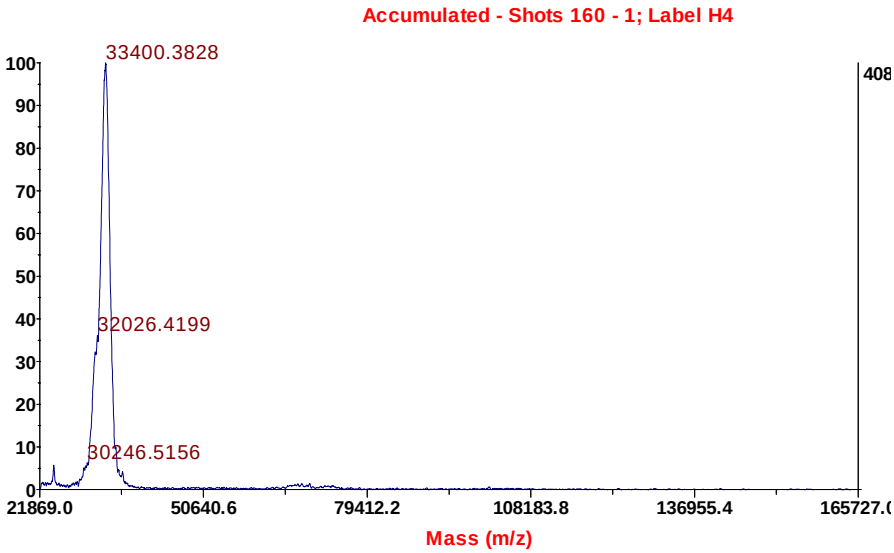

Table S1. The detected molecular weight of the double charged HSA by MALDI-TOF/TOF, and the calculated molecular weight of the singly charged species.

$[HSA]^{2+}$	$[HSA + \mathbf{4a}]^{2+}$	$[HSA]^{+}$	$[HSA + \mathbf{4a}]^{+}$
33321.0742	33459.7461	66641.1484	66918.4922
33330.1445	33477.6211	66659.289	66954.2422
33300.3594	33487.8906	66599.7188	66974.7812
33270.9805	33543.1445	66540.961	67085.289
33229.9805	33497.6875	66458.961	66994.375
33301.875	33470.3828	66602.75	66939.7656
33328.2227	33481.6797	66655.4454	66962.3594
33315.0117	33514.3424	66629.0234	67027.6848
33290.1328	33486.3984	66579.2656	66971.7968
33299.4805	33518.5391	66597.961	67036.0782
33298.72618[a]	**33493.74322**[a]	**66596.45236**[a]	**66986.48644**[a]

[a] The everage value from 10 spectra

Table S2. The detected molecular weight of the double charged BSA by MALDI-TOF/TOF, and the calculated molecular weight of the singly charged species.

$[BSA]^{2+}$	$[BSA + \mathbf{4a}]^{2+}$	$[BSA]^{+}$	$[BSA + \mathbf{4a}]^{+}$
33216.2266	33387.2578	66431.4532	66773.5156
33240.793	33399.918	66480.586	66798.836
33218.2227	33407.6523	66435.4454	66814.3046
33250.8125	33401.1133	66500.625	66801.2266
33206.3555	33395.5547	66411.711	66790.1094
33207.9648	33388.4805	66414.9296	66775.961
33269.5	33425.9258	66538	66850.8516
33288.7188	33388.4805	66576.4376	66775.961
33202.1094	33377.2422	66403.2188	66753.4844
33244.2422	33400.3828	66487.4844	66799.7656
33234.49455[a]	**33397.20079**[a]	**66467.9891**[a]	**66793.40158**[a]

[a] The everage value from 10 spectra

7. DNA cross-linking experiments with naphthols

The ability of naphthols to cross-link DNA molecules was assayed by alkaline agarose electrophoresis. Plasmid DNA (1 μg) was mixed with bis-naphthols **4a**-**4e** (500 μM) or psoralen (20 μM) in PBS buffer, and then irradiated for 30 min at 350 nm in a Luzchem Reactor. After the irradiation, the alkaline agarose gel electrophoresis was performed. Psoralen was used as a positive control. Interstrand cross-linking activity of psoralen was evident as X-band of circular (X-CC) form. However, no X-bands and no difference in migratory ability compared to control DNA were observed in the presence of **4**, suggesting that bis-naphthols do not cross-link plasmid DNA (Fig S43). Another explanation is that agarose electrophoresis may not be sensitive enough to detect subtle epigenetic changes in DNA.

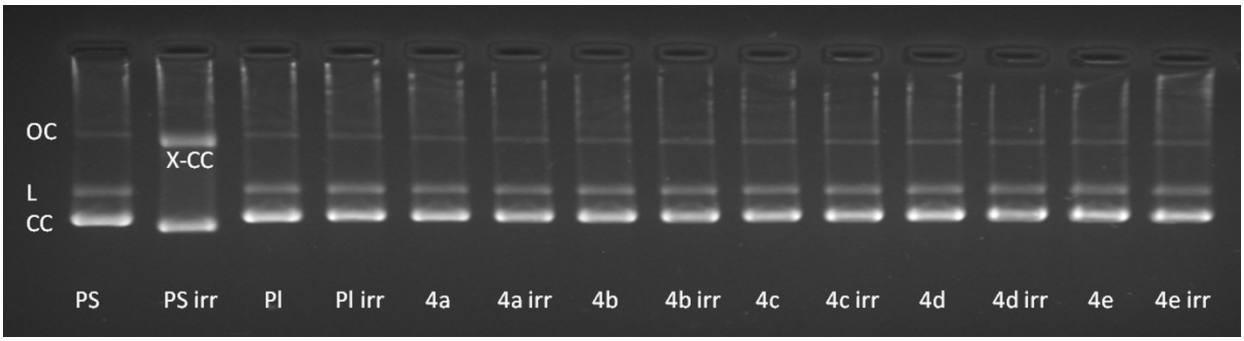

Fig S44. Alkaline agarose gel electrophoresis: pCMVbeta plasmid DNA (1 μg) in PBS buffer (pH = 7.4) was mixed with 4a-4e (500 μM). After 30 min of irradiation at 350nm, samples were loaded and the gel was running for 5 h. In parallel, all of the samples without irradiation were loaded onto the gel. PS-psoralen, Pl-plasmid DNA, irr-irradiated, CC-closed circular DNA, OC-open circular DNA, L-linear DNA, X- cross -linked DNA.

Experimental procedure for the alkaline agarose gel assay

Plasmid CMVbeta DNA (1 μg) was mixed with bis-naphthols **4a-4e** (500 μM) or psoralen (20μM) in PBS buffer, and then irradiated for 30 min at 350nm in a Luzchem Reactor. Irradiated solutions and non-irradiated controls were added to alkaline agarose gel loading buffer [50 mM NaOH, 1 mM ethylenediaminetetraacetic acid (EDTA), 3% Ficoll, and 0.02% bromophenol blue] and loaded on a 1% agarose gel. Prior to the loading, the gel was soaked in 50 mM NaOH and 1 mM EDTA for 1h, and the same solution was used as the running buffer. Gels were run at 30 V constant voltage in horizontal electrophoresis system (BIO-RAD, USA) for 5 h. After the run, gels were neutralized with 0,5M Tris (pH 7) for 30 min, and stained with ethidium bromide (1 μg/mL) for 30 min. Resulting products were visualized and documented with UV light at 254 nm (Image Master VDS, Pharmacia Biotech, Sweden).

8. Antiproliferative investigation

Cell lines and cell culture conditions

The experiments were carried out on 3 human tumor cell lines: NCI-H1299 (lung carcinoma), MCF-7 (breast adenocarcinoma) and SUM159 (pleomorphic breast carcinoma). NCI-H1299 and MCF-7 cells were cultured as monolayers and maintained in DMEM medium, supplemented with 10% fetal bovine serum (FBS), 2 mM L-glutamine, 100 U/mL penicillin and 100 μg/mL streptomycin, while SUM159 cell line was maintained in Ham's F12 medium supplemented with 5% fetal bovine serum, 2 mM L-glutamine, 100 U/mL penicillin and 100 μg/mL streptomycin, 5 μg/mL insulin, 1 μg/mL hydrocortisone, in a humidified atmosphere with 5% CO_2 at 37 °C.

Proliferation assay

Cells were seeded at 2×10^4 cells/mL for SUM159 and NCI-H1299, and 3×10^4 cells/ml for MCF7, depending on the doubling times of specific cell line, in two standard 96-well microtiter plates and left to attach. Next day, test compounds were added at five 10-fold dilutions (10^{-8} to 10^{-4} M) in quadruplicates. For each cell line one of the plates was left in the dark, while the other was irradiated in a Luzchem reactor (6 lamps 350 nm, 5 min) four h after the addition of compounds and subsequently 24 h and 48 h after the first irradiation. The percentage of growth (PG) was evaluated after 72 hours of incubation by adding MTT reagent (Sigma-Aldrich), as described previously.[6] The results were expressed as GI_{50}, a concentration necessary for 50% of inhibition. The GI_{50} values for each compound were calculated from dose-response curves using linear regression analysis by fitting the test concentrations that give PG values above and below the respective reference value. If all of the tested concentrations produce PGs exceeding the respective reference level of effect (e.g. PG value of 50), then the highest tested concentration is assigned as the default value, which is preceded by a ">" sign. Each result is a mean value from at least two separate experiments.

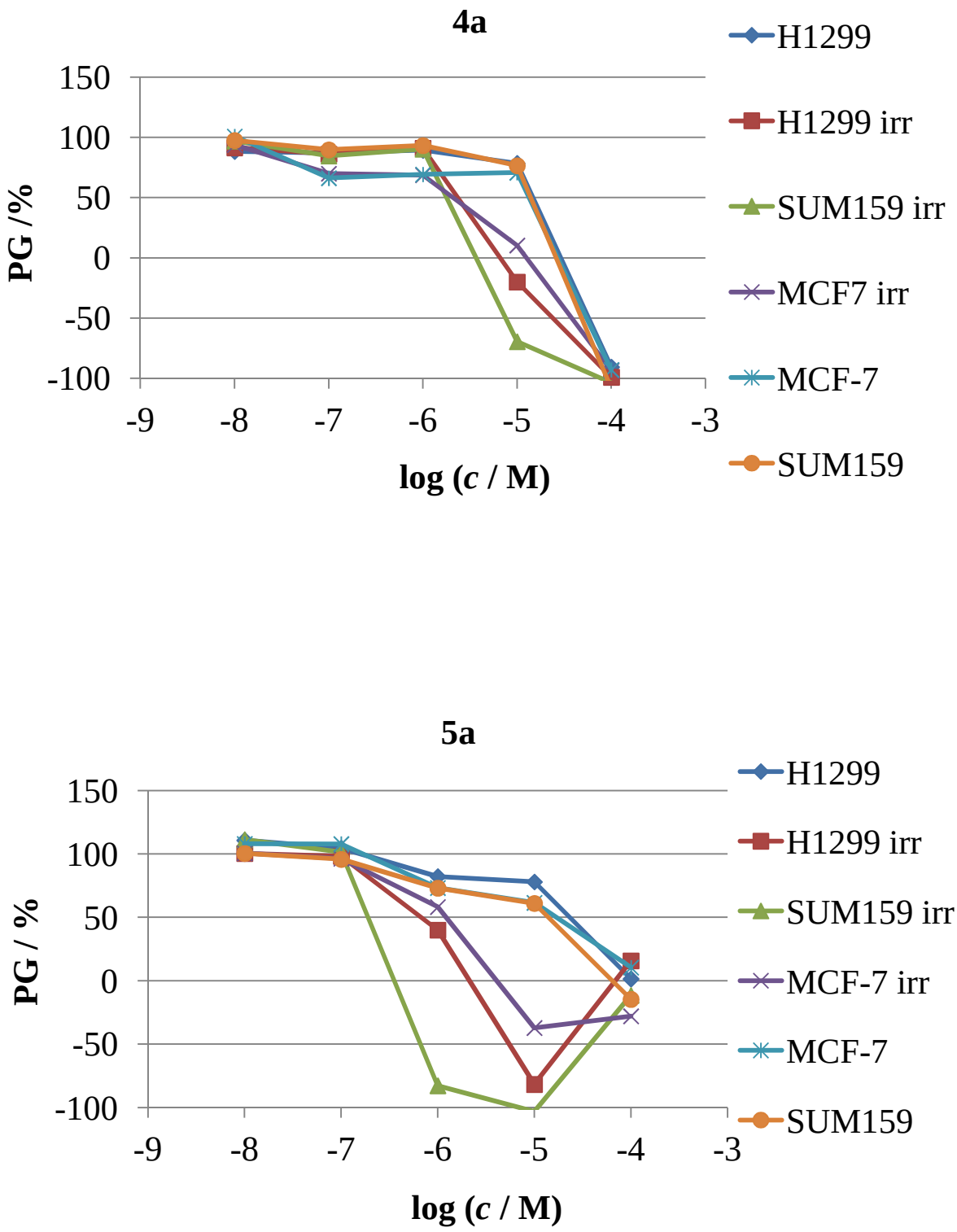

Fig S45. Dose-response profiles for compounds **4a** (top) and **5a** (bottom) tested *in vitro* on H1299, SUM159 and MCF-7 cell lines. PG- percentage of growth, irr-irradiation.

9. NMR spectra

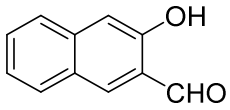

^{1}H NMR ($CDCl_3$, 600 MHz)

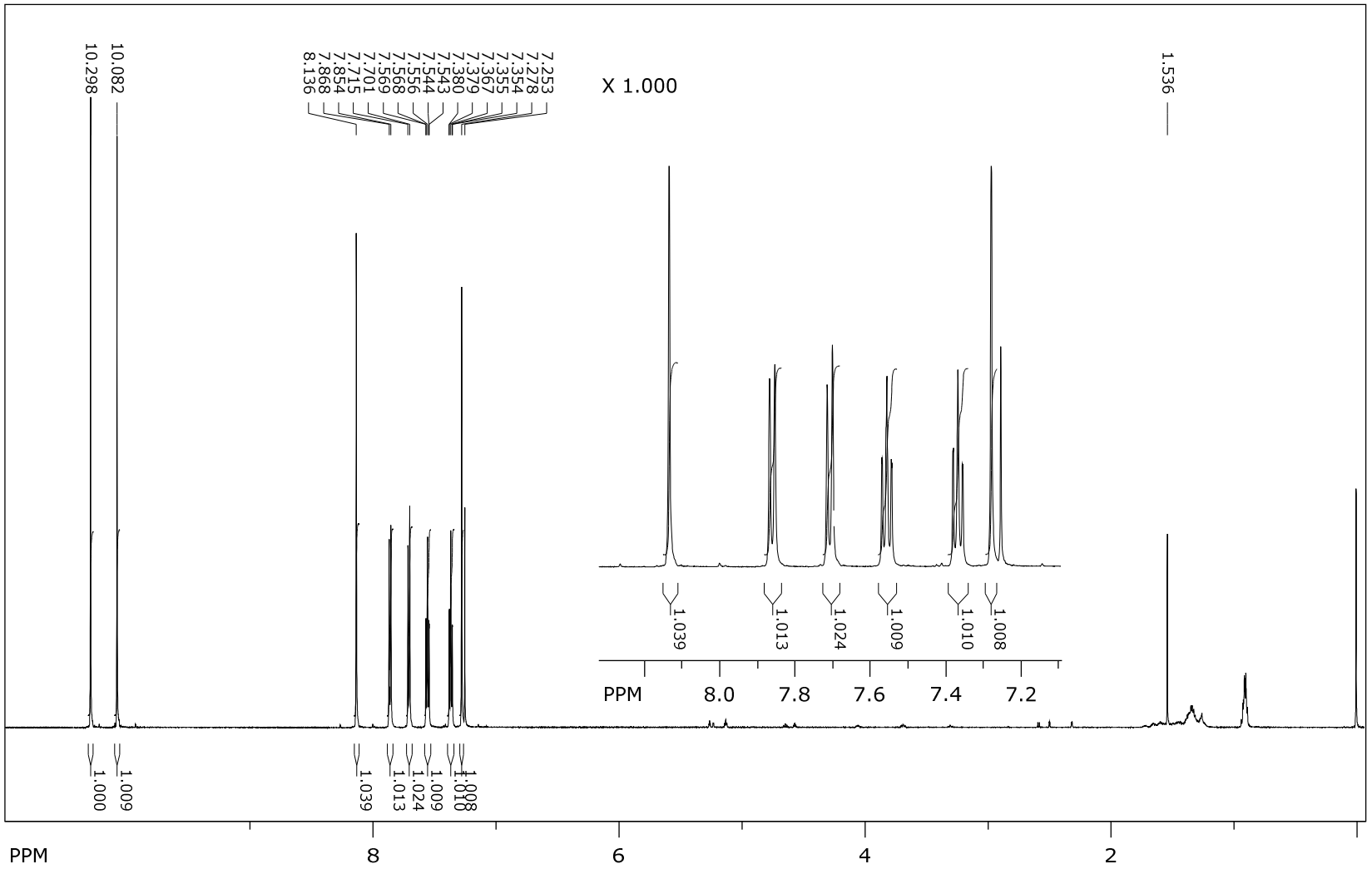

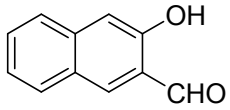

^{13}C NMR ($CDCl_3$, 150 MHz)

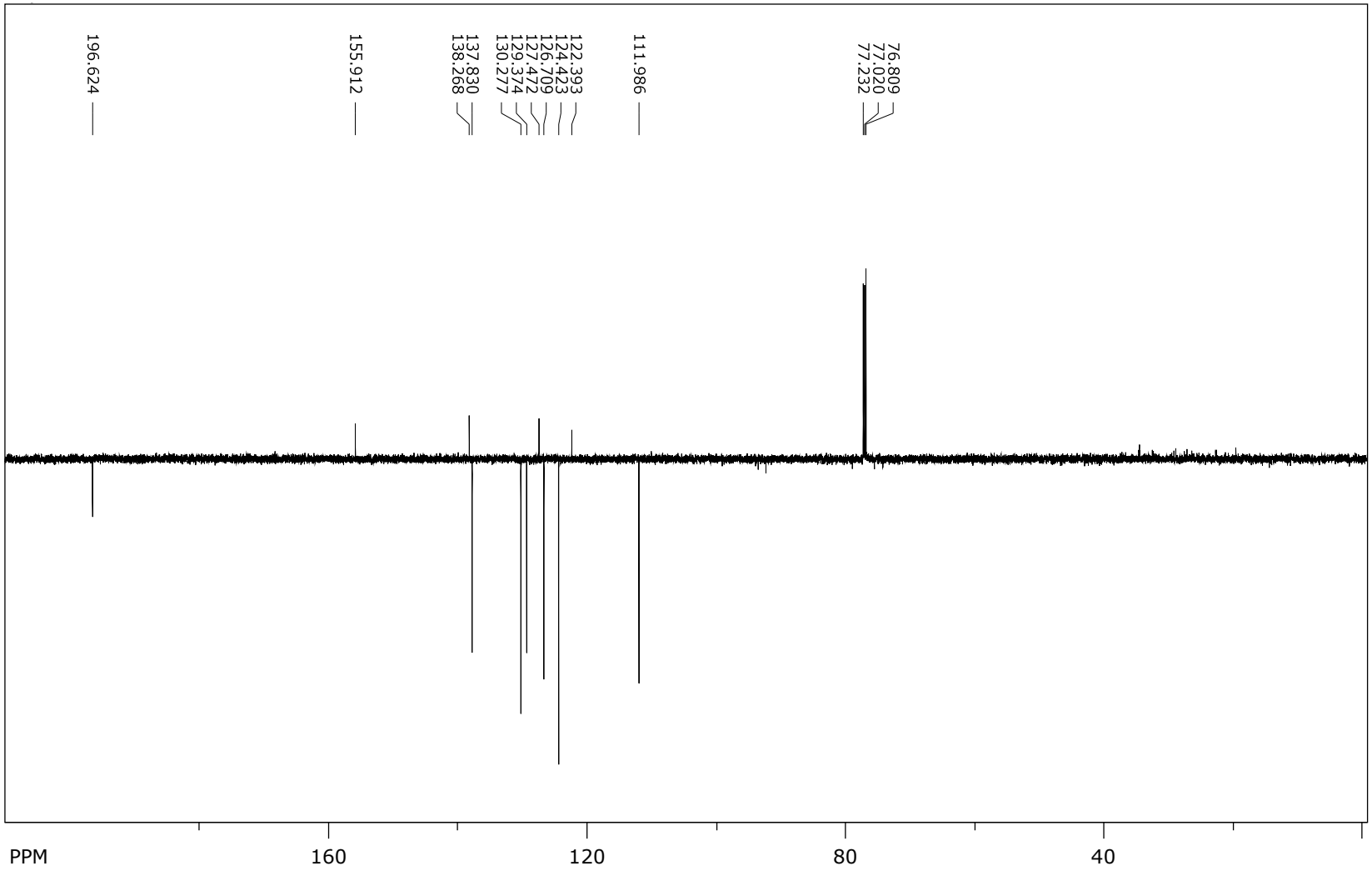

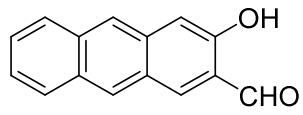

^{1}H NMR ($CDCl_3$, 300 MHz)

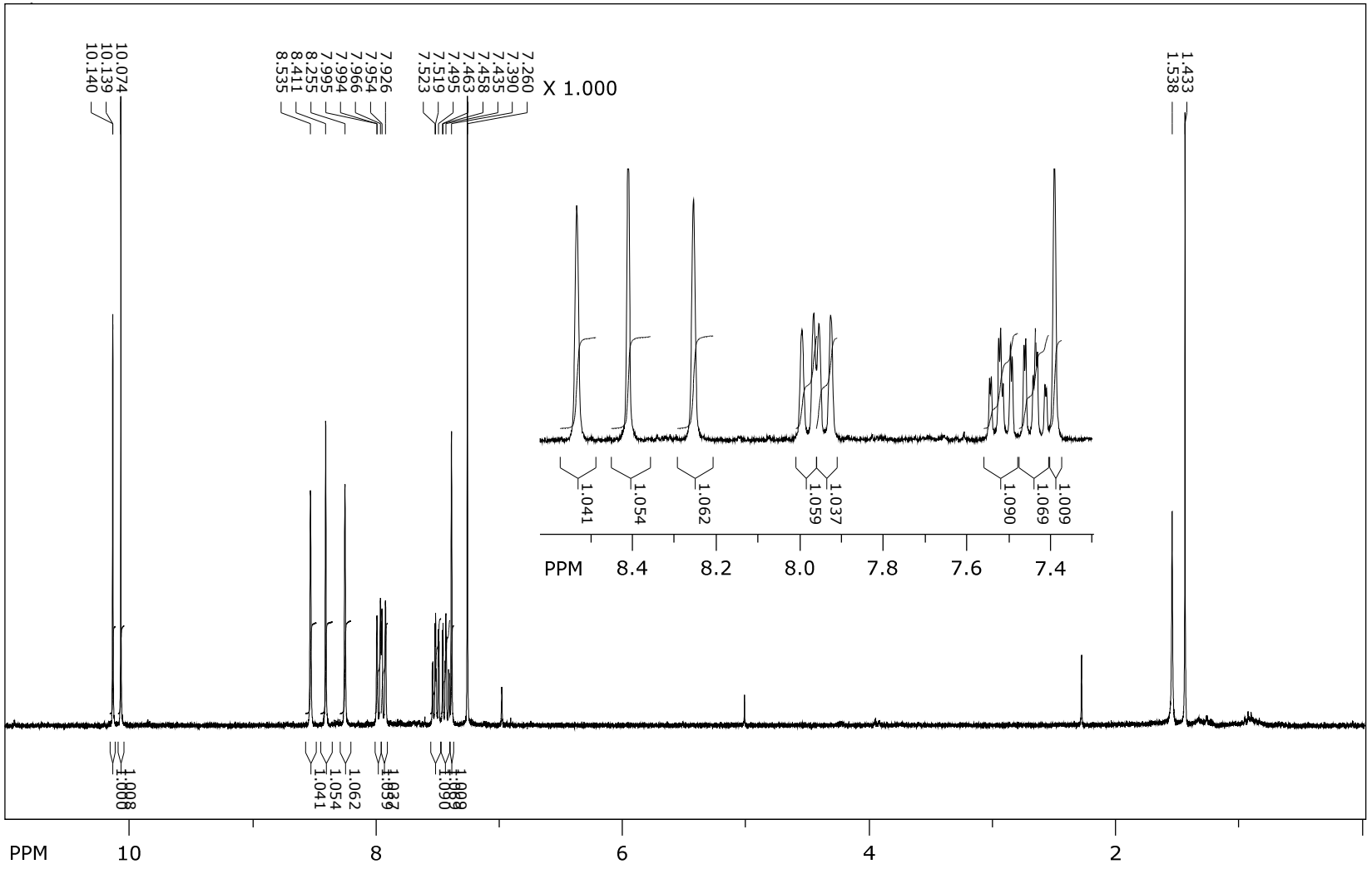

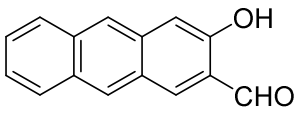

^{13}C NMR ($CDCl_3$, 75 MHz)

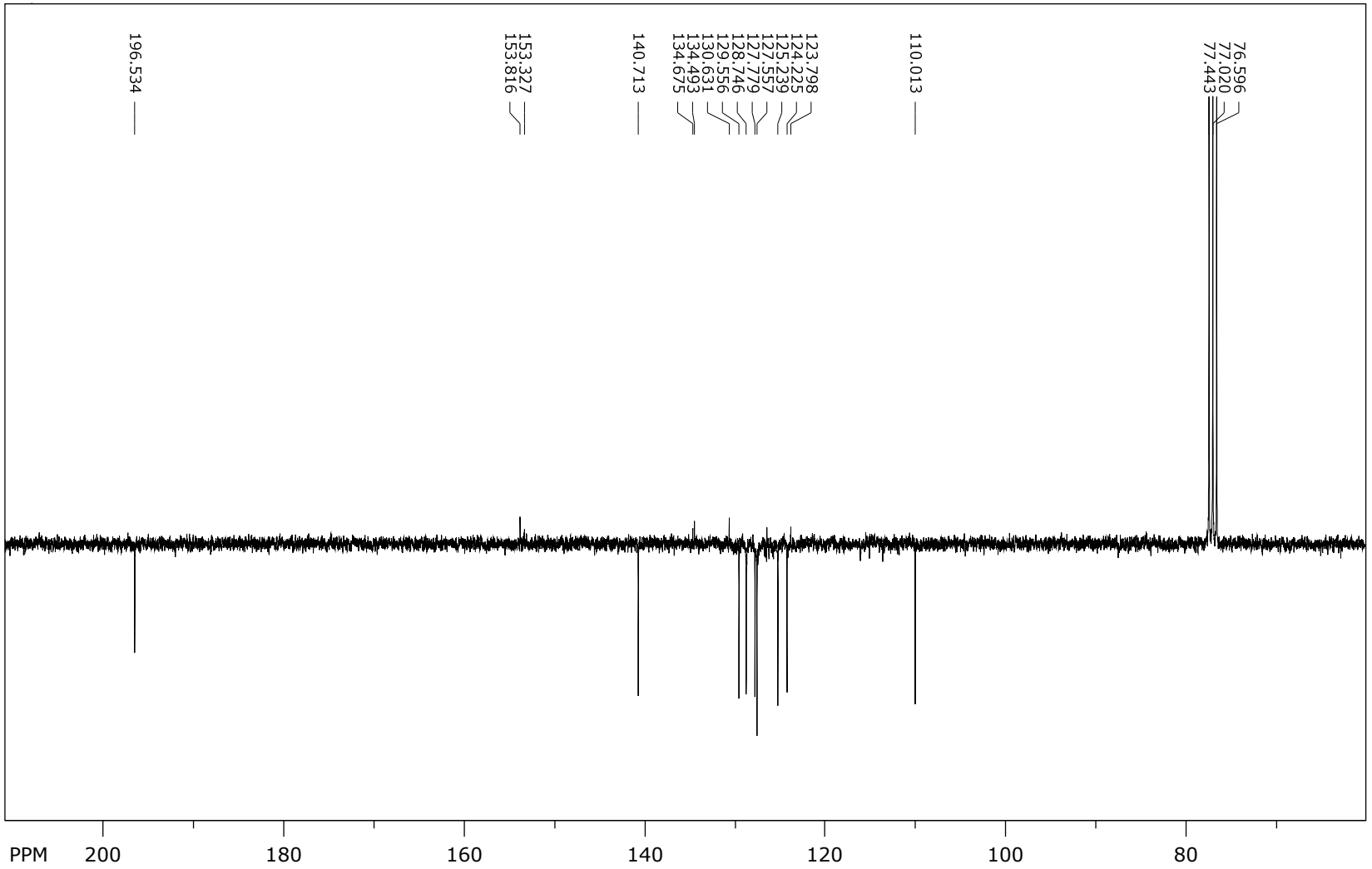

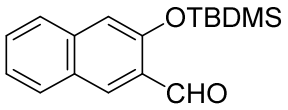

^{1}H NMR ($CDCl_3$, 300 MHz) of **6**

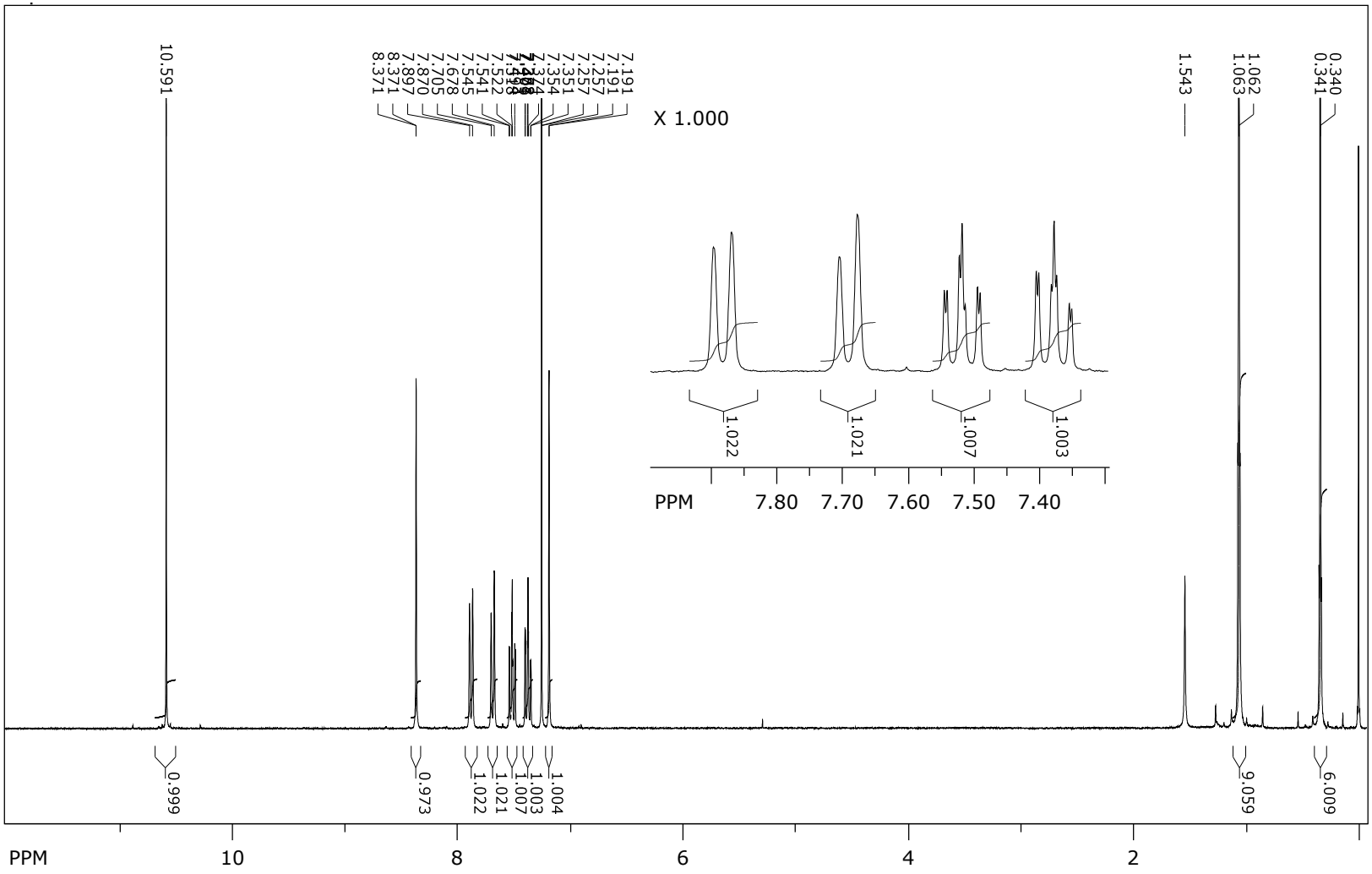

^{13}C NMR ($CDCl_3$, 150 MHz) of **6**

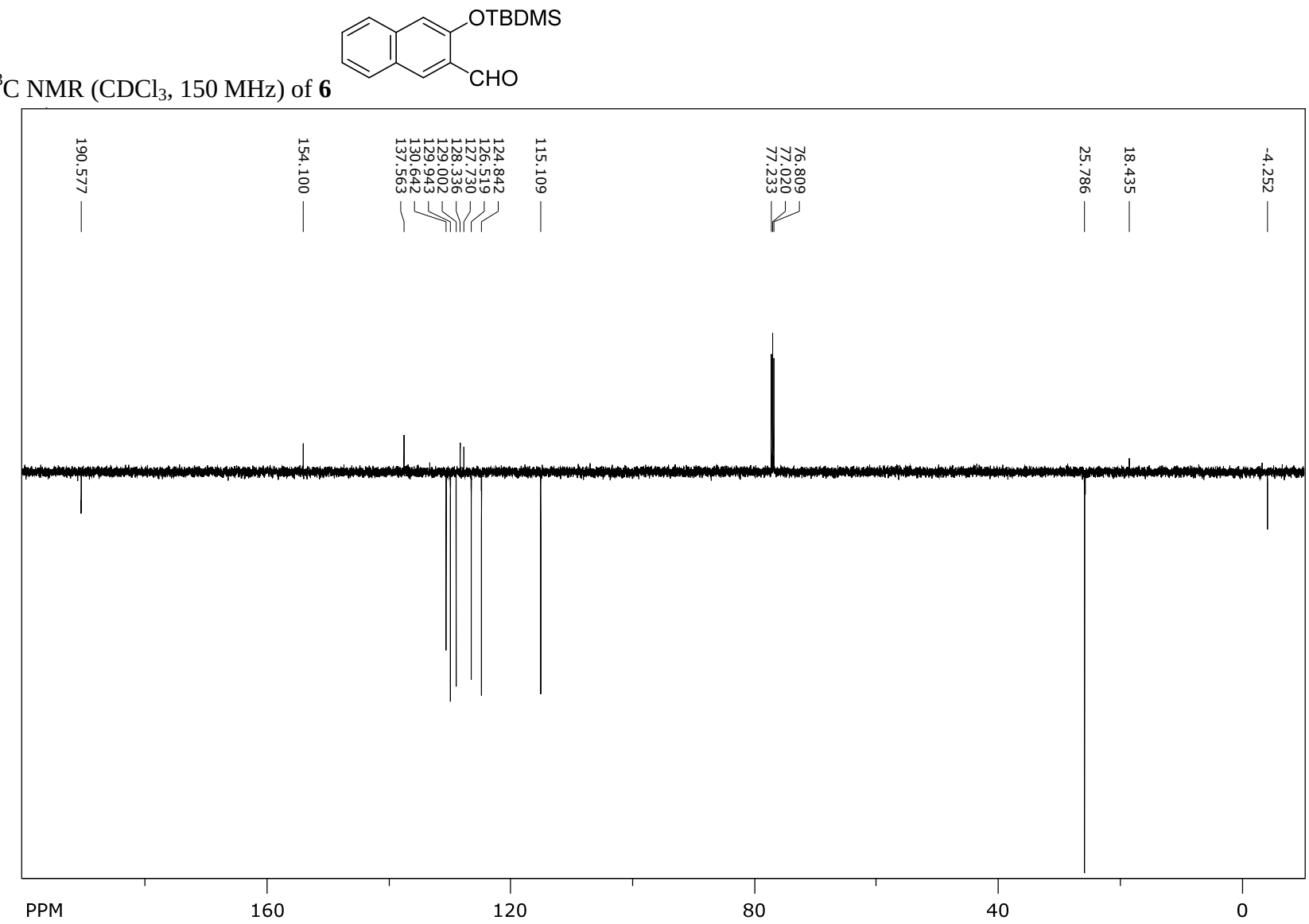

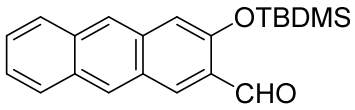

^{1}H NMR ($CDCl_3$, 400 MHz) of **8**

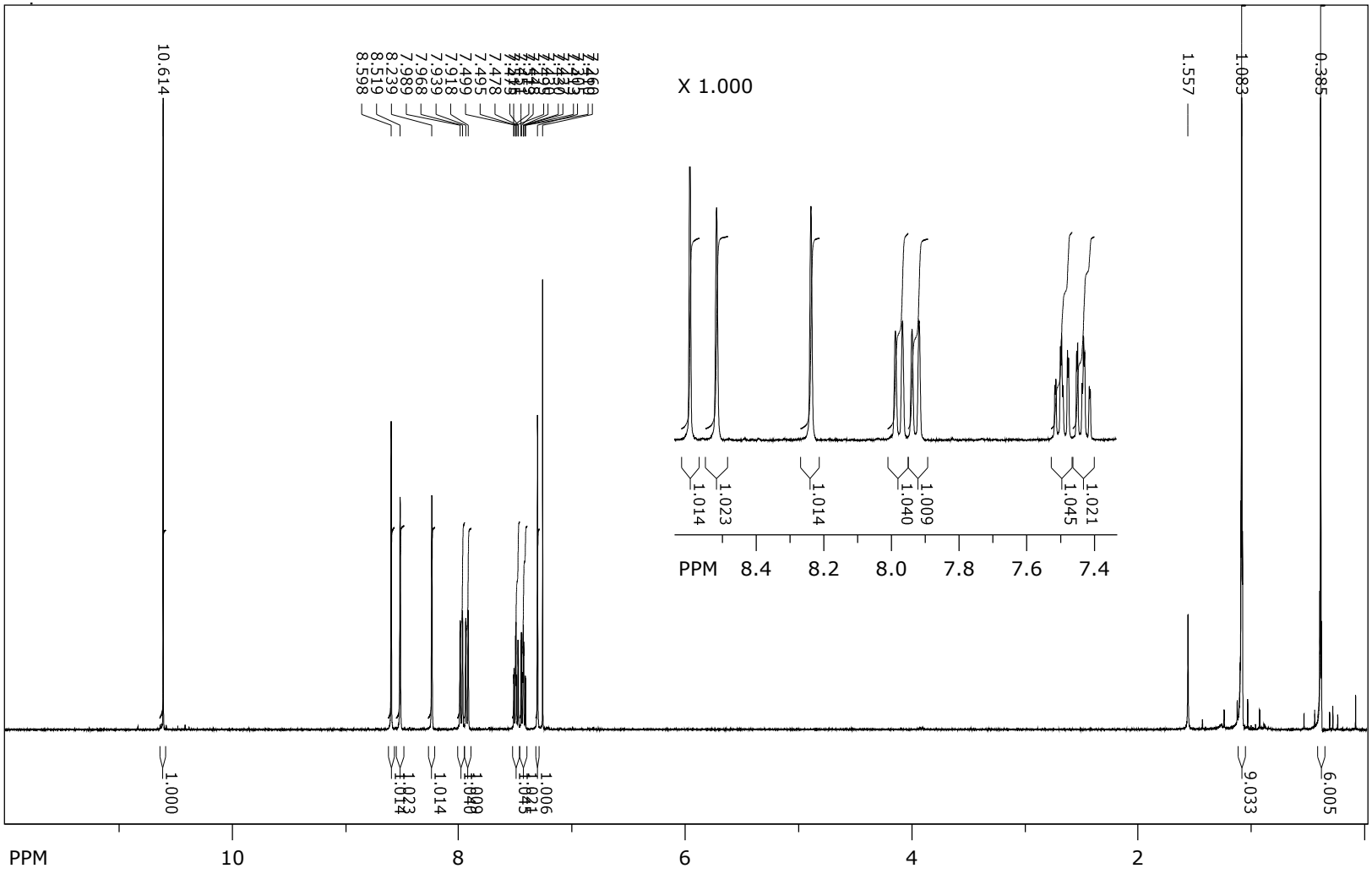

^{13}C NMR ($CDCl_3$, 100 MHz) of **8**

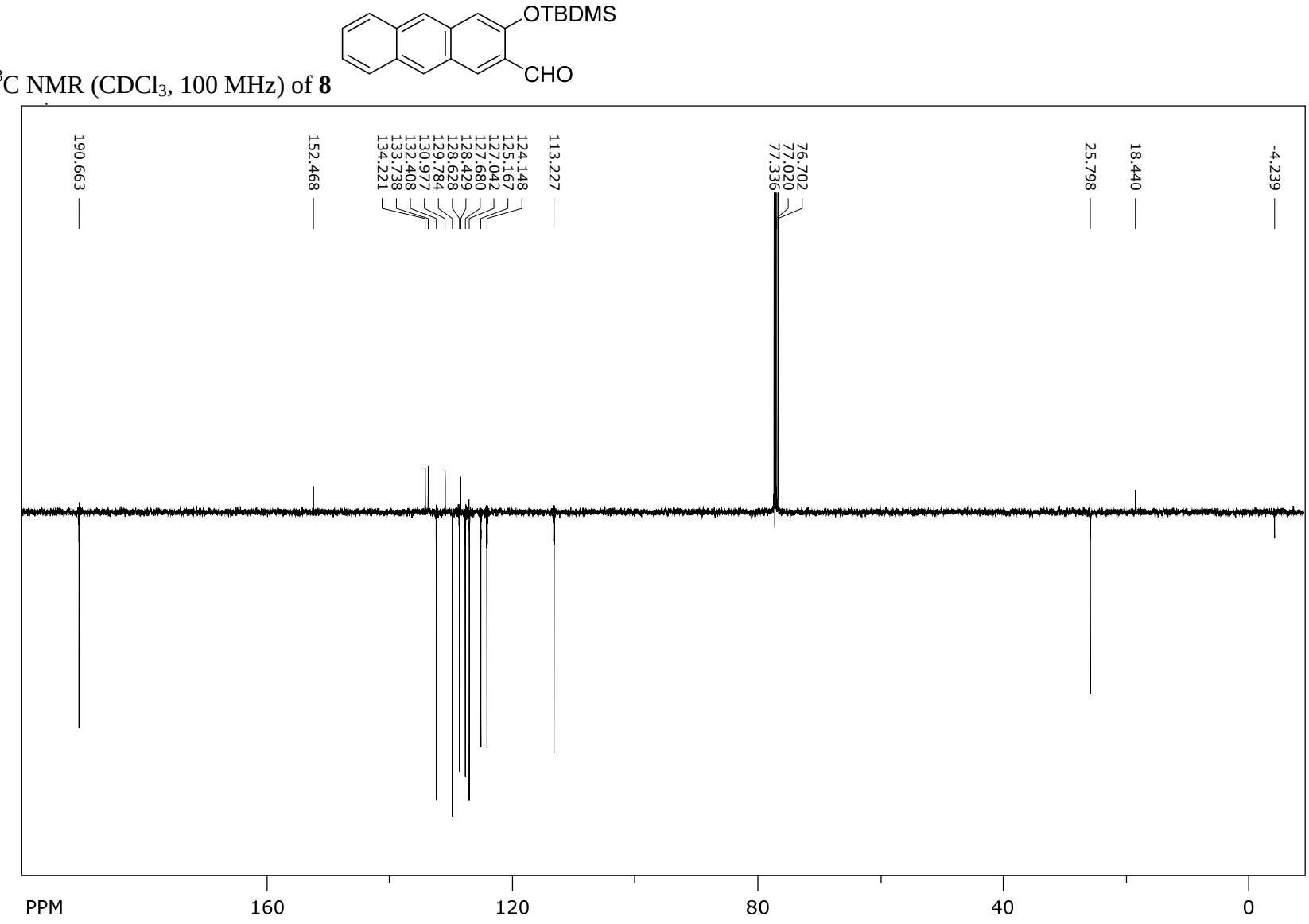

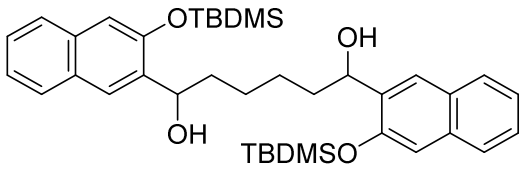

^{1}H NMR ($CDCl_3$, 400 MHz) of **7a**

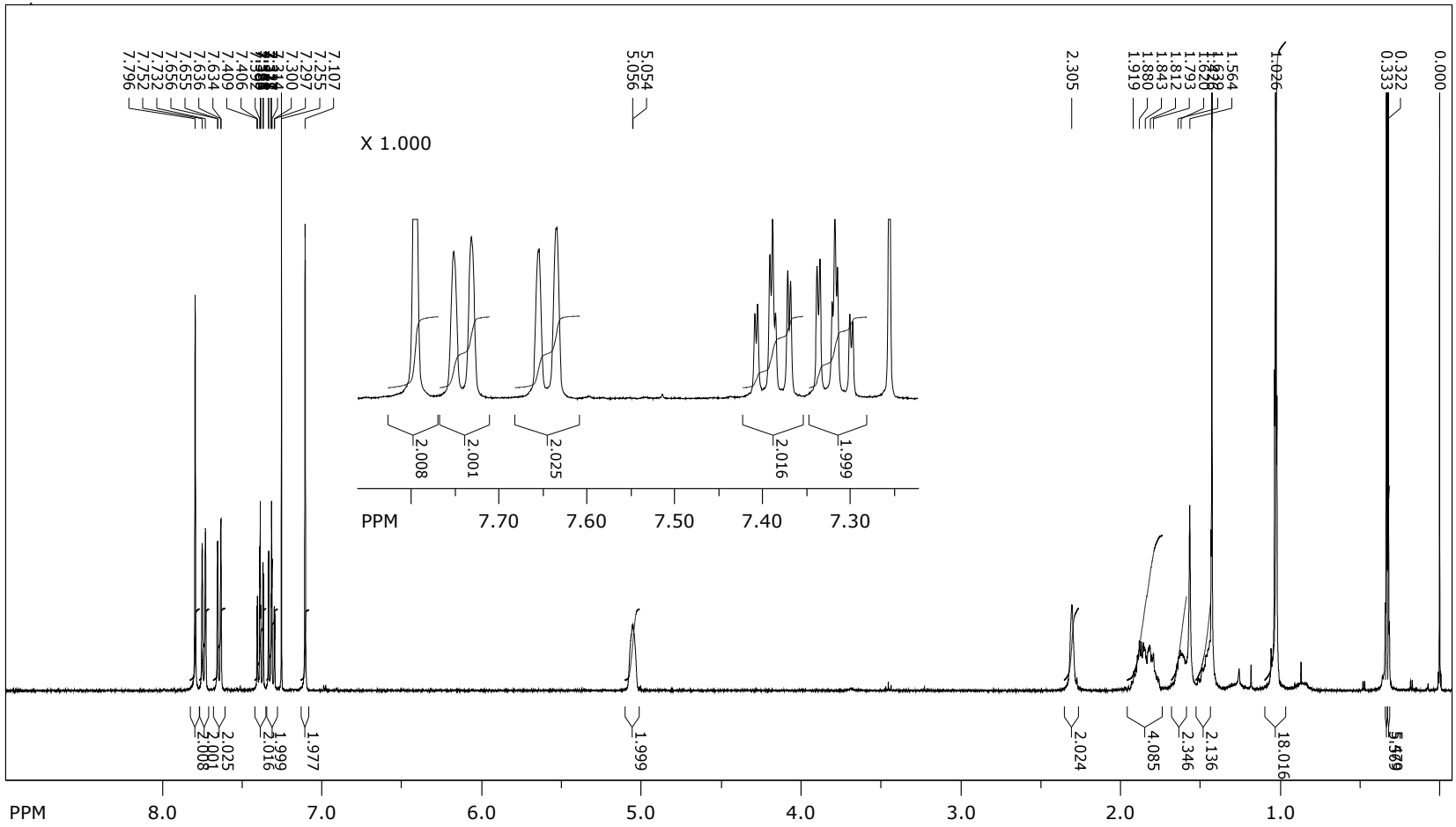

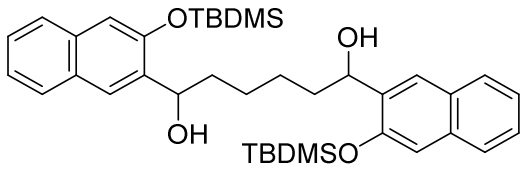

^{13}C NMR ($CDCl_3$, 100 MHz) of **7a**

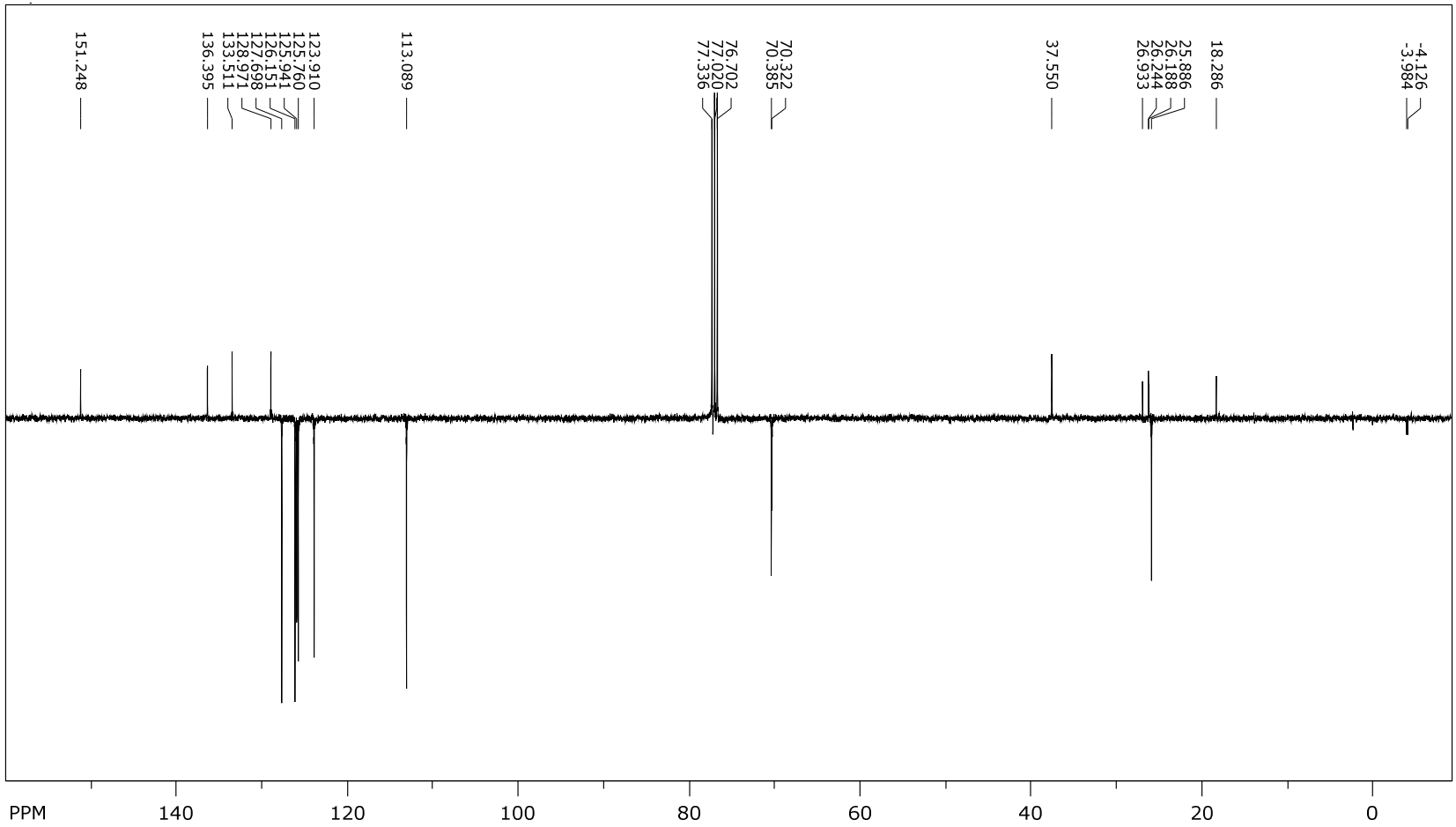

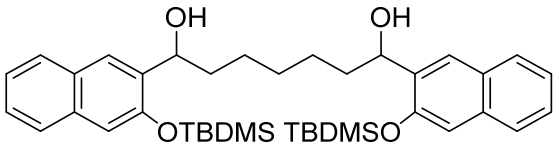

^{1}H NMR ($CDCl_3$, 400 MHz) of **7b**

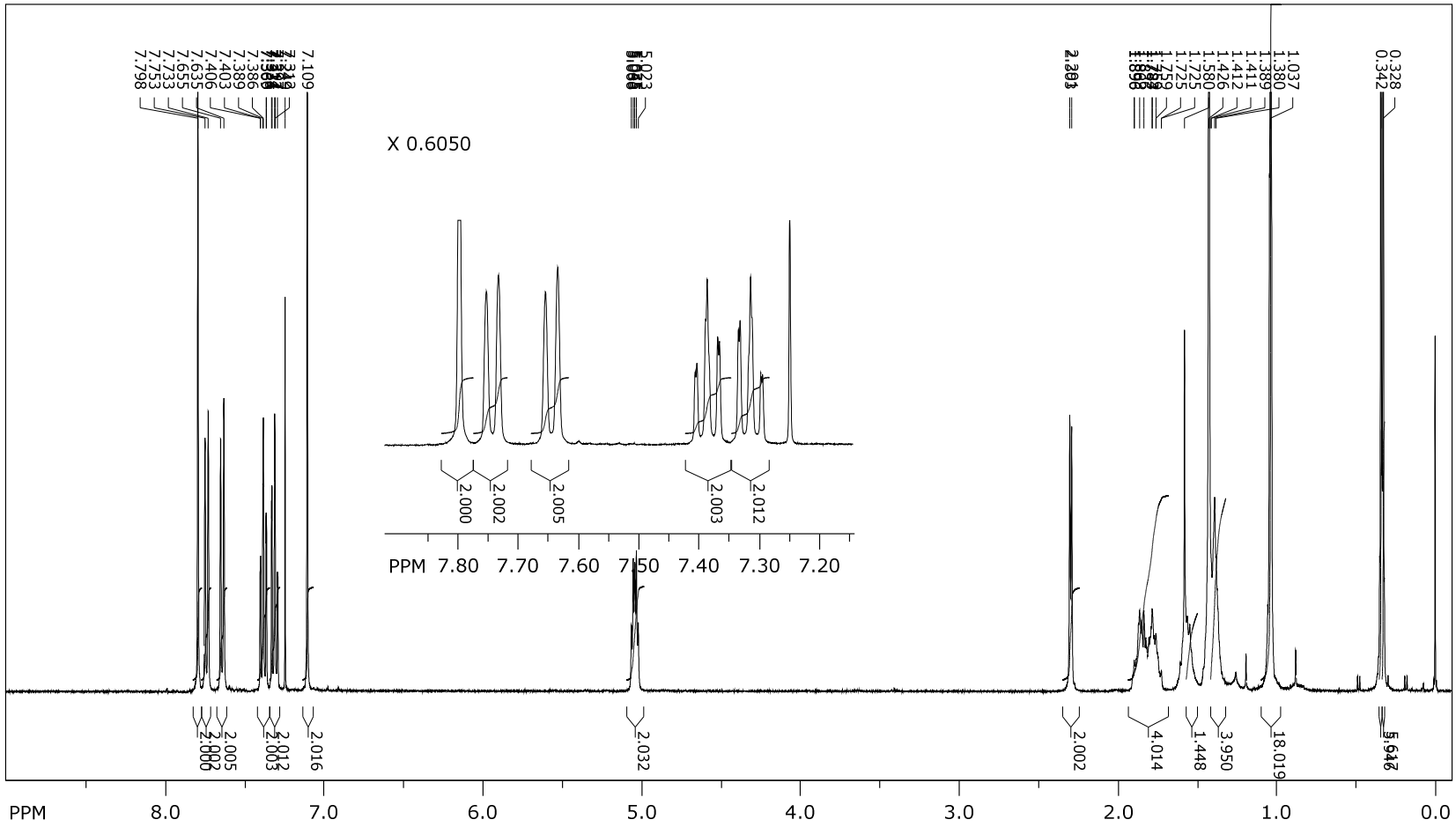

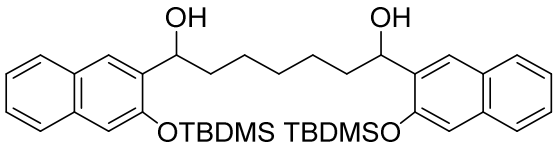

^{13}C NMR ($CDCl_3$, 100 MHz) of **7b**

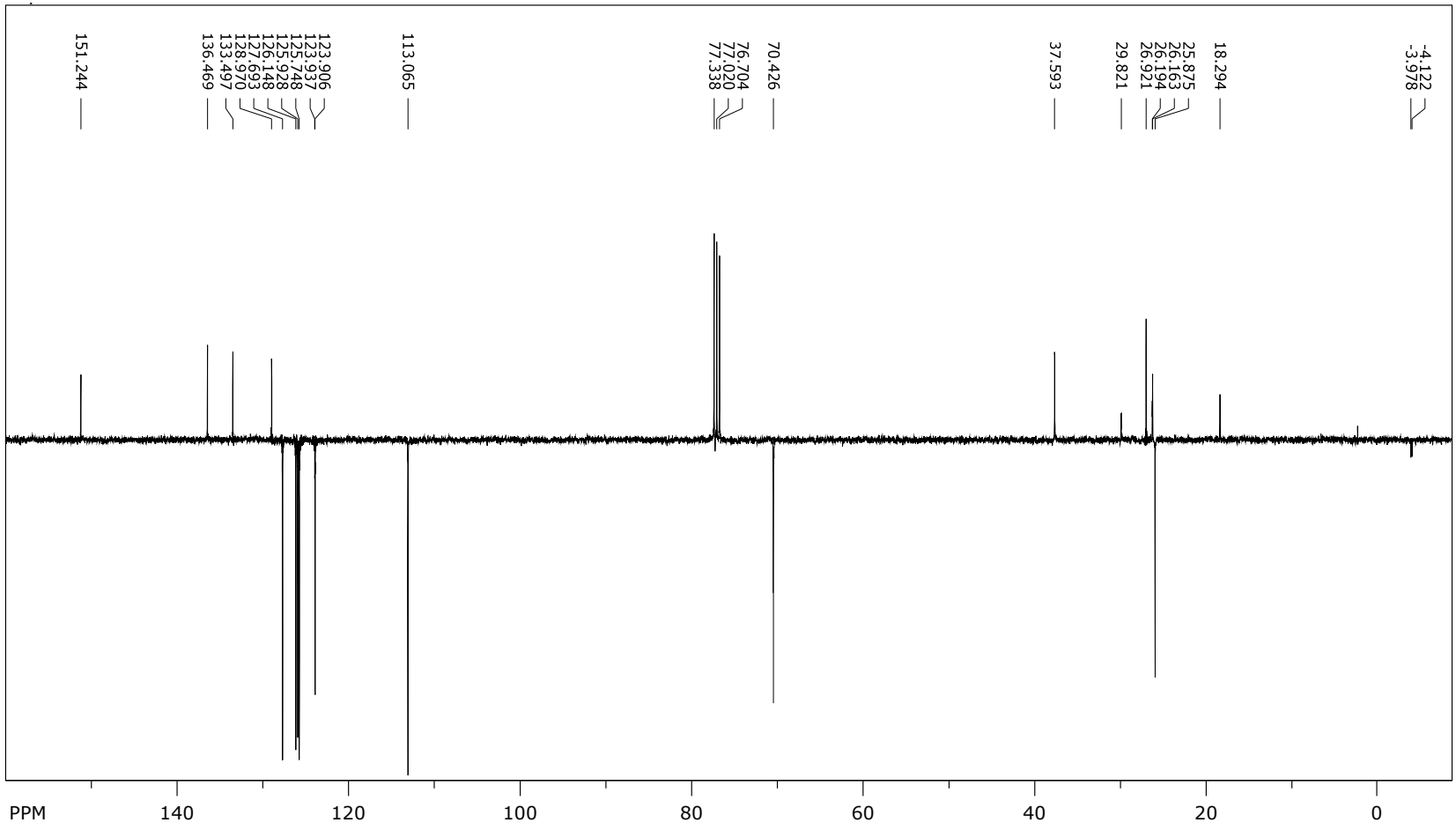

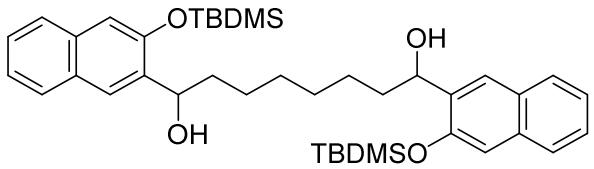

^{1}H NMR ($CDCl_3$, 400 MHz) of **7c**

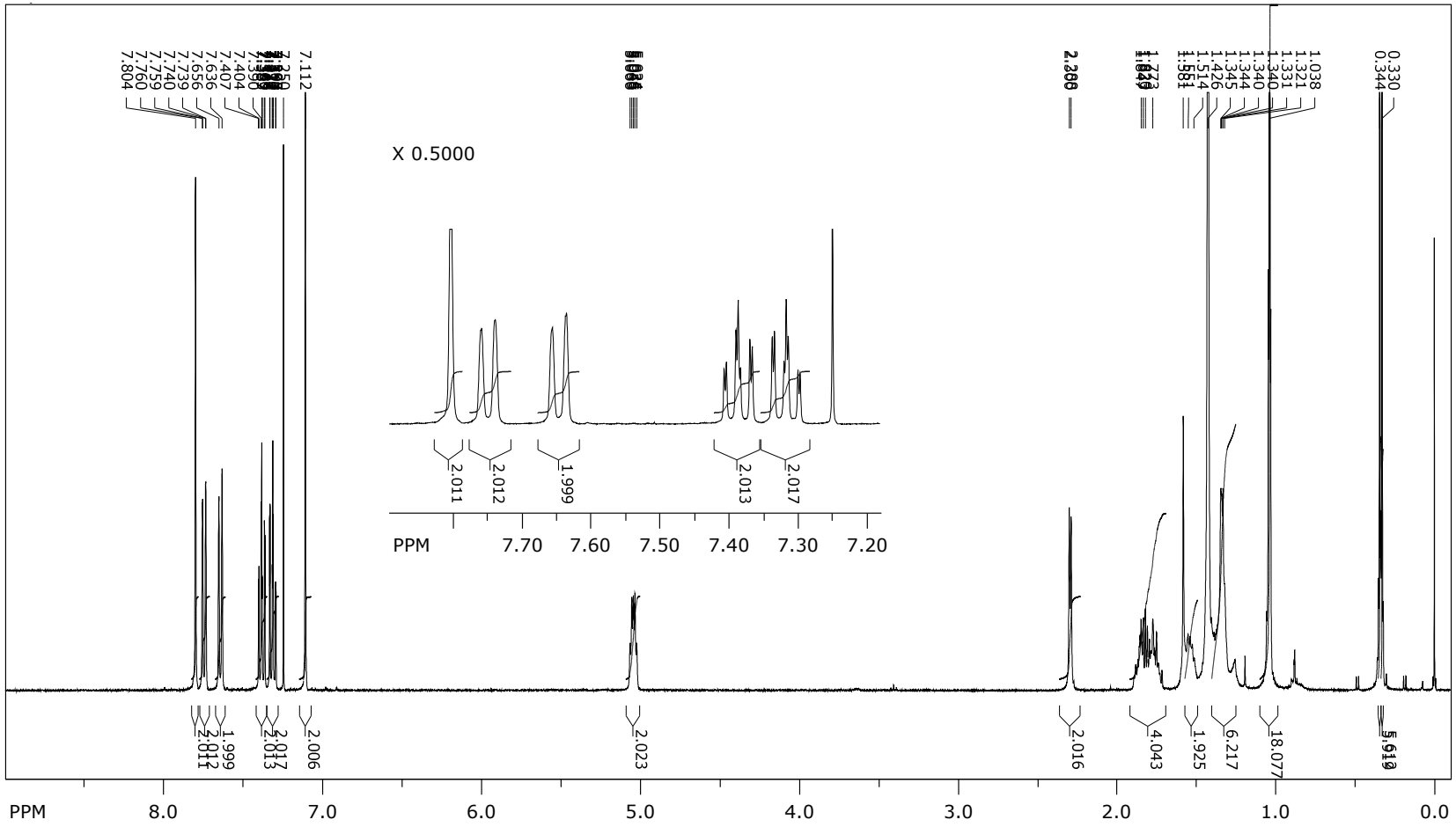

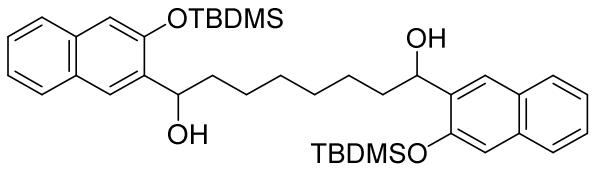

^{13}C NMR ($CDCl_3$, 100 MHz) of **7c**

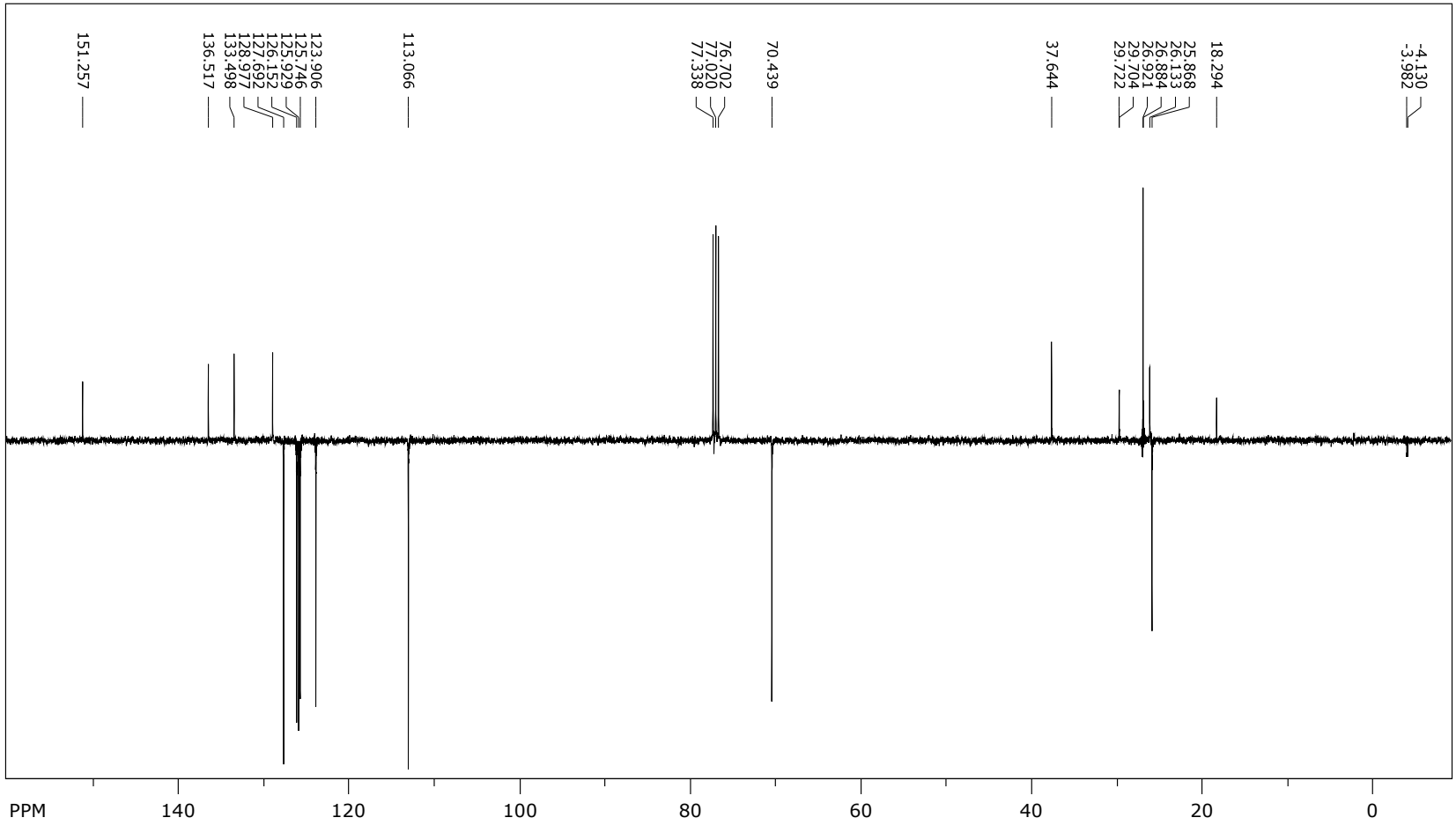

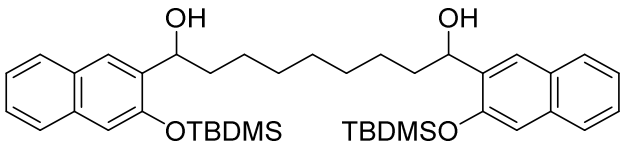

^{1}H NMR ($CDCl_3$, 400 MHz) of **7d**

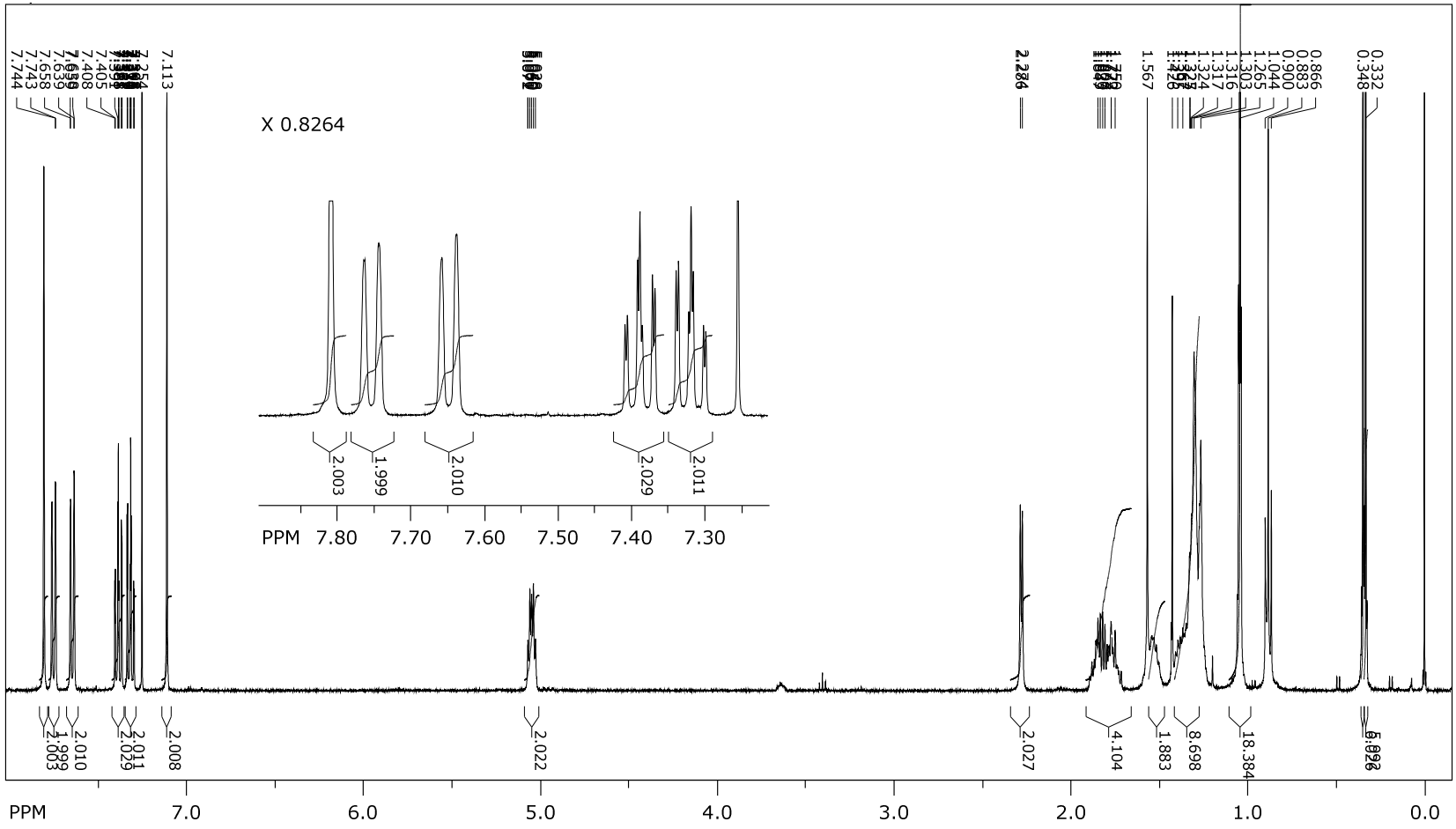

^{13}C NMR ($CDCl_3$, 100 MHz) of **7d**

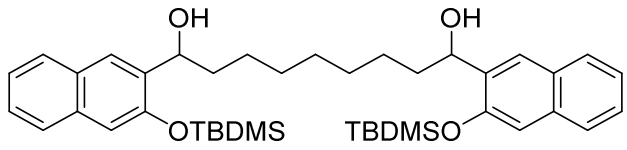

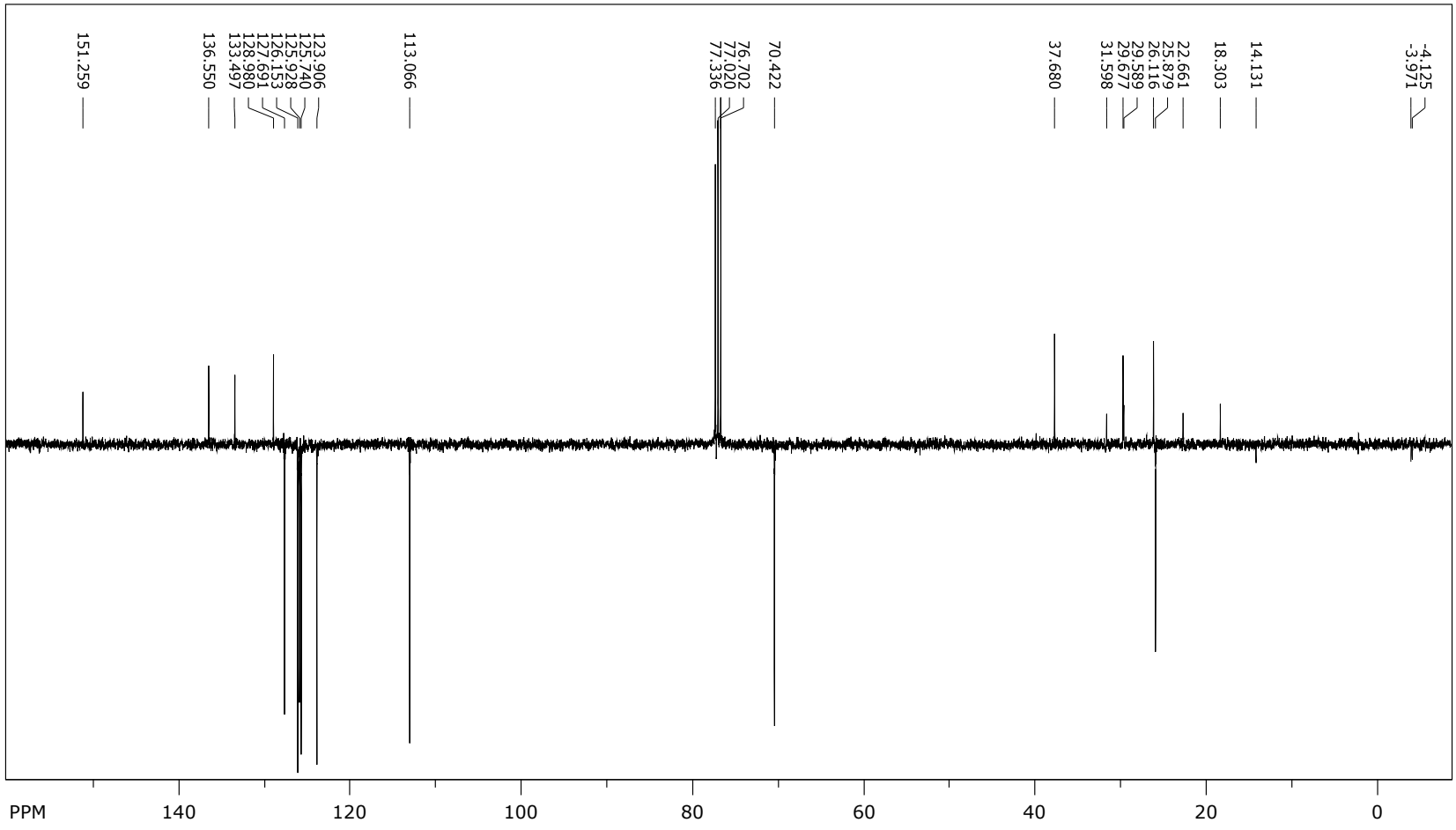

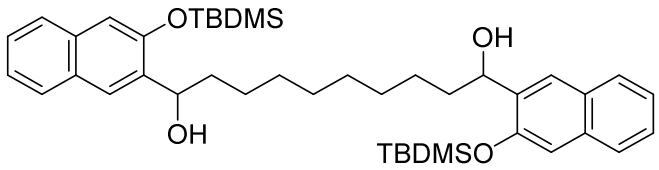

^{1}H NMR ($CDCl_3$, 400 MHz) of **7e**

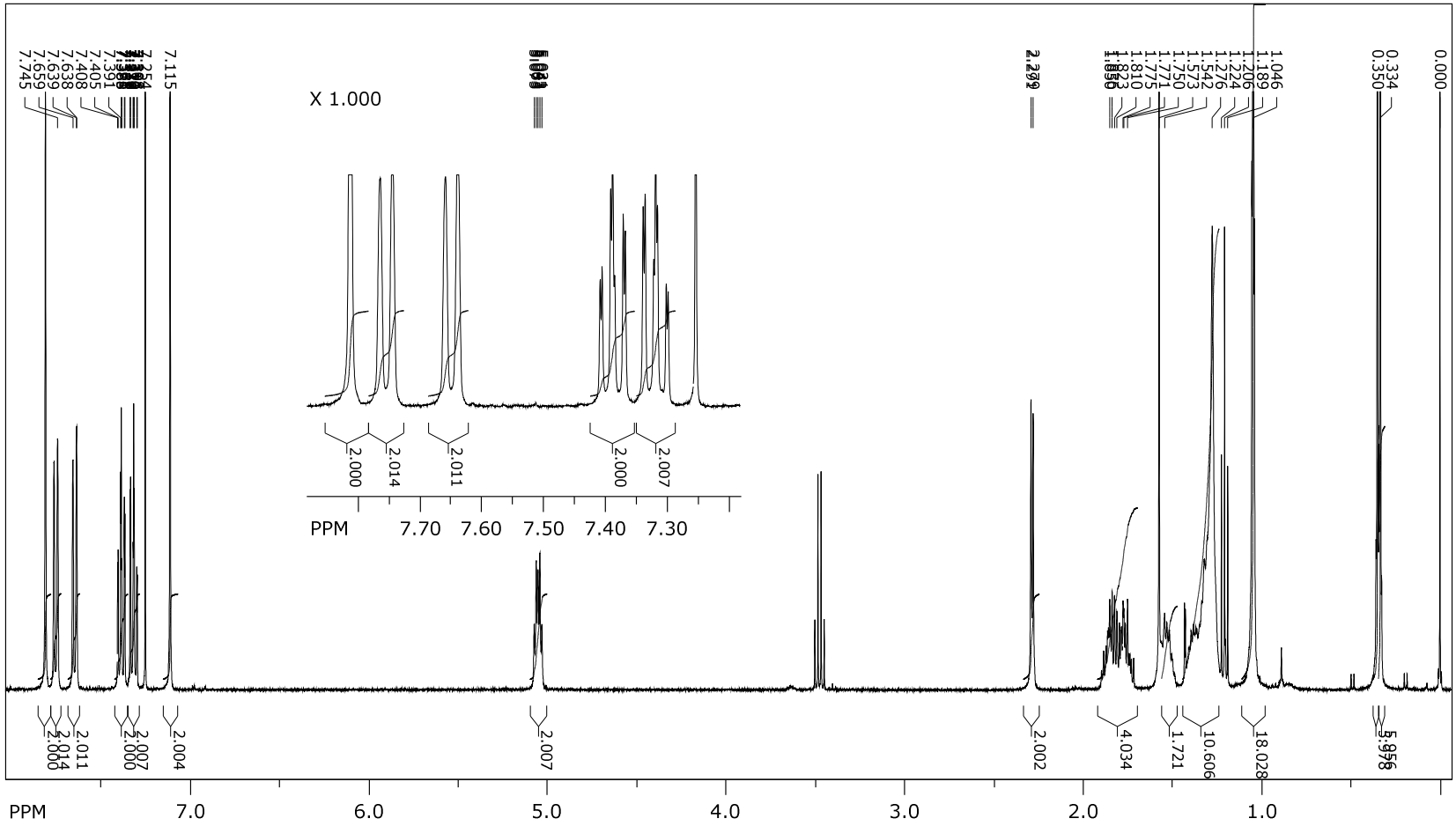

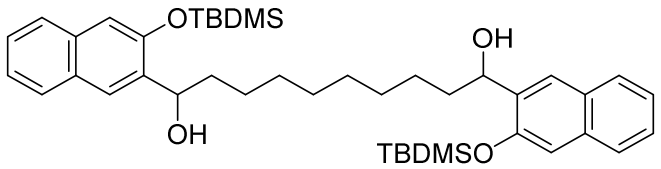

^{13}C NMR ($CDCl_3$, 100 MHz) of **7e**

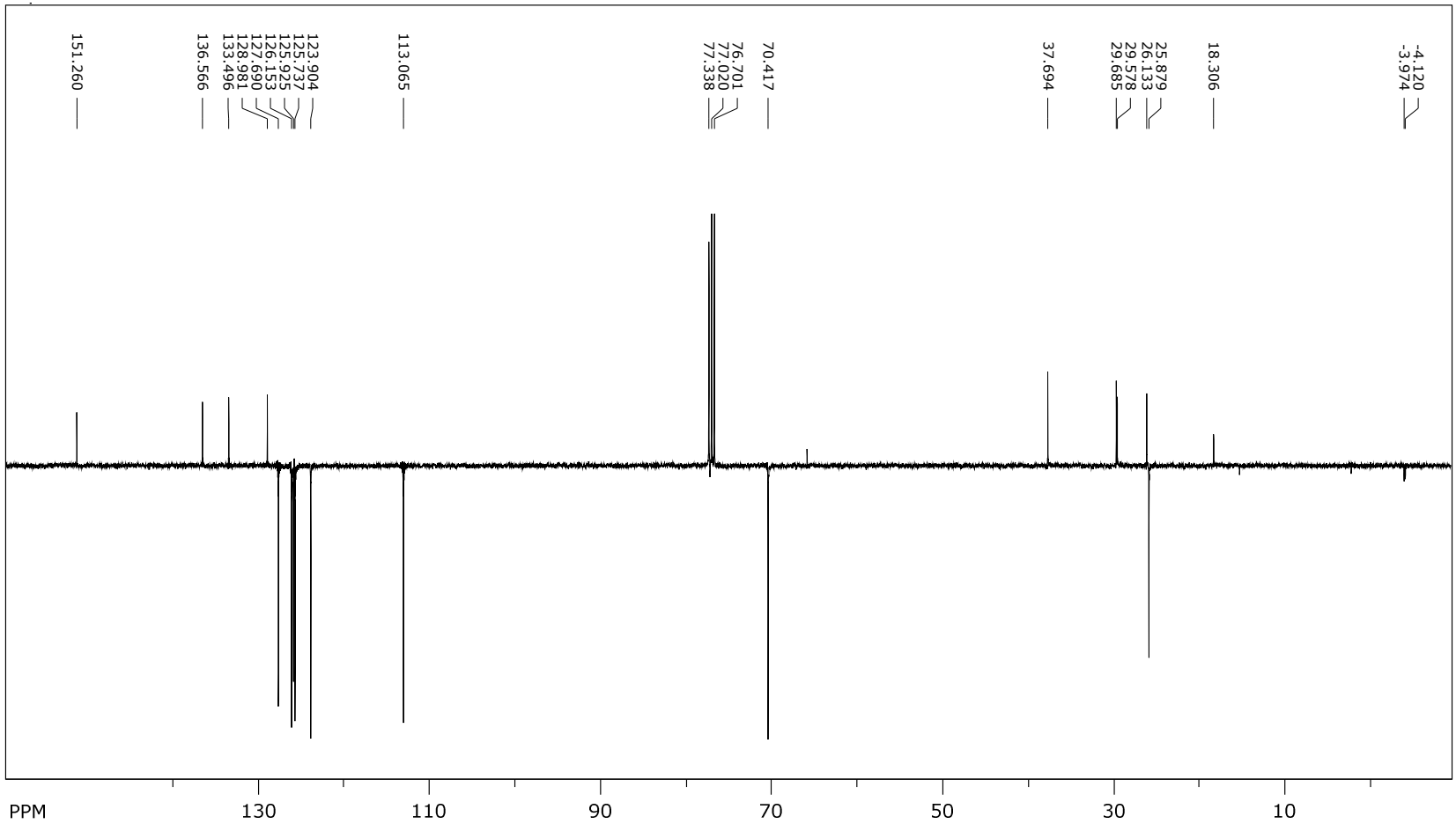

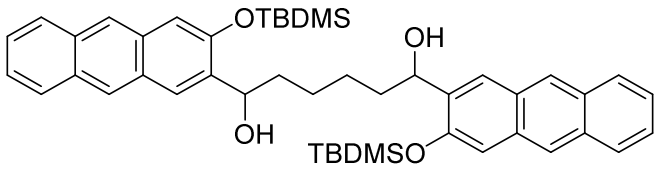

^{1}H NMR ($CDCl_3$, 500 MHz) of **9a**

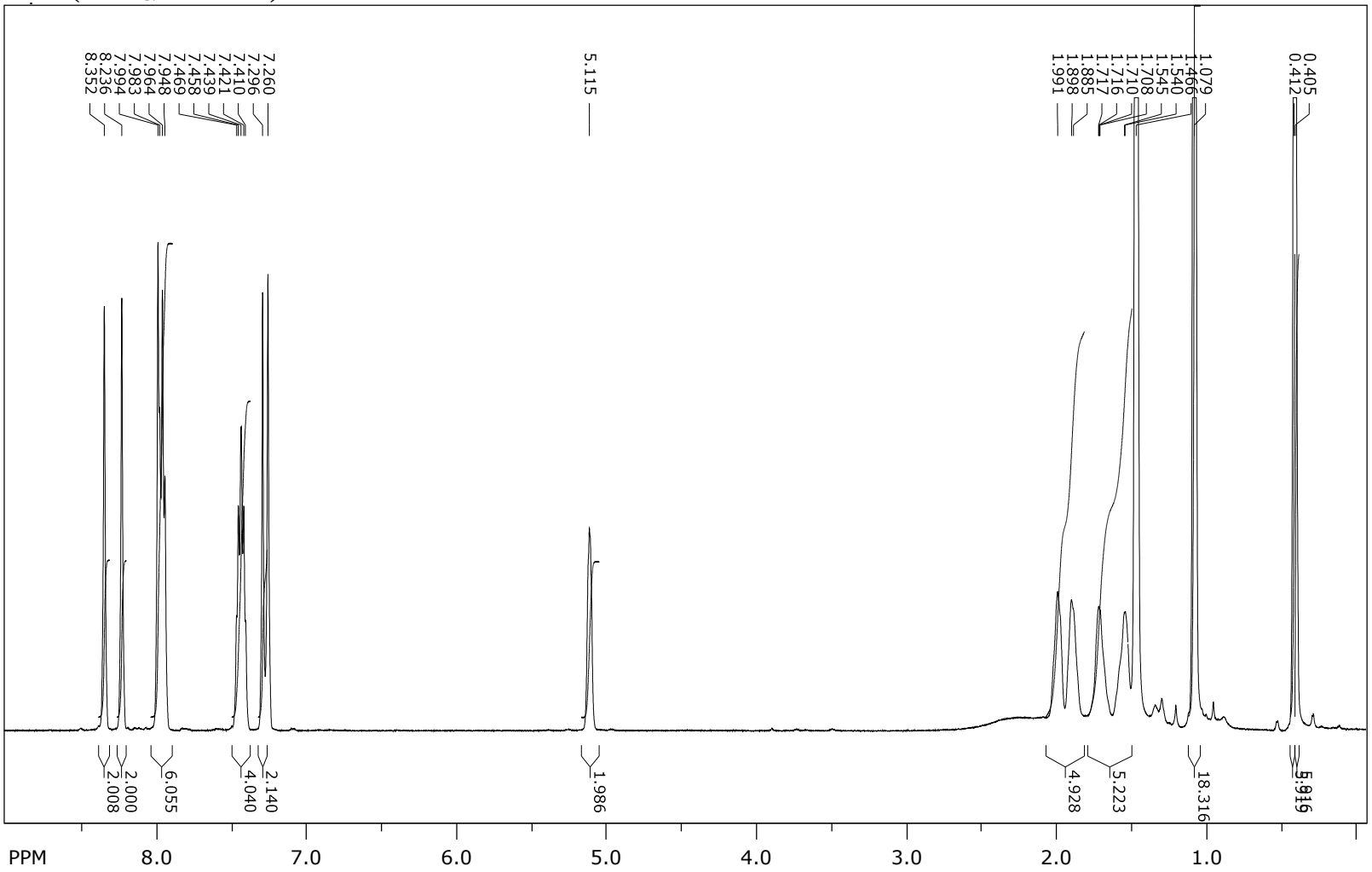

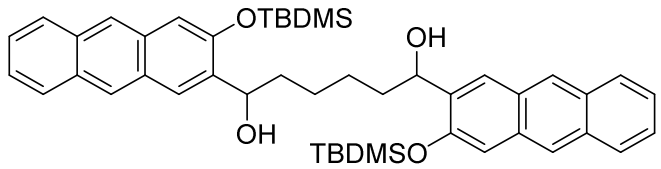

^{13}C NMR ($CDCl_3$, 125 MHz) of **9a**

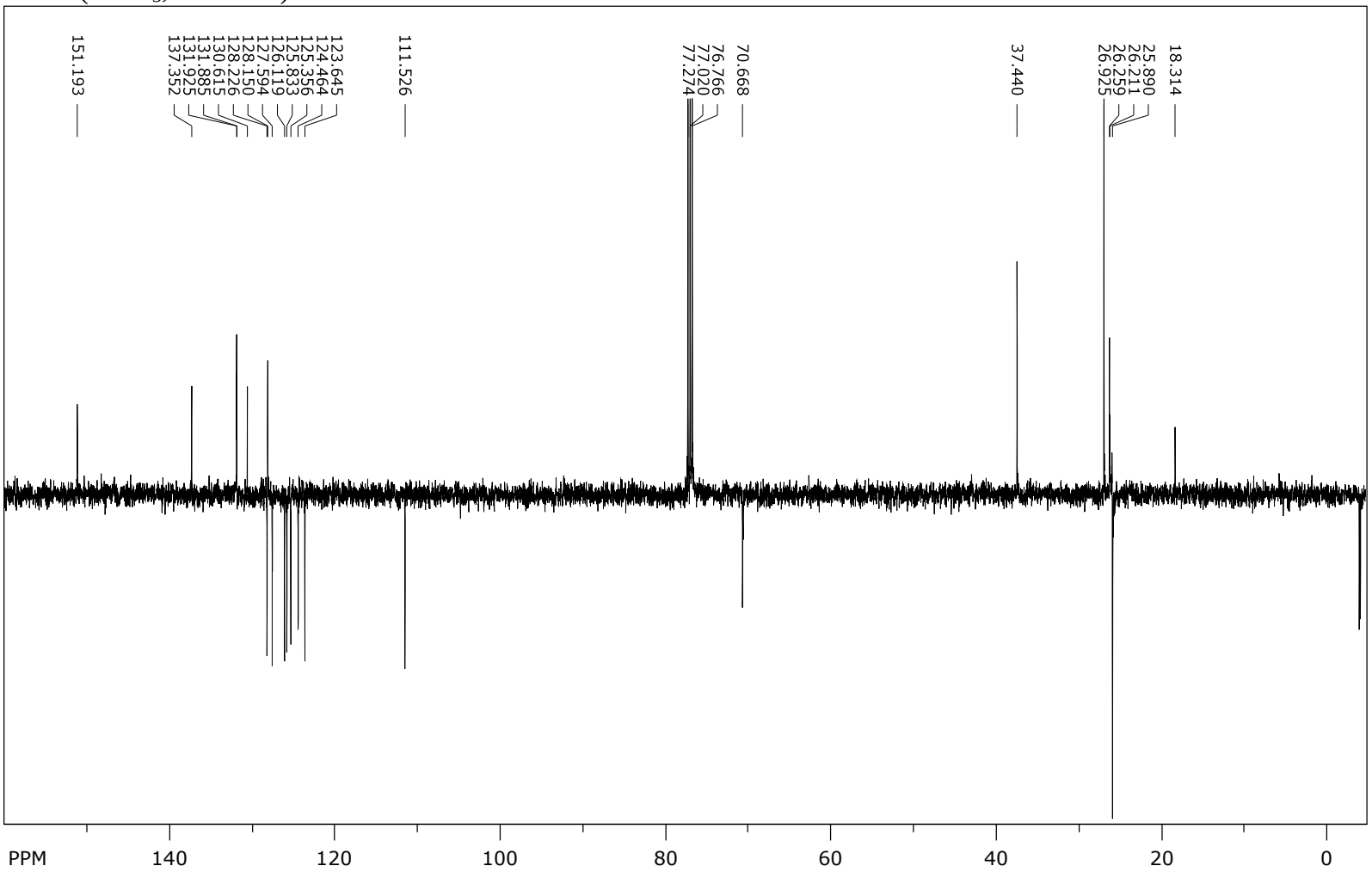

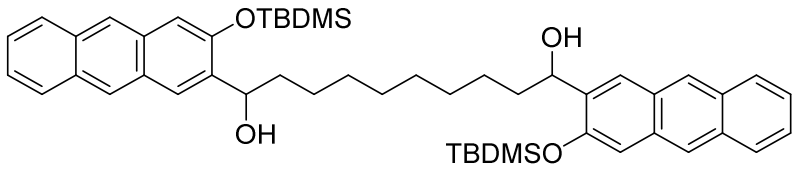

^{1}H NMR ($CDCl_3$, 500 MHz) of **9e**

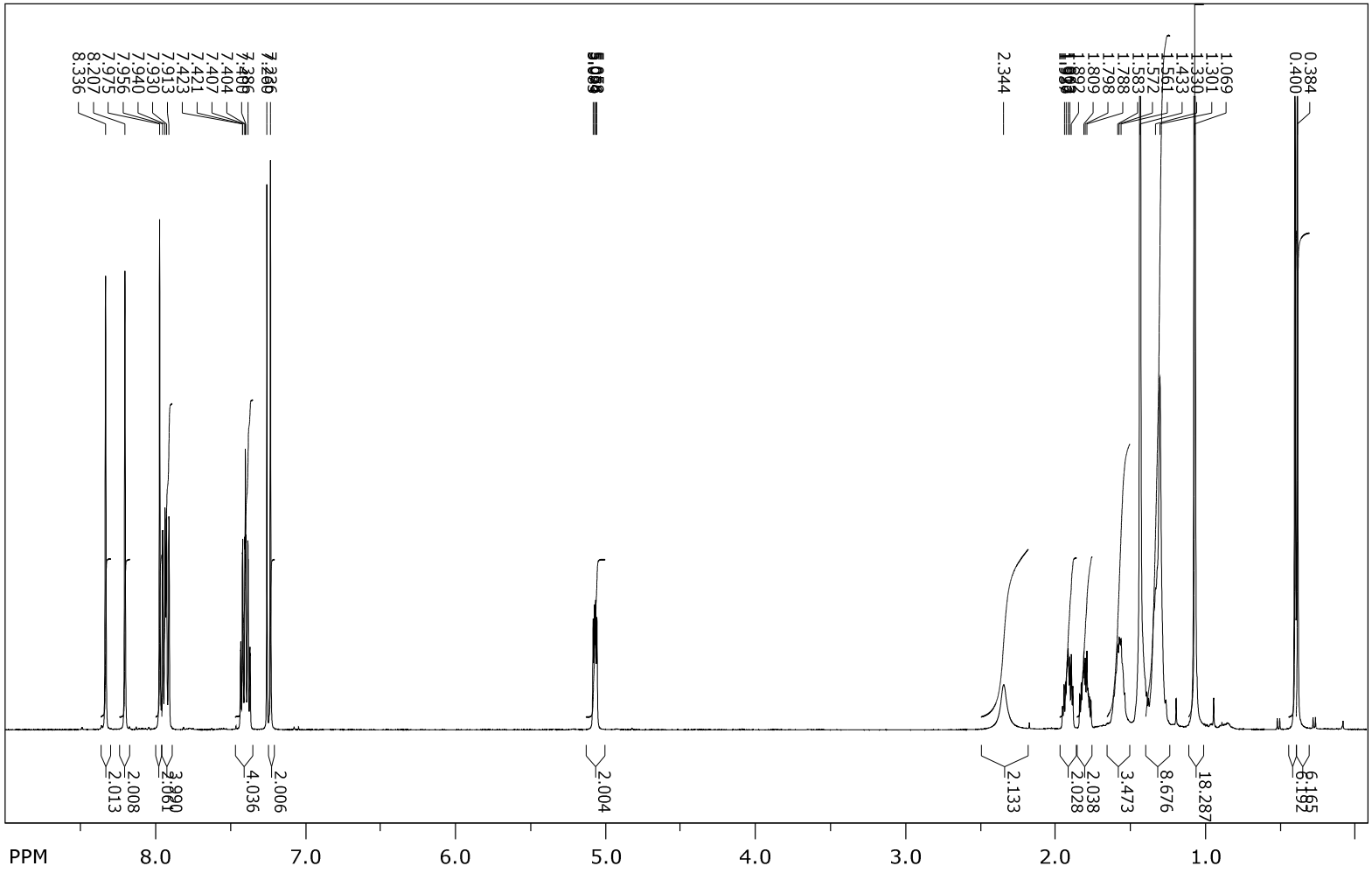

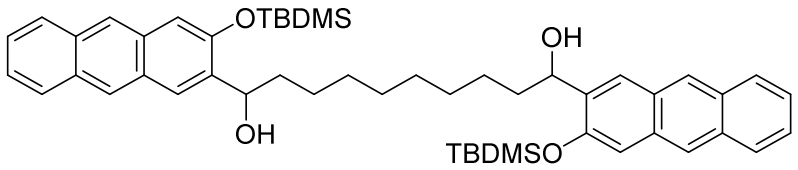

^{13}C NMR ($CDCl_3$, 125 MHz) of **9e**

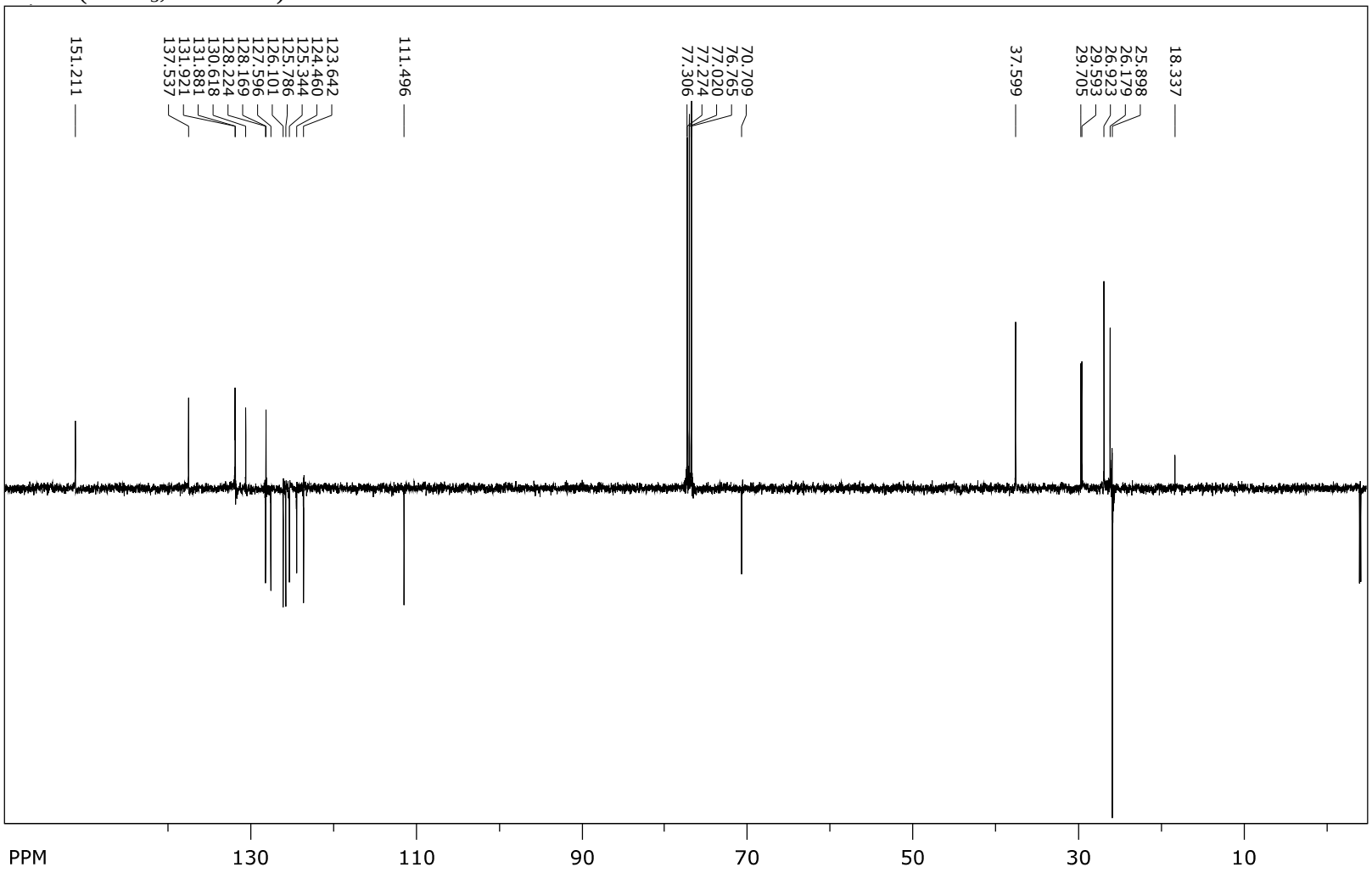

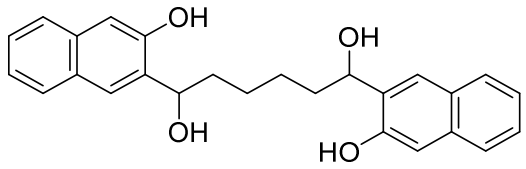

^{1}H NMR (DMSO-d_6, 500 MHz) of **4a**

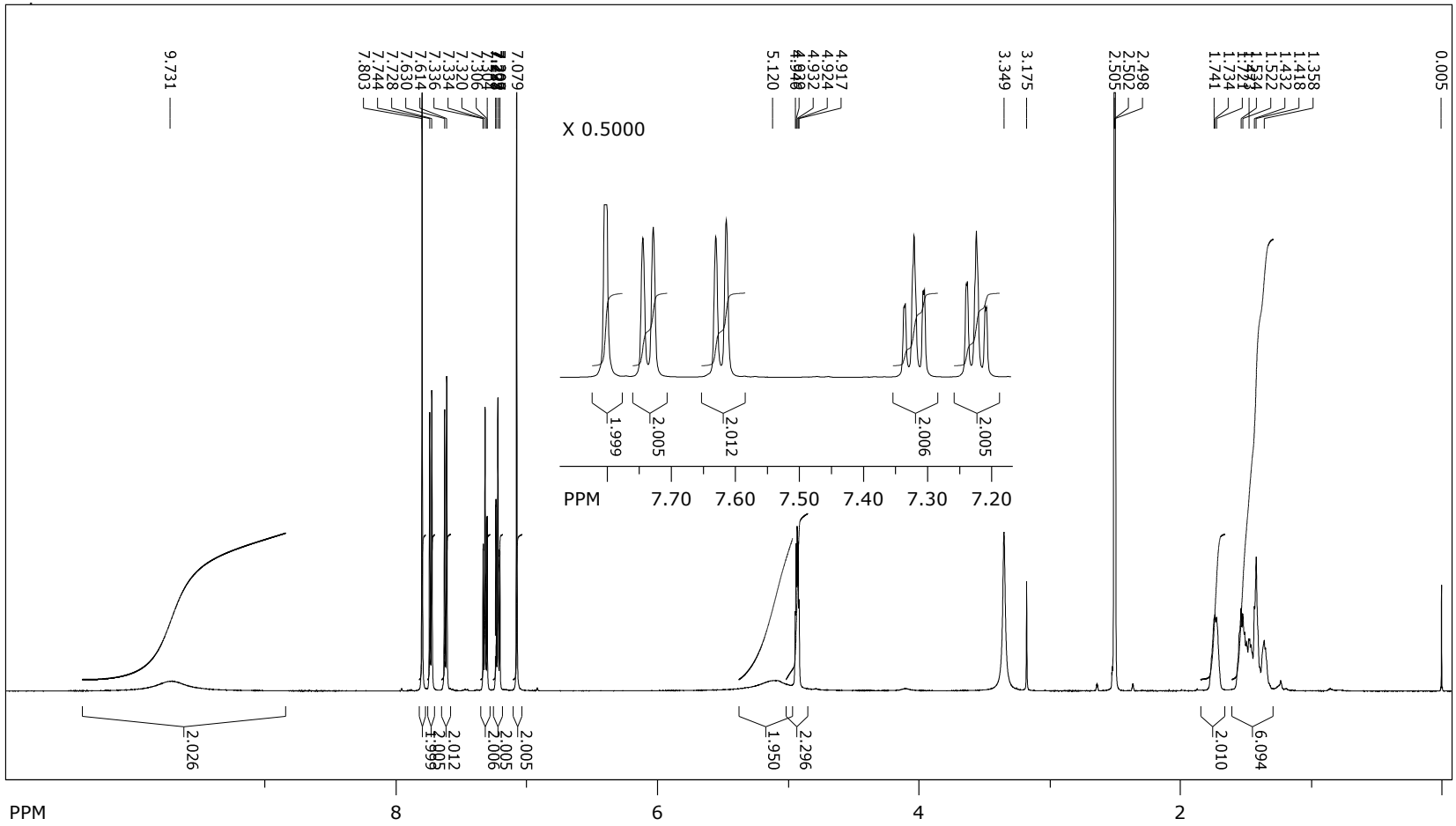

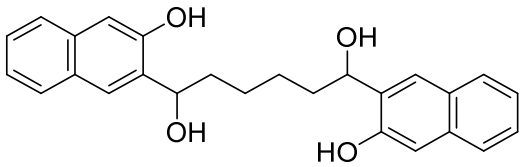

^{13}C NMR (DMSO-d_6, 125 MHz) of **4a**

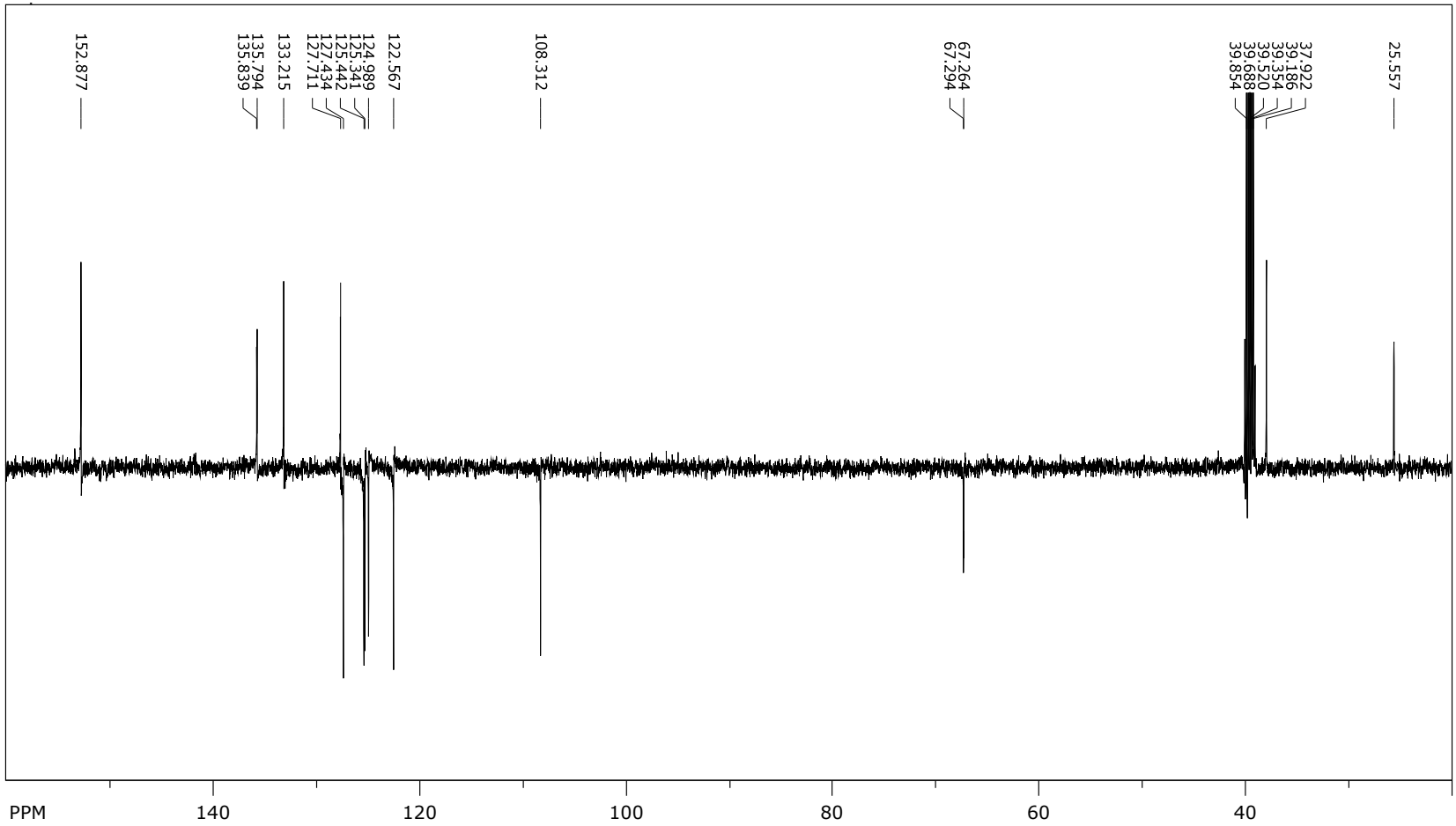

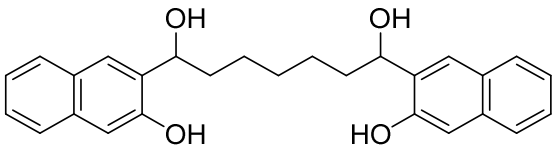

^{1}H NMR (DMSO-d_6, 400 MHz) of **4b**

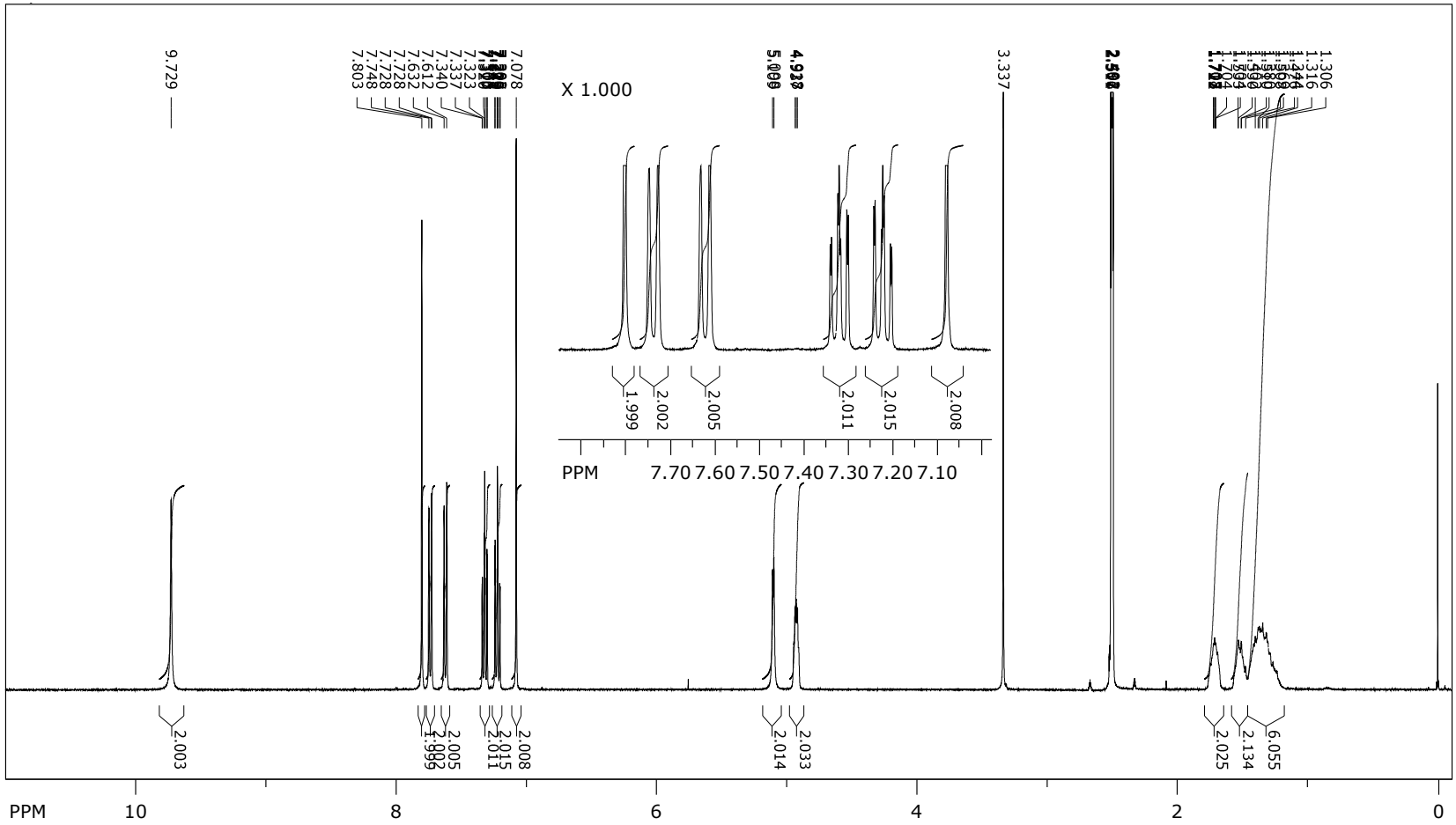

^{13}C NMR (DMSO-d_6, 100 MHz) of **4b**

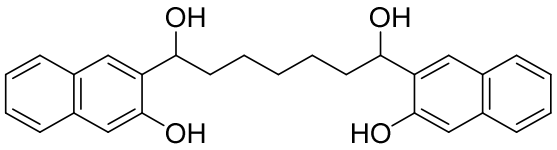

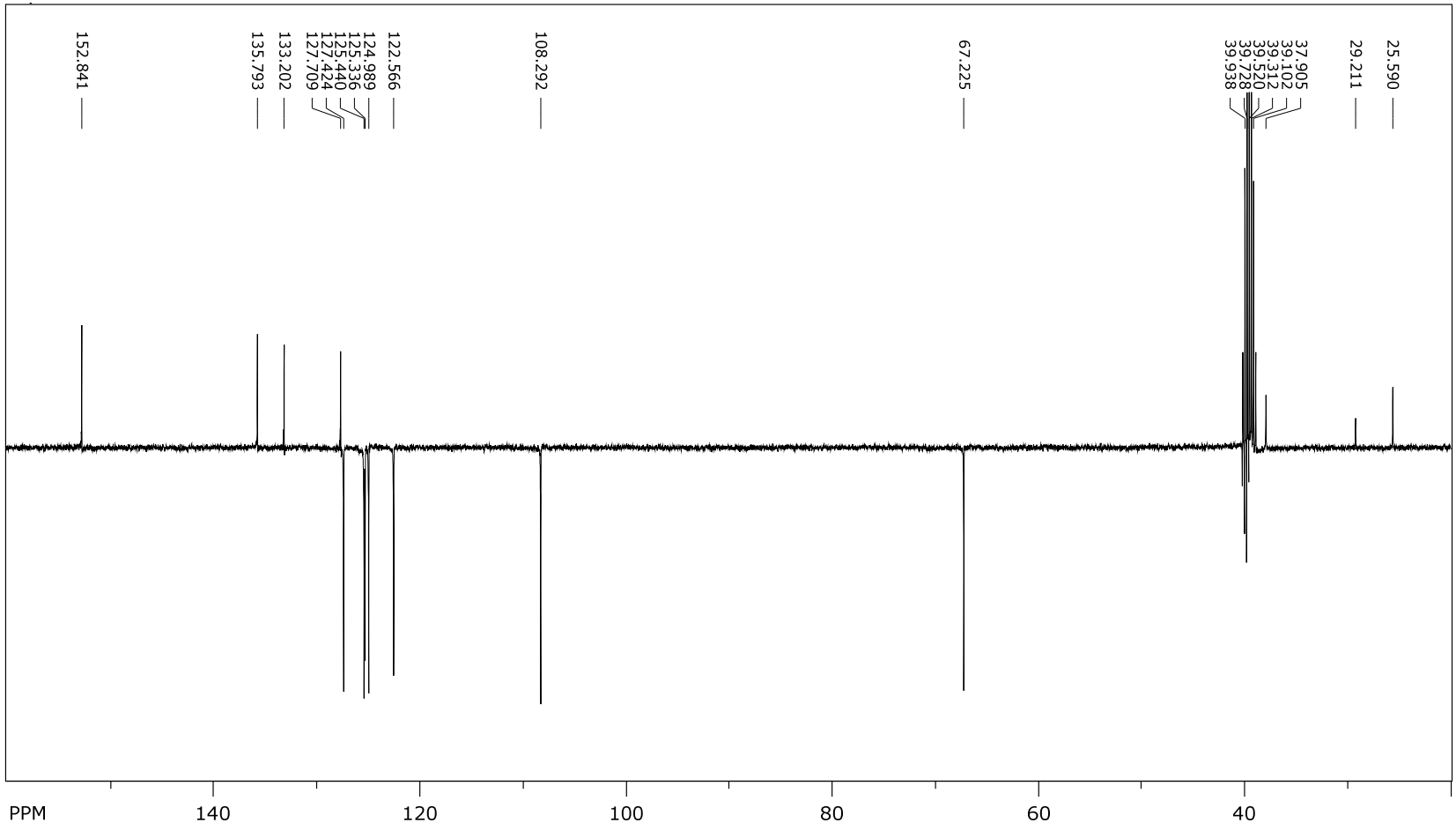

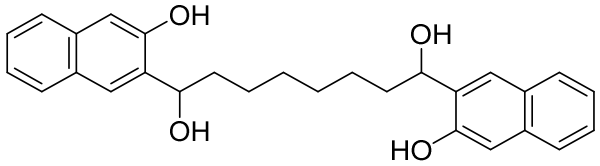

^{1}H NMR (DMSO-d_6, 400 MHz) of **4c**

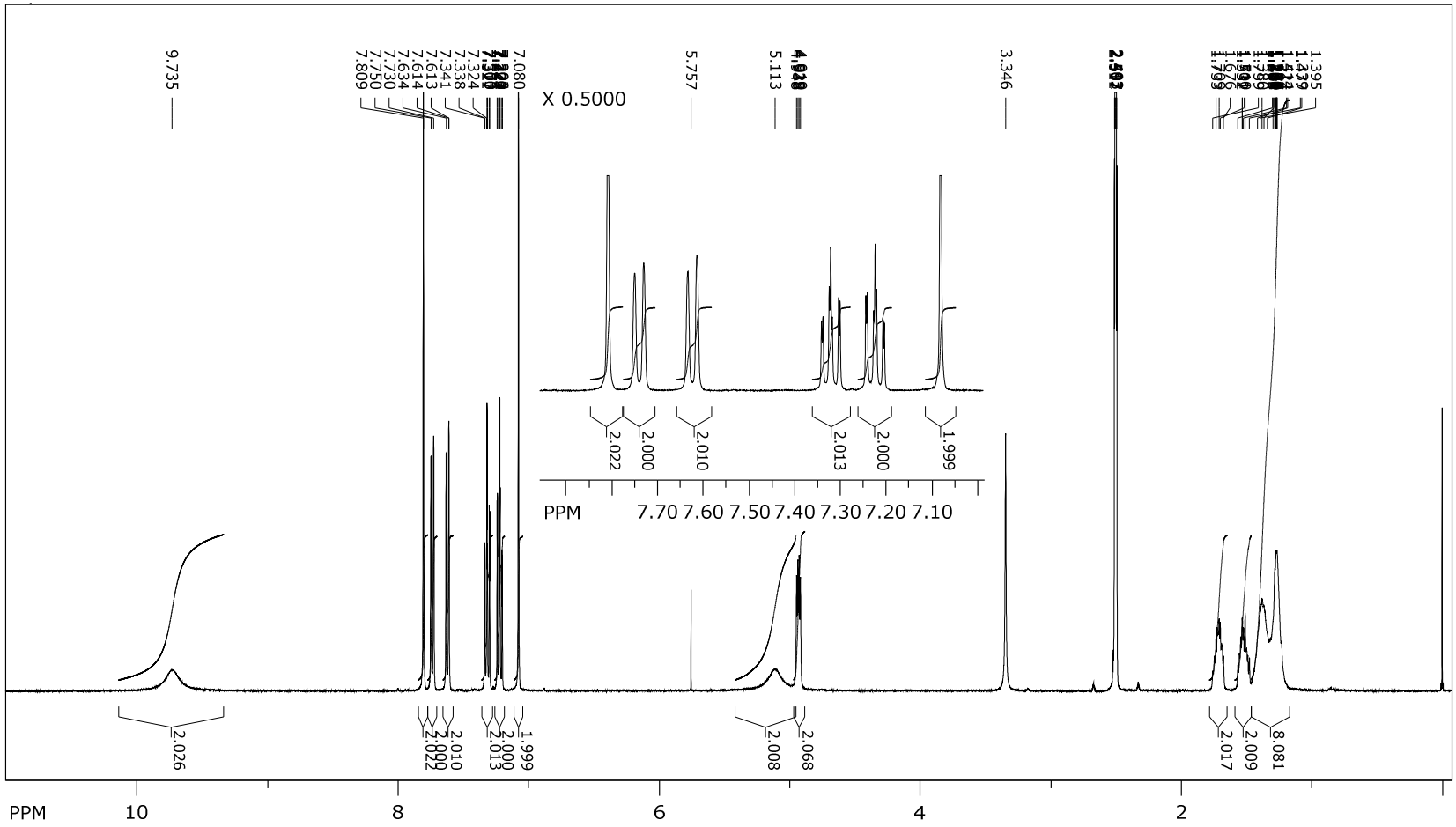

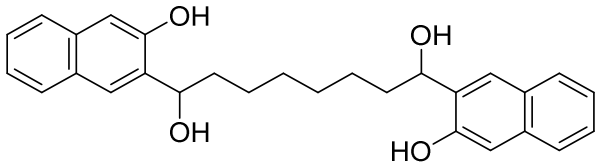

^{13}C NMR (DMSO-d_6, 100 MHz) of **4c**

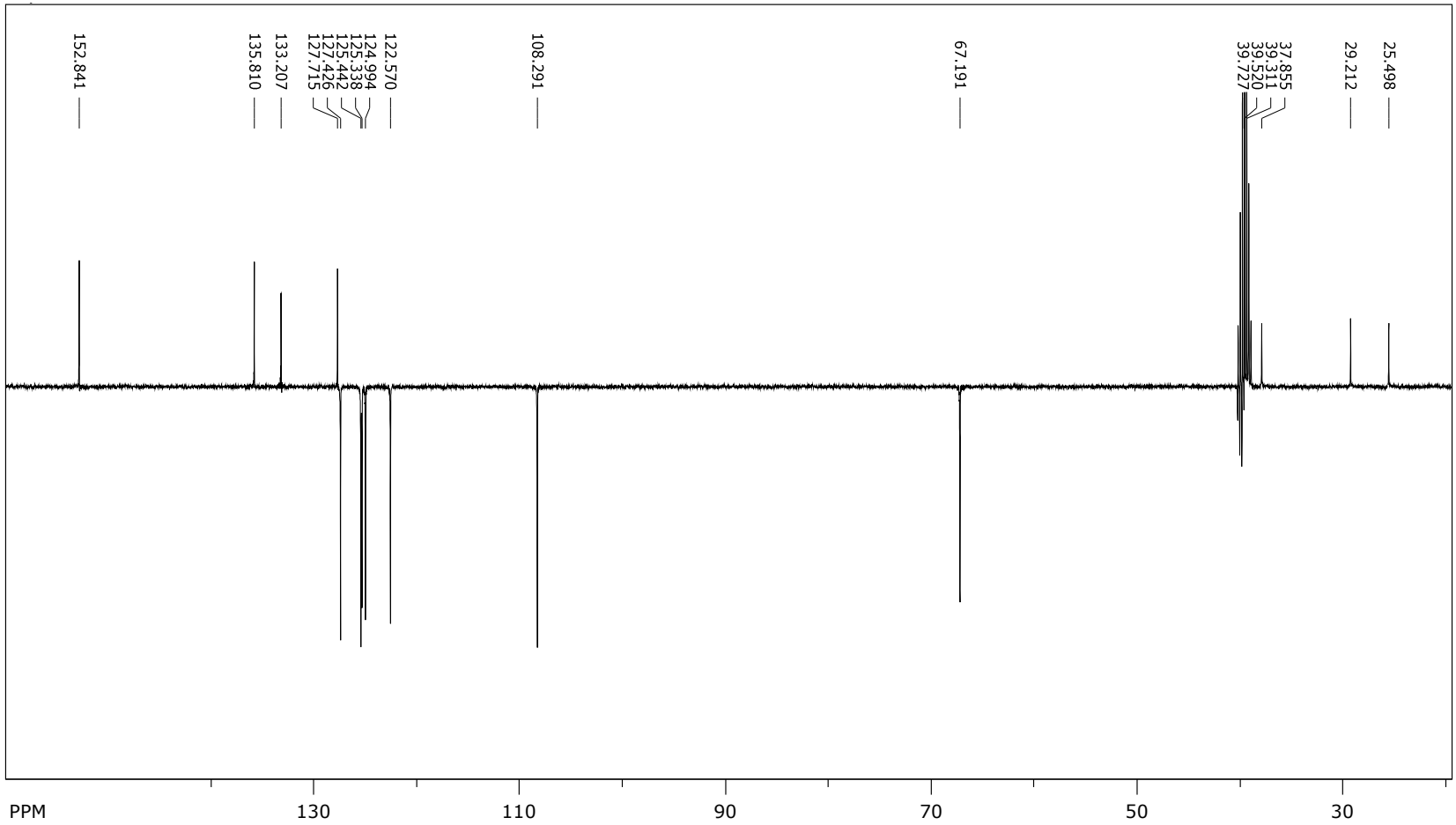

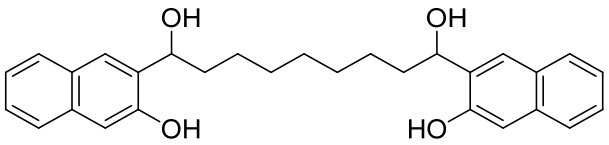

^{1}H NMR (DMSO-d_6, 400 MHz) of **4d**

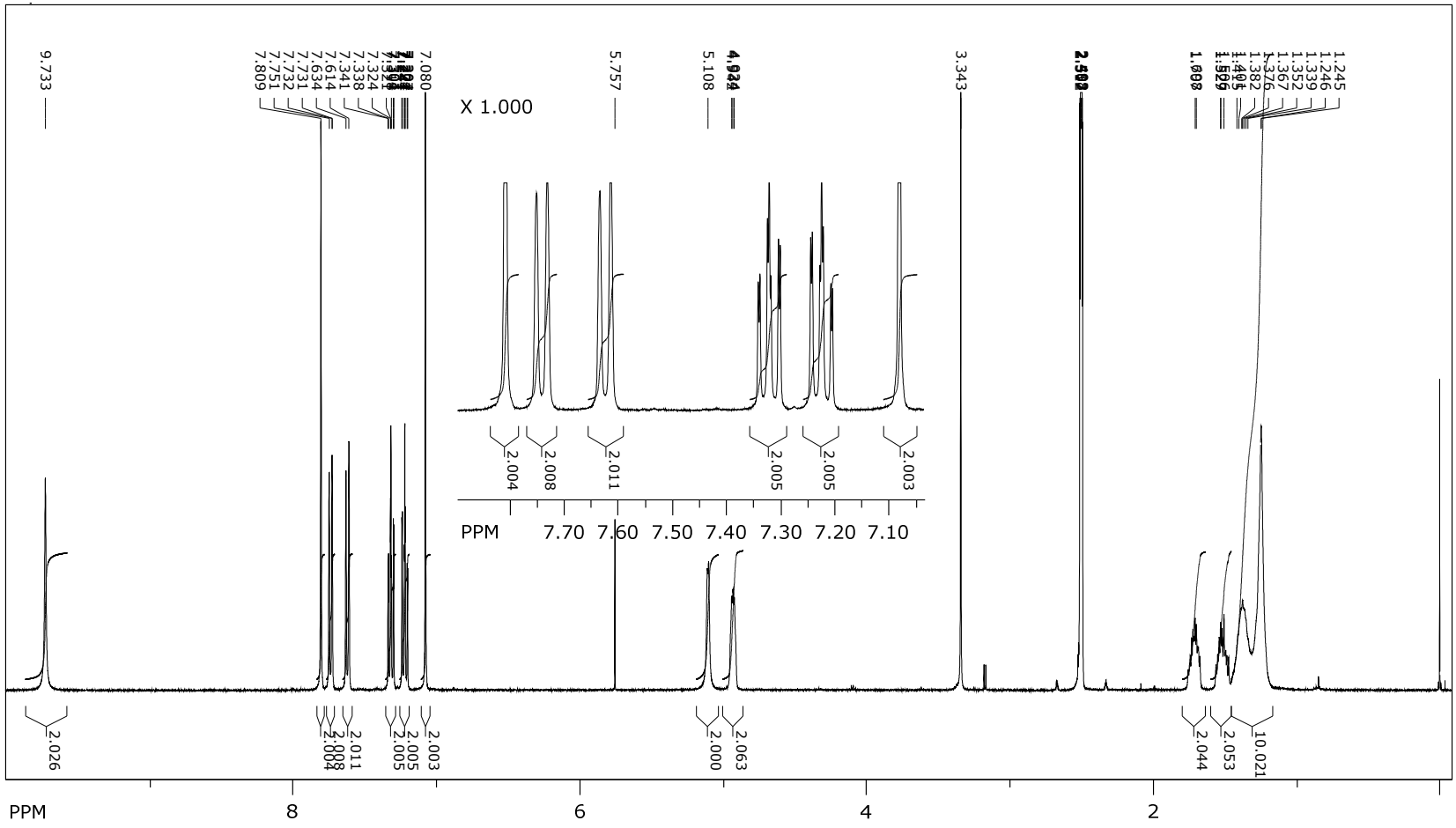

^{13}C NMR (DMSO-d_6, 100 MHz) of **4d**

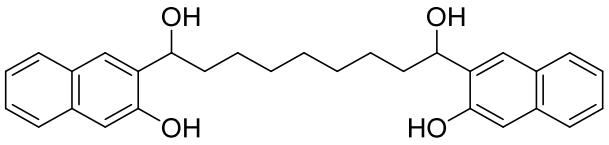

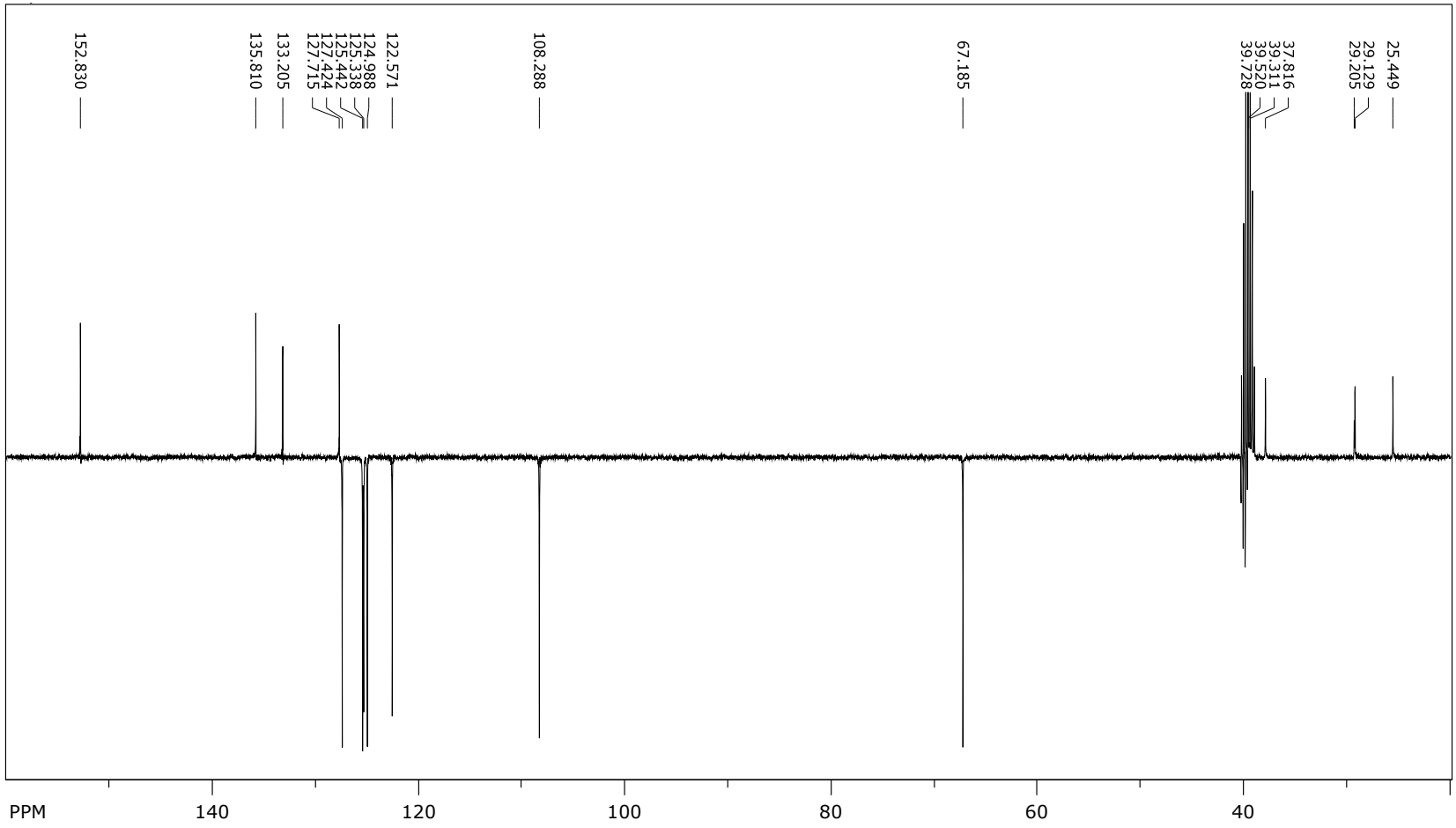

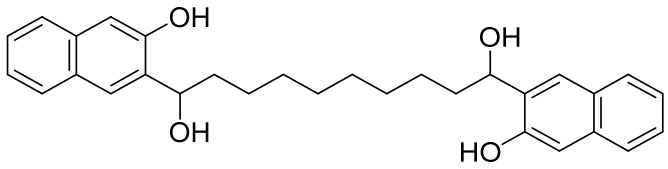

^{1}H NMR (DMSO-d_6, 400 MHz) of **4e**

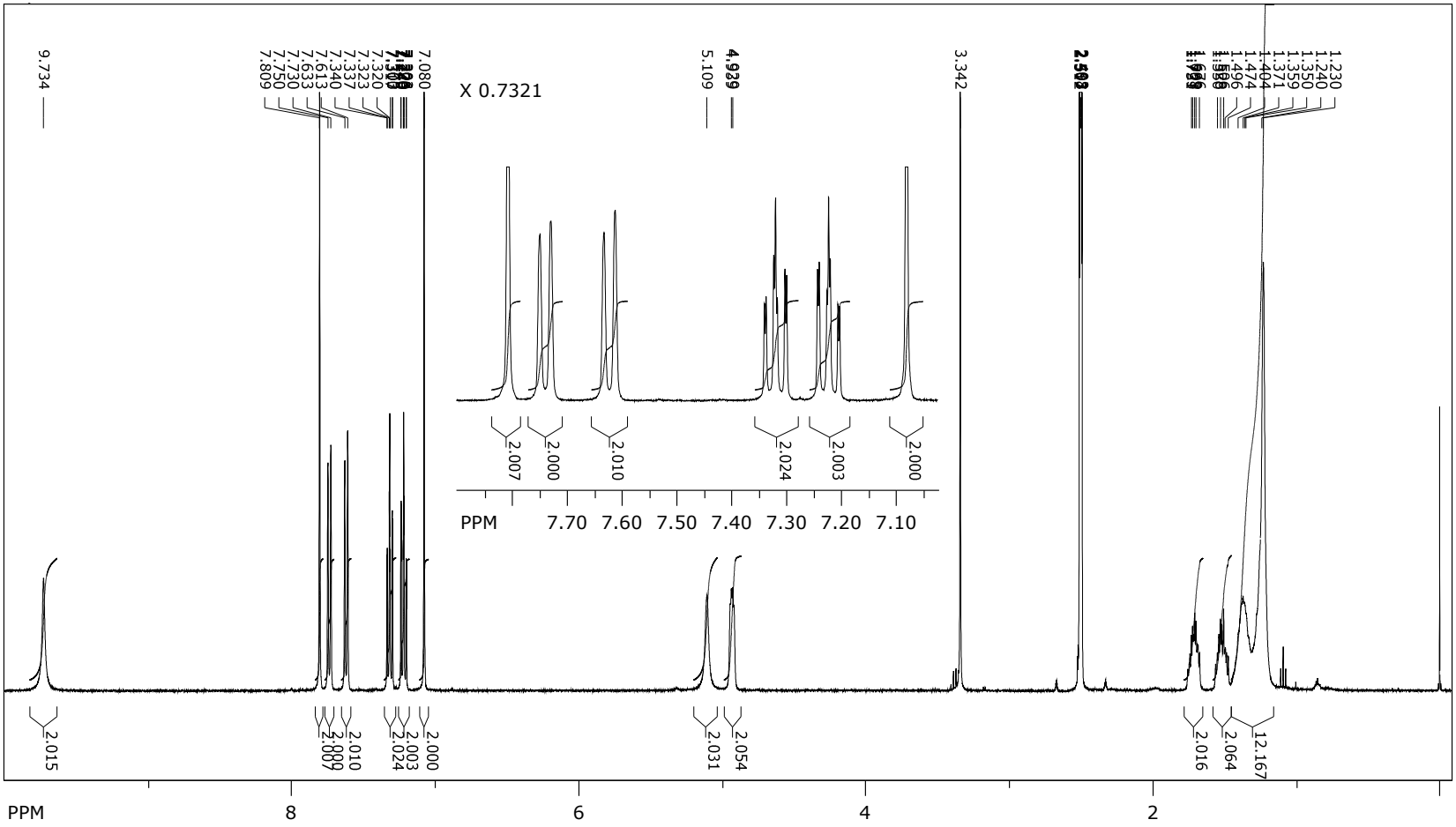

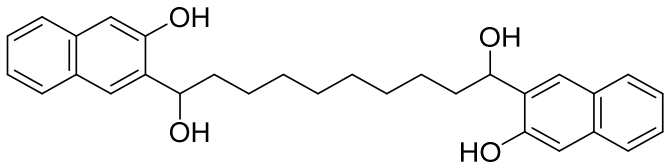

^{13}C NMR (DMSO-d_6, 100 MHz) of **4e**

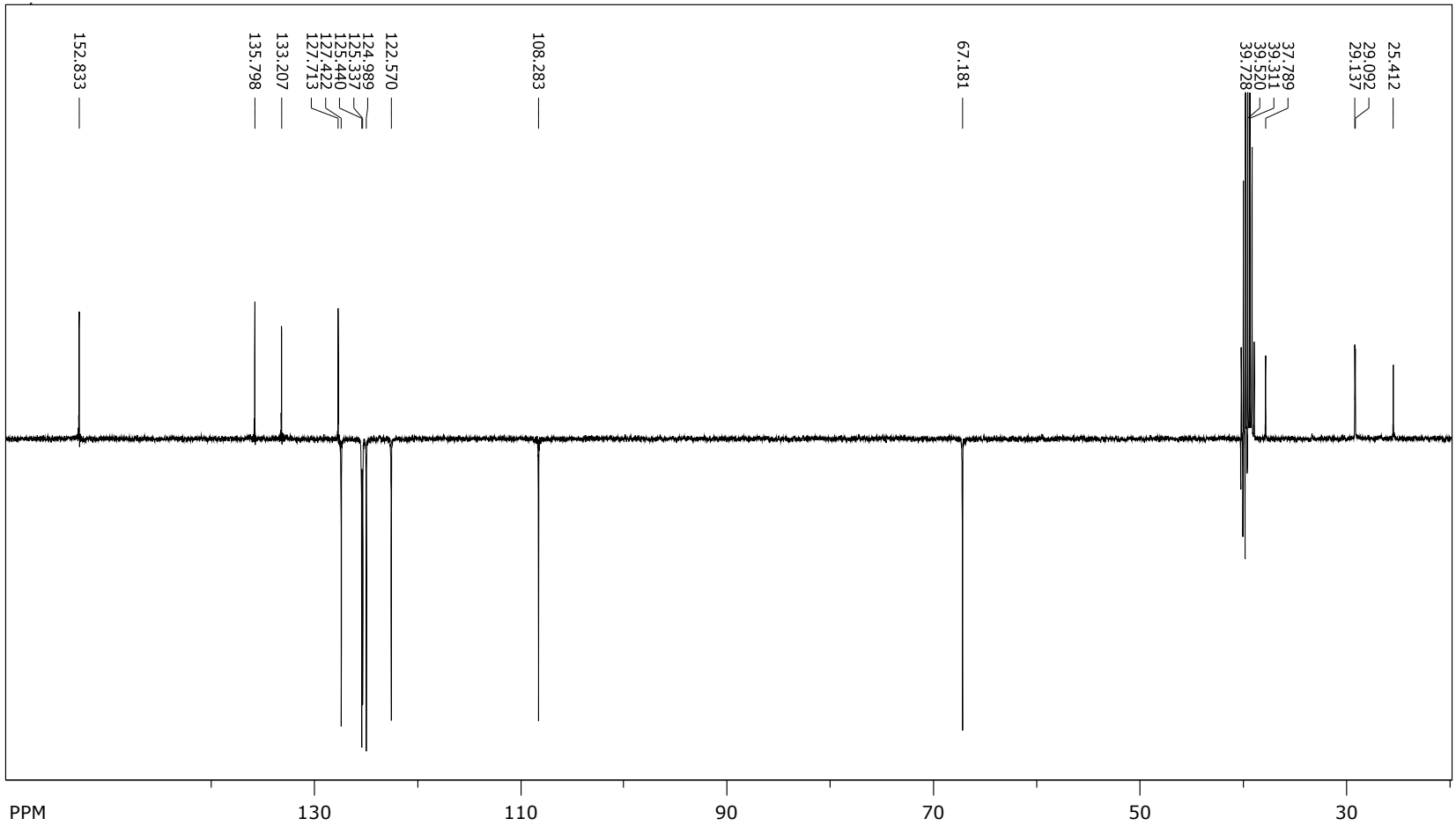

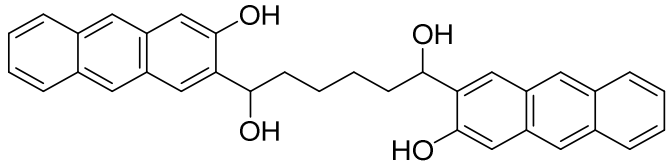

^{1}H NMR (DMSO-d_6, 600 MHz) of **5a**

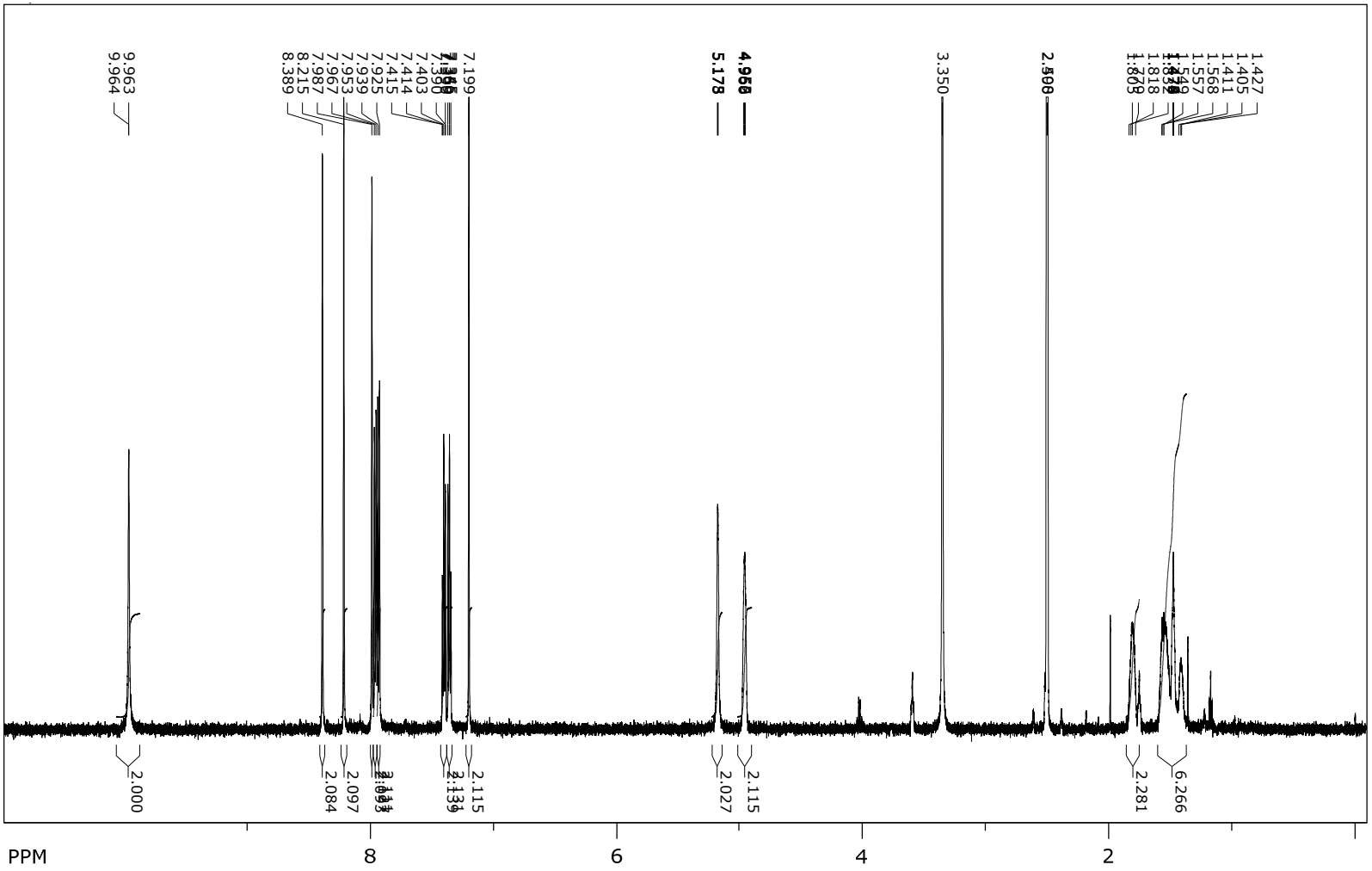

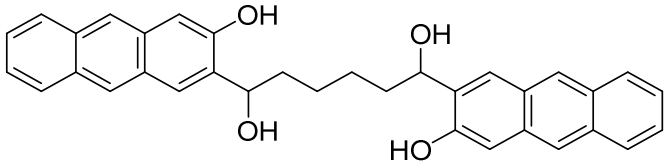

^{13}C NMR (DMSO-d_6, 150 MHz) of **5a**

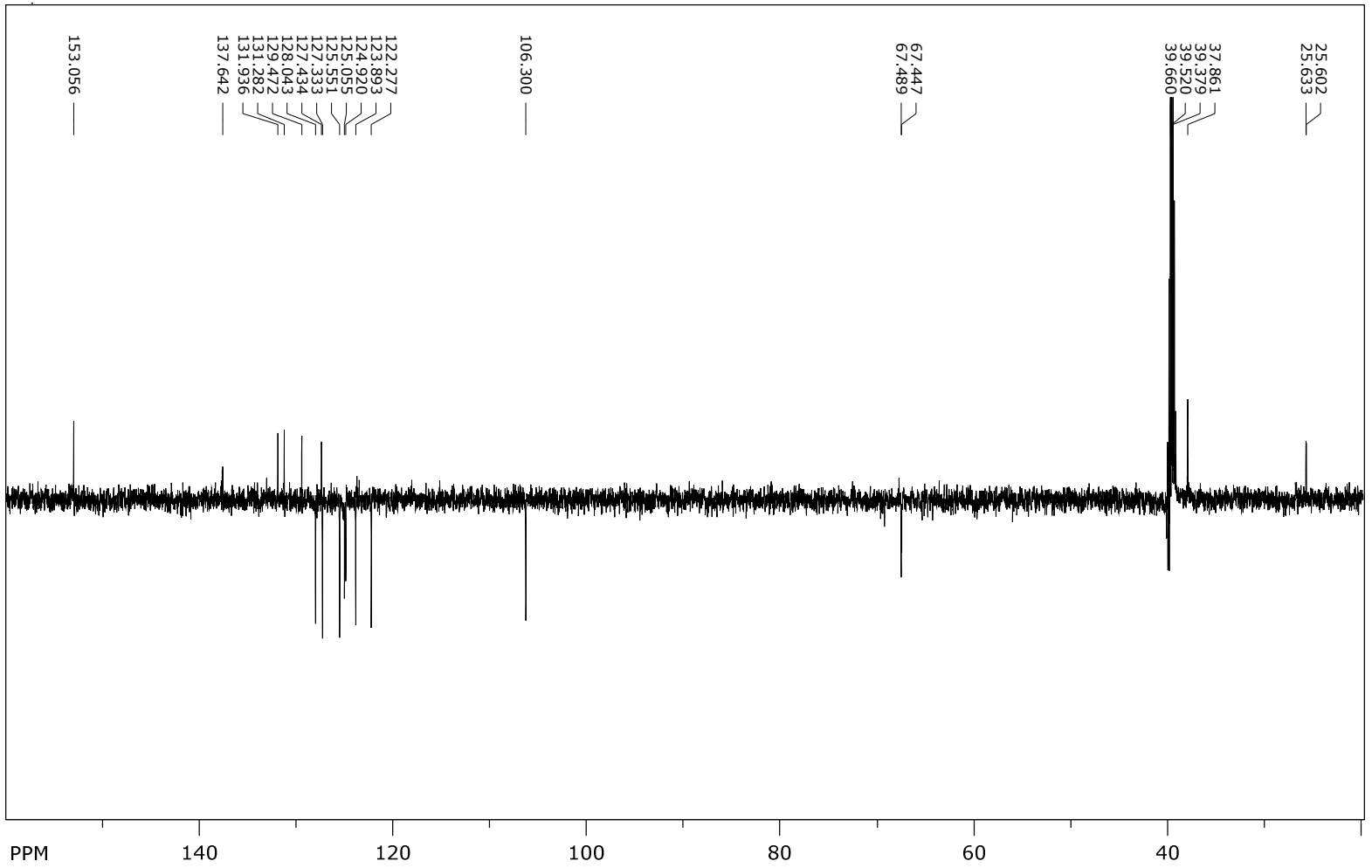

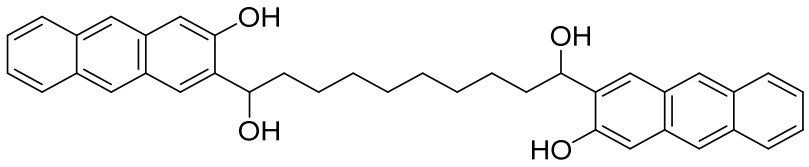

^{1}H NMR (DMSO-d_6, 400 MHz) of **5e**

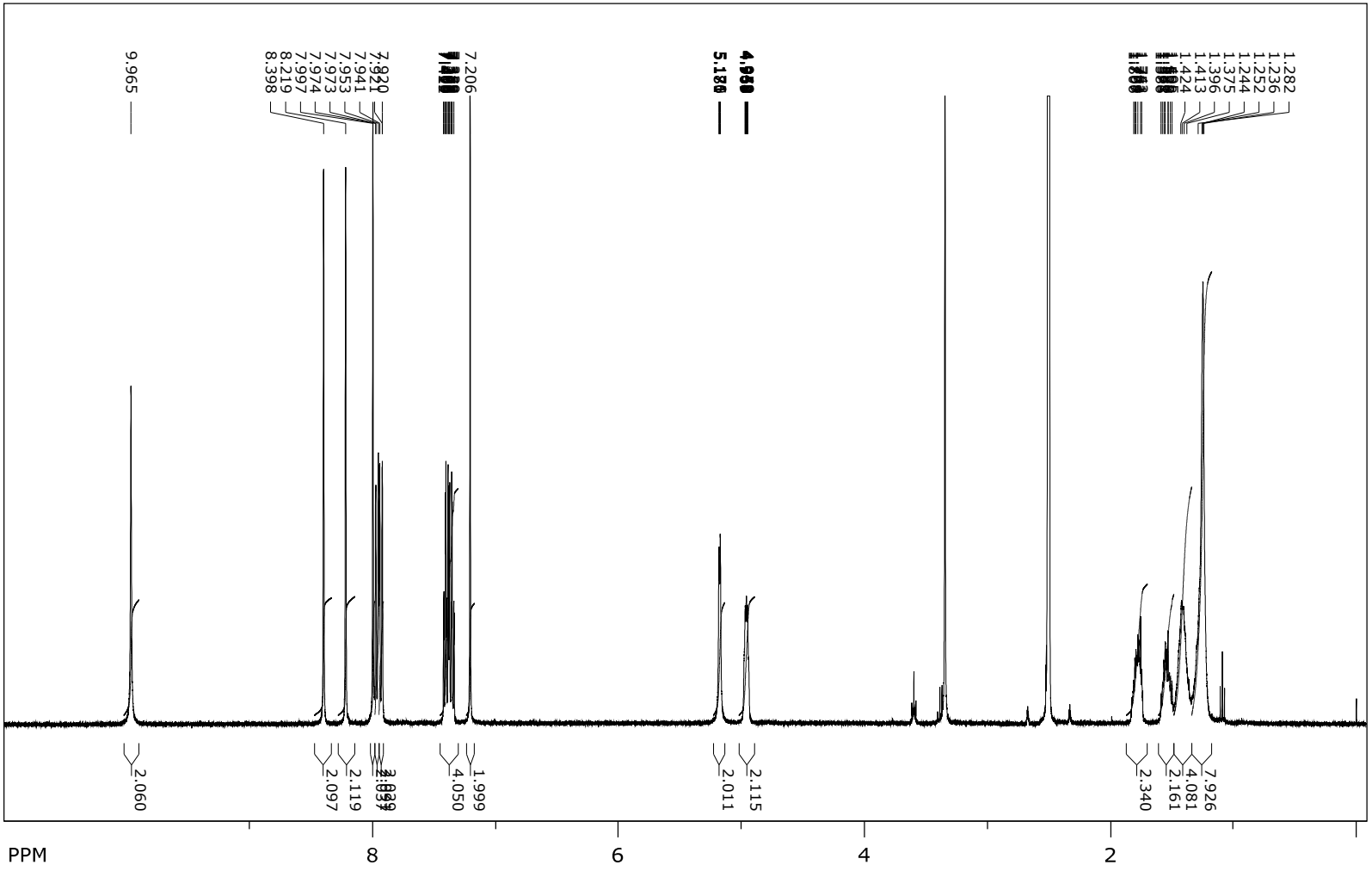

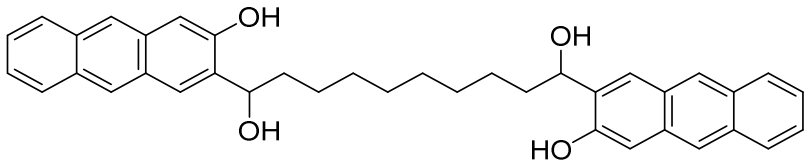

^{13}C NMR (DMSO-d_6, 100 MHz) of **5e**

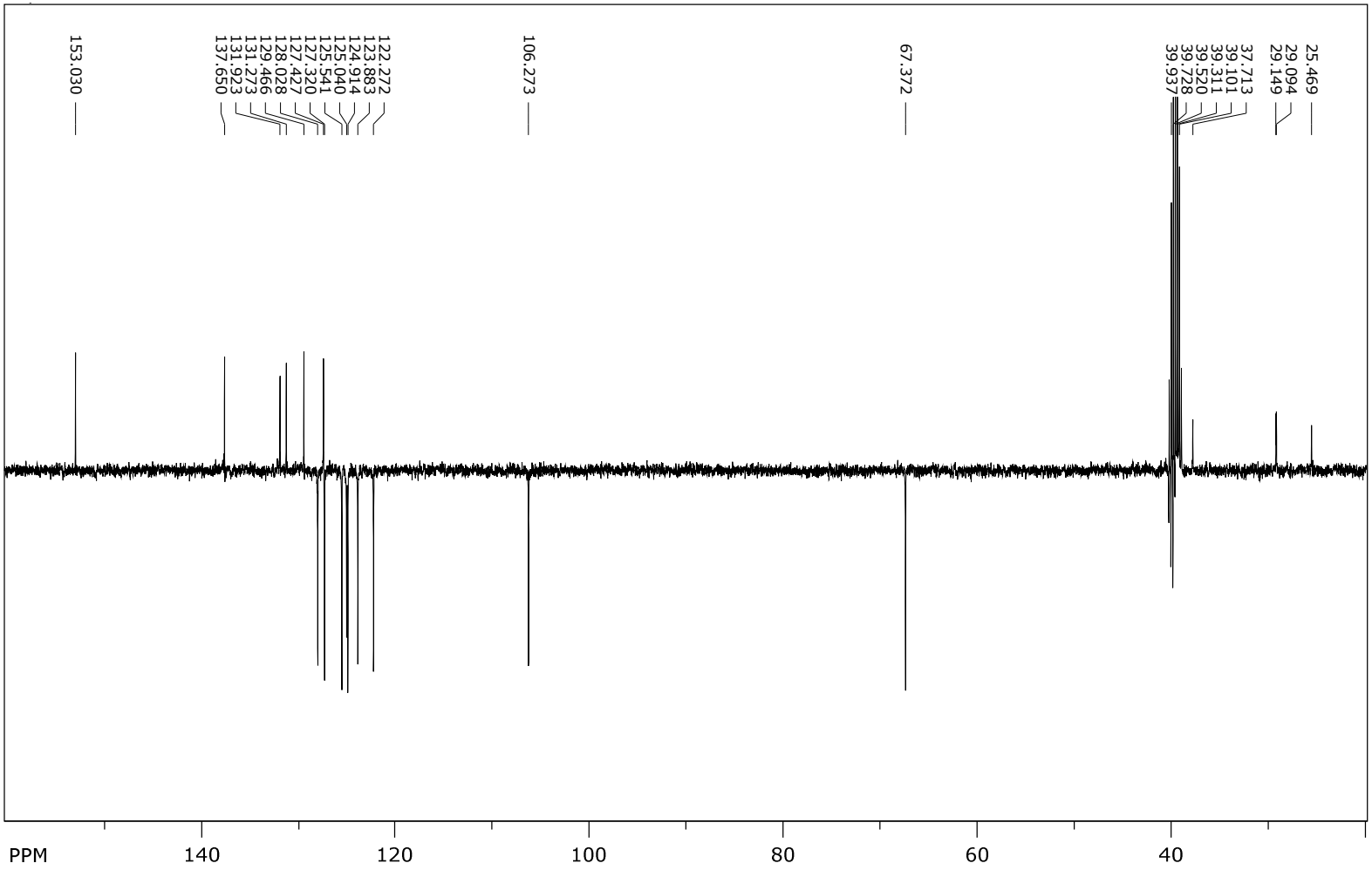

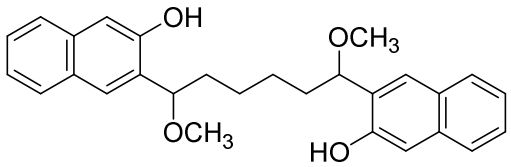

^{1}H NMR ($CDCl_3$, 400 MHz) of **11a**

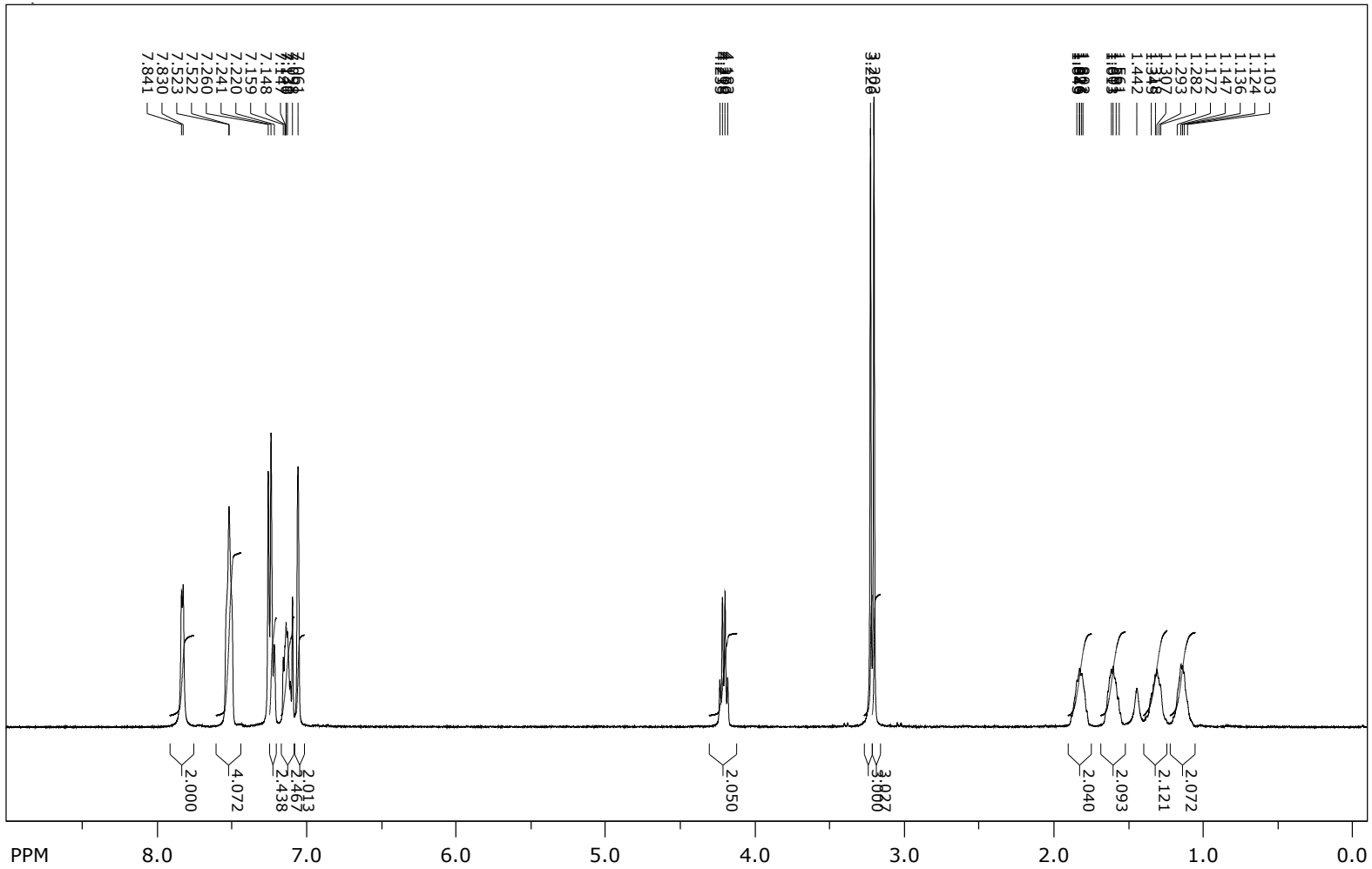

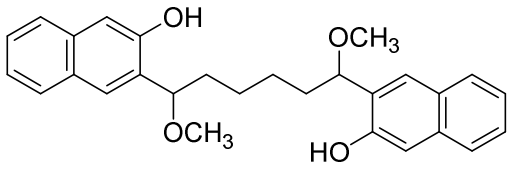

^{13}C NMR ($CDCl_3$, 100 MHz) of **11a**

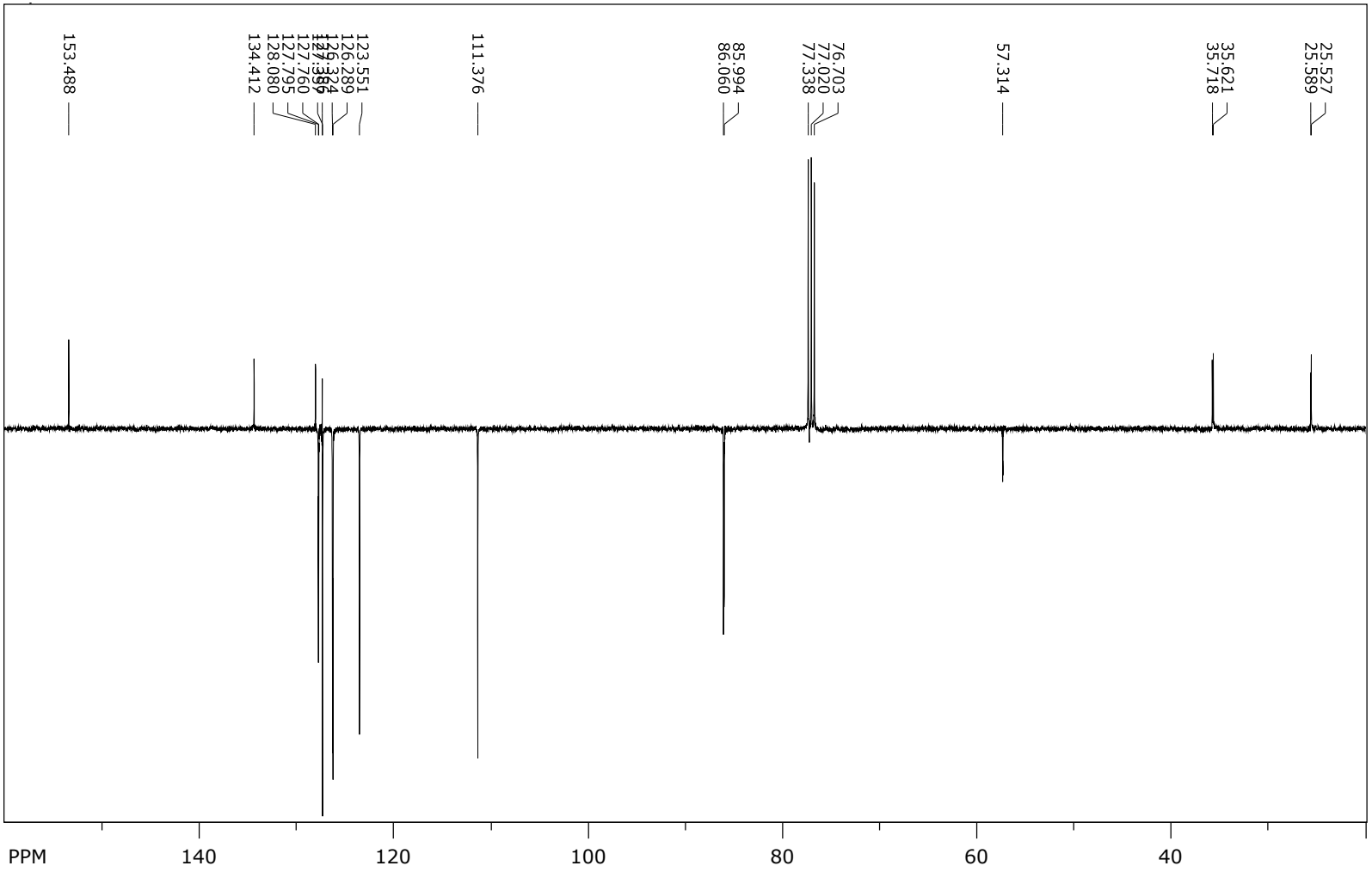

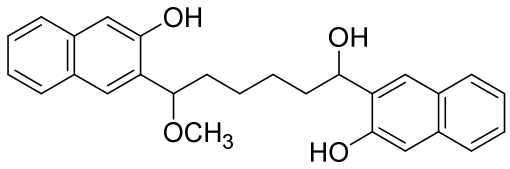

^{1}H NMR ($CDCl_3$, 400 MHz) of **10a**

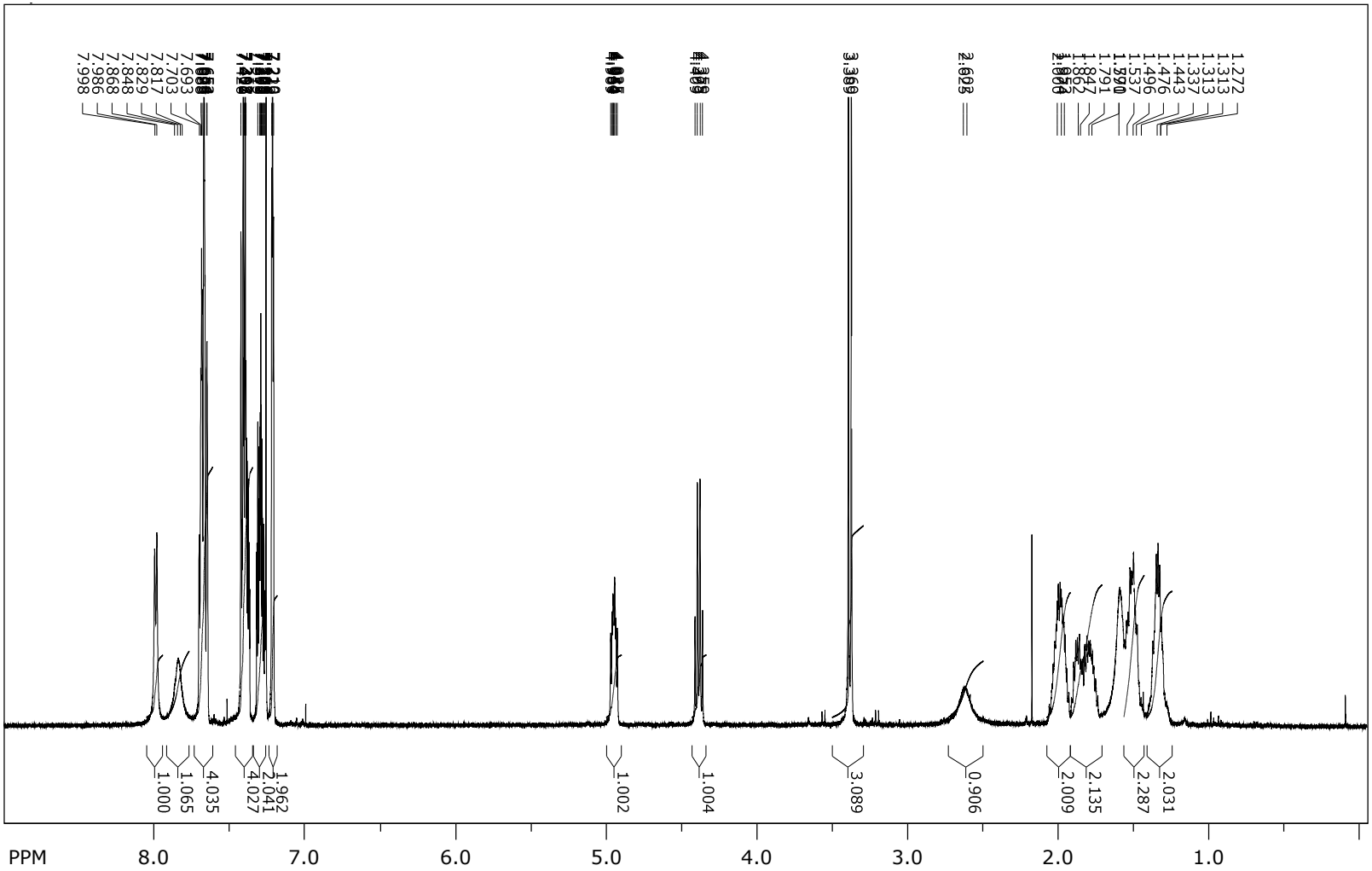

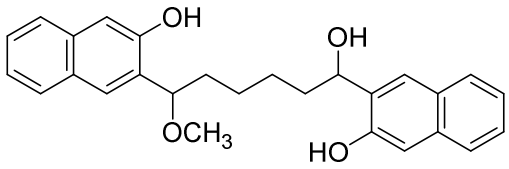

^{13}C NMR ($CDCl_3$, 100 MHz) of **10a**

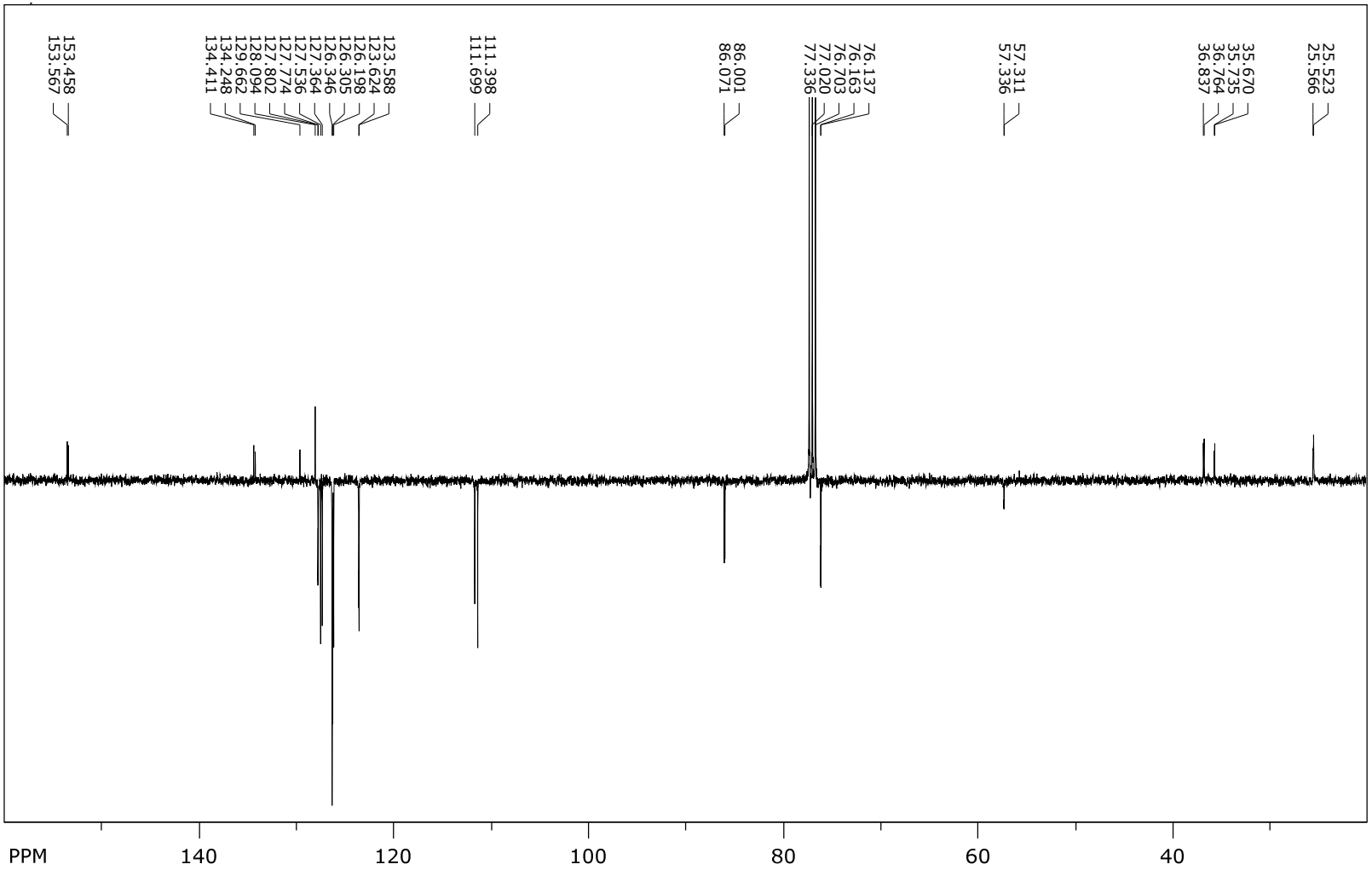

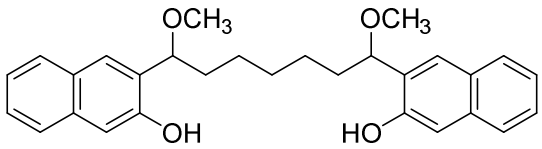

^{1}H NMR ($CDCl_3$, 500 MHz) of **11b**

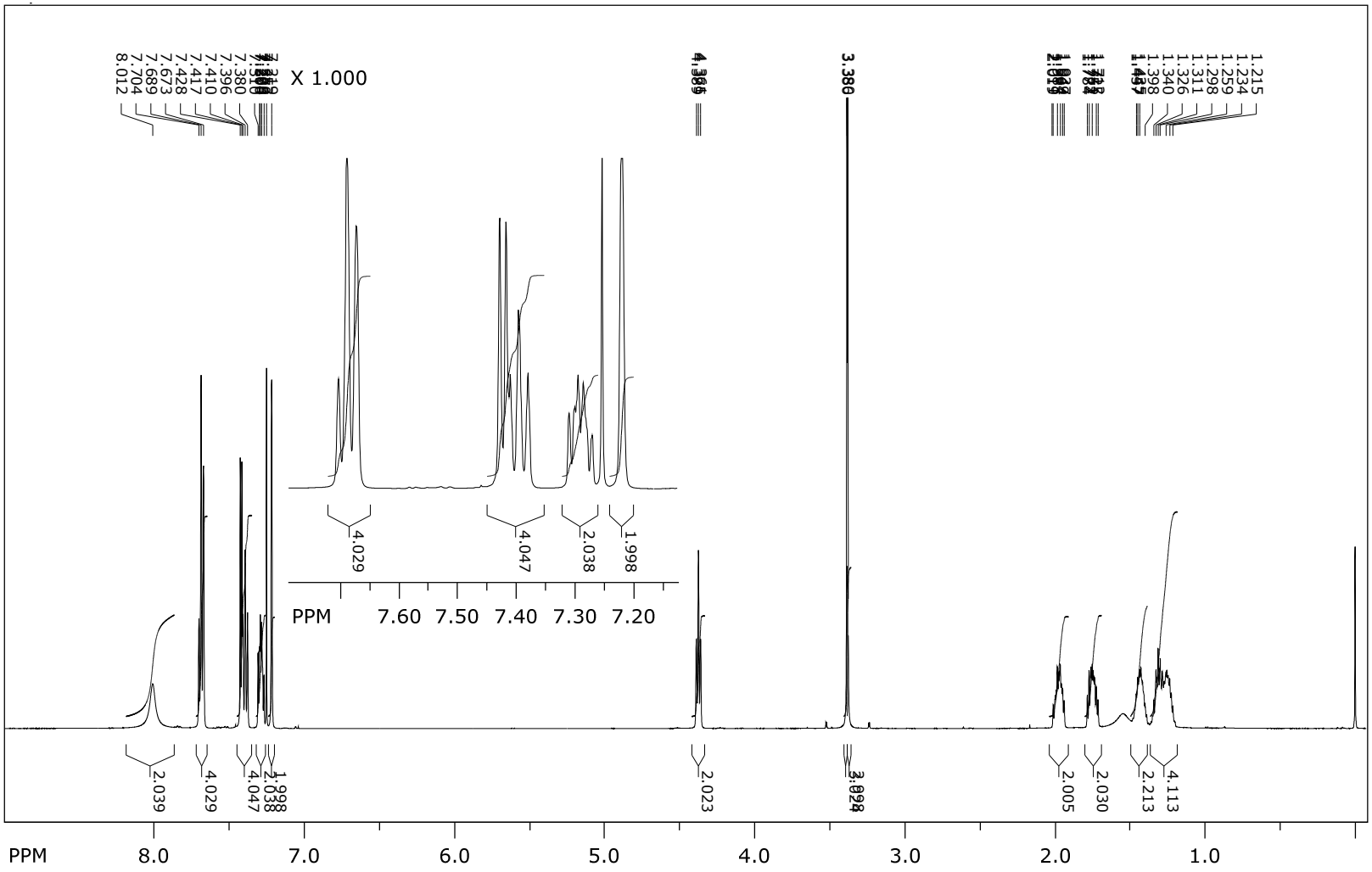

^{13}C NMR ($CDCl_3$, 125 MHz) of **11b**

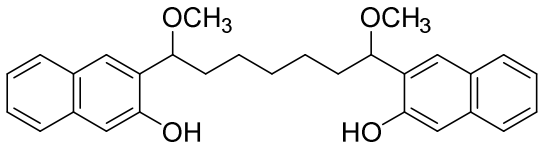

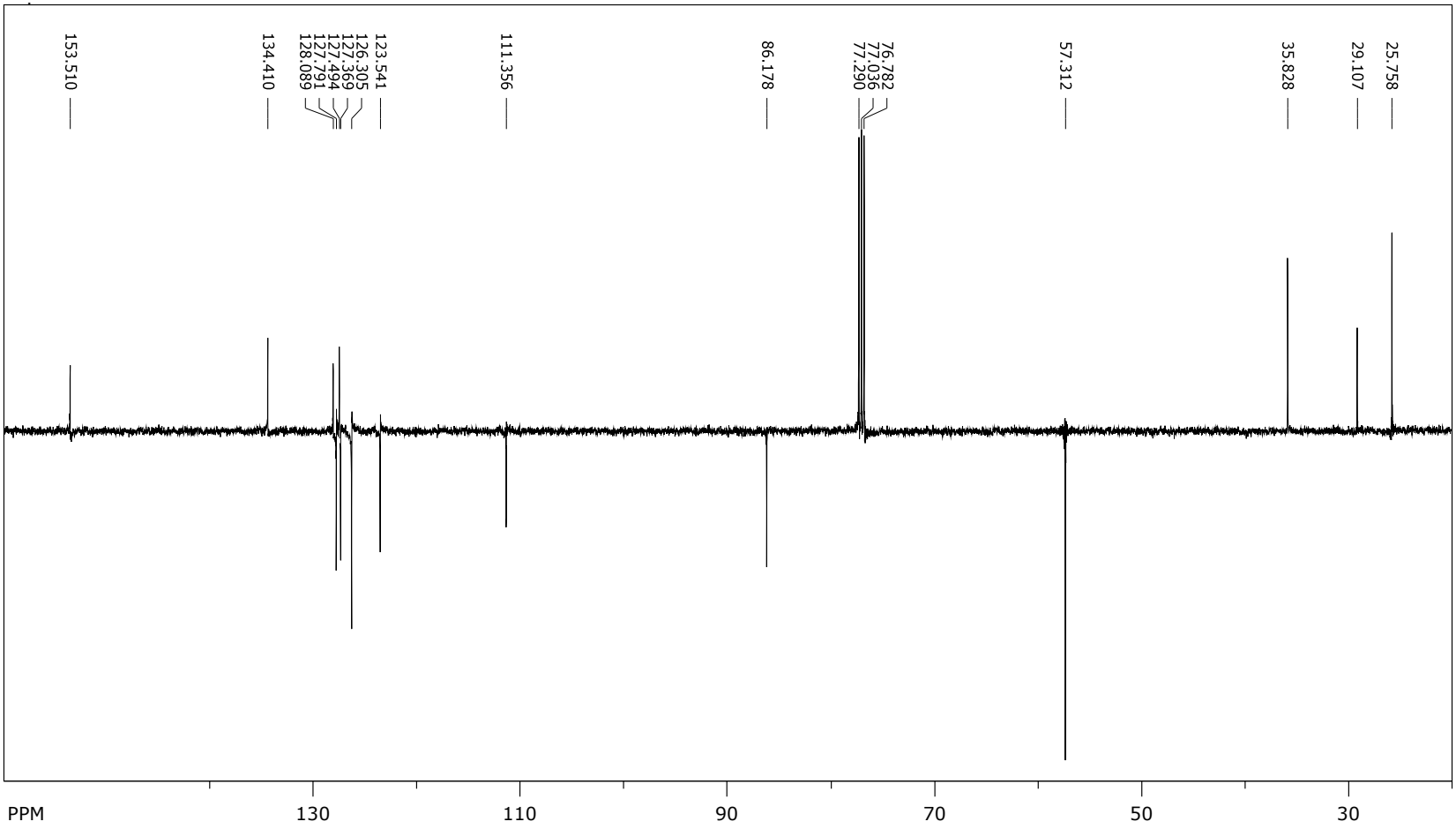

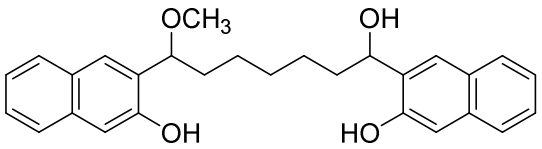

^{1}H NMR ($CDCl_3$, 500 MHz) of **10b**

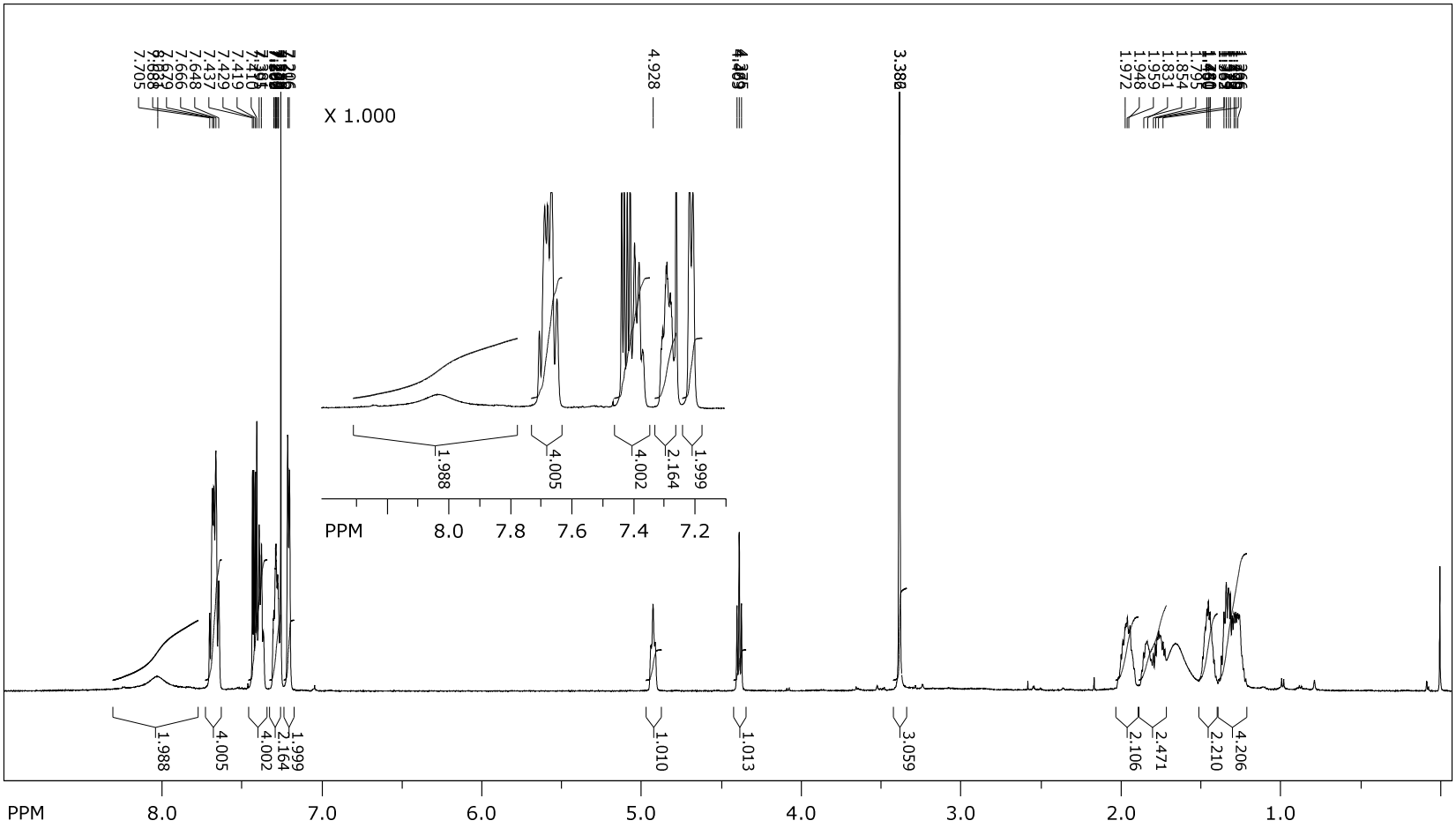

^{13}C NMR ($CDCl_3$, 125 MHz) of **10b**

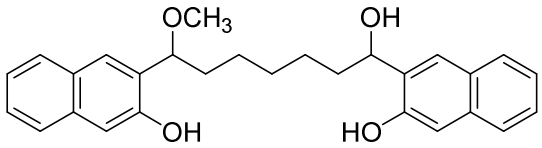

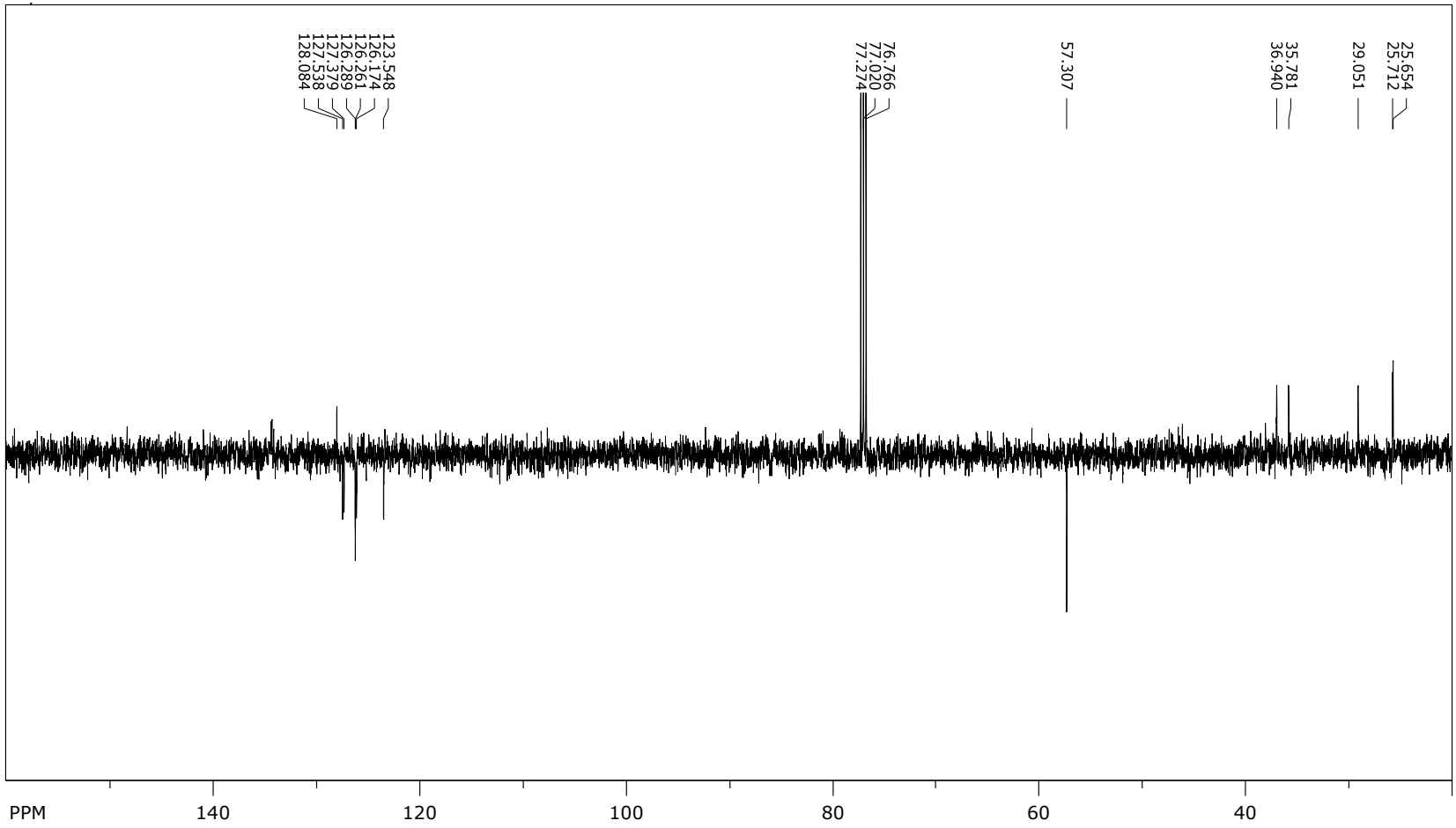

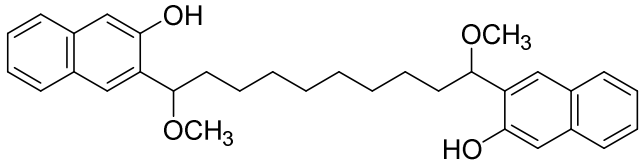

^{1}H NMR ($CDCl_3$, 500 MHz) of **11e**

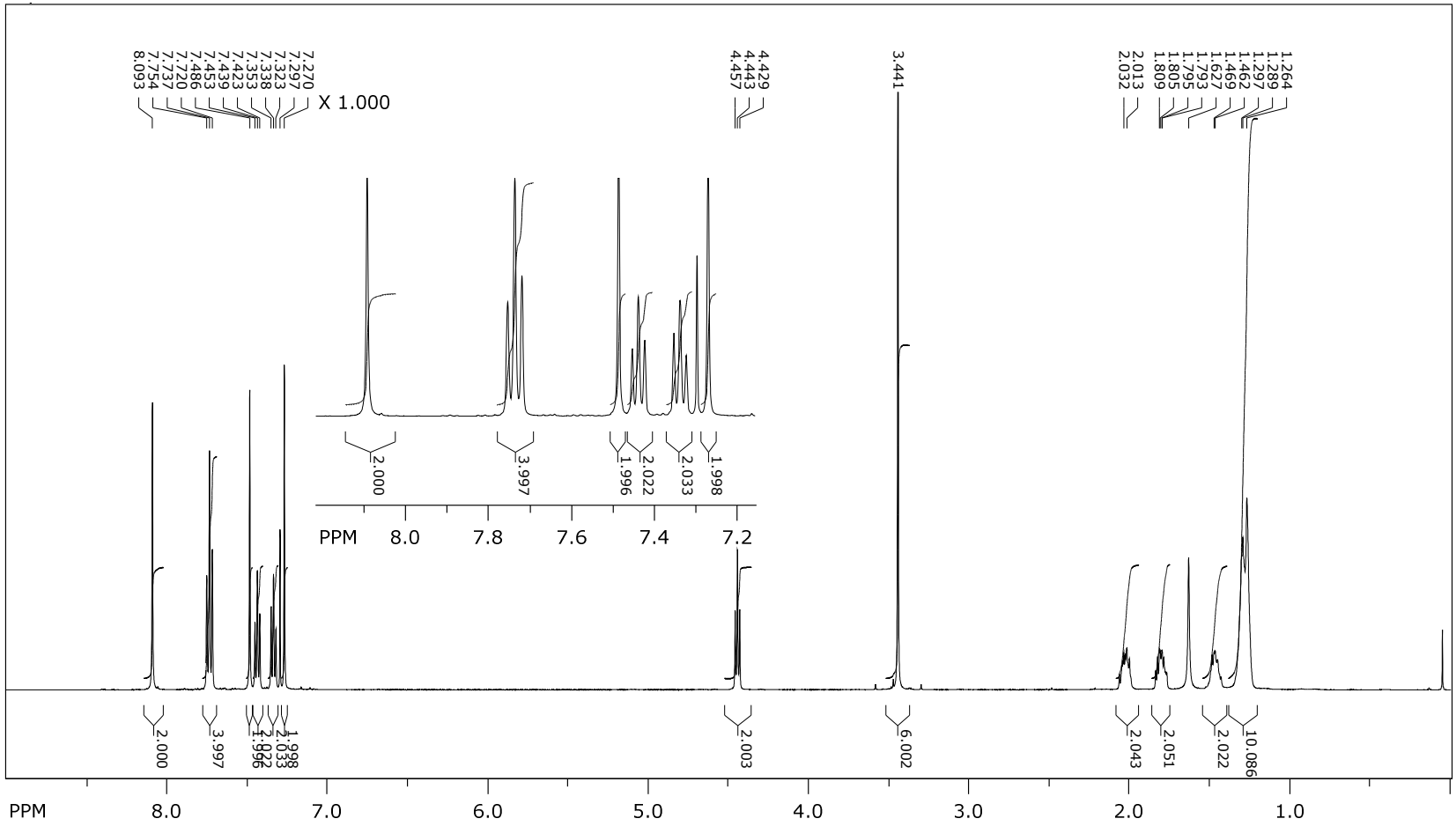

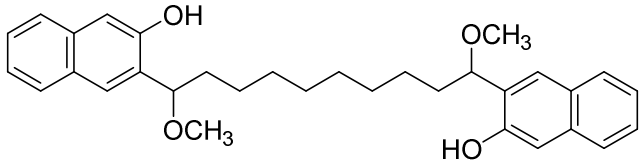

^{13}C NMR ($CDCl_3$, 125 MHz) of **11e**

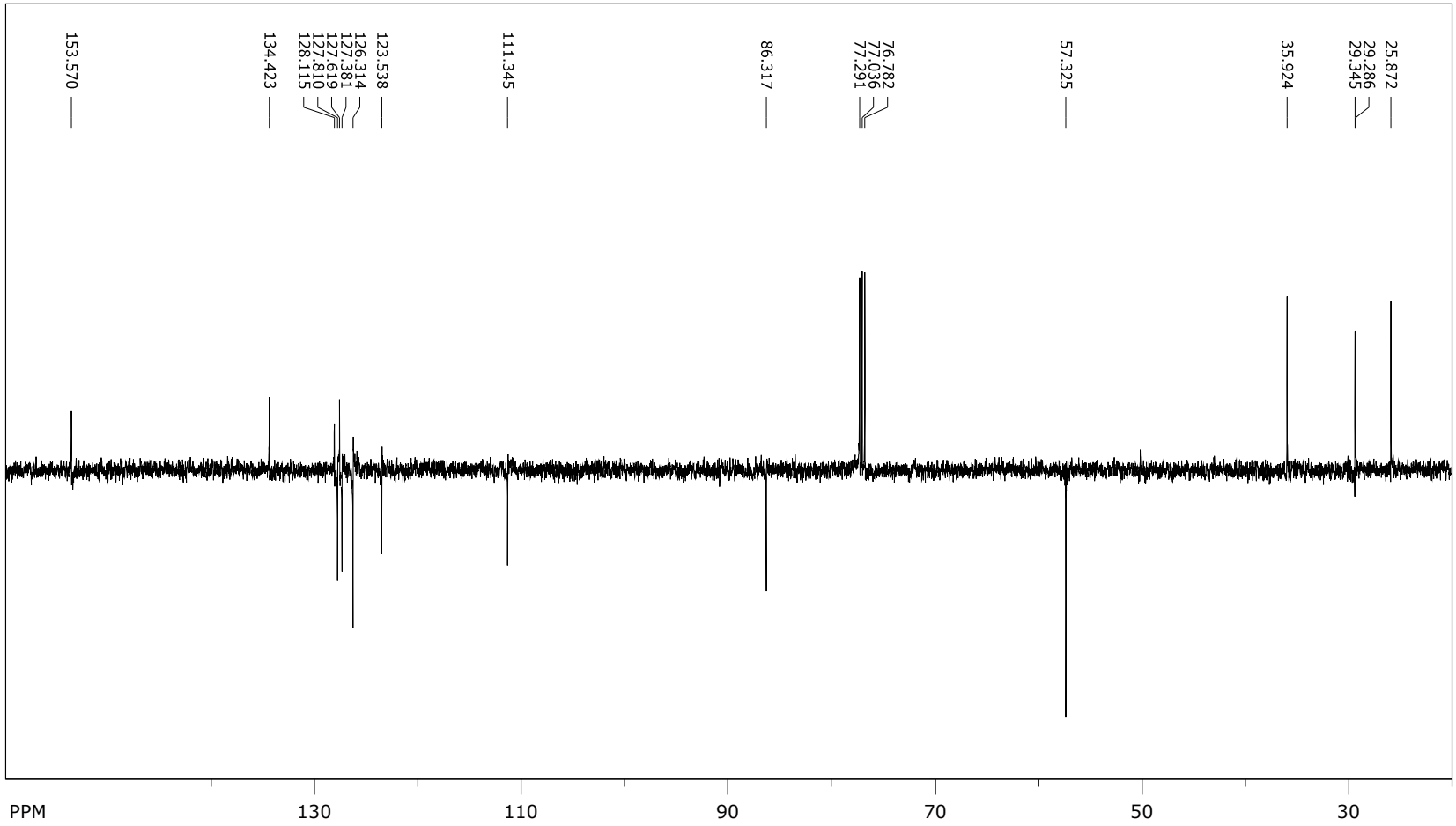

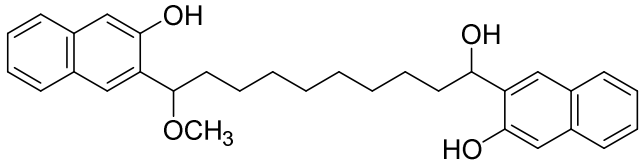

^{1}H NMR ($CDCl_3$, 500 MHz) of **10e**

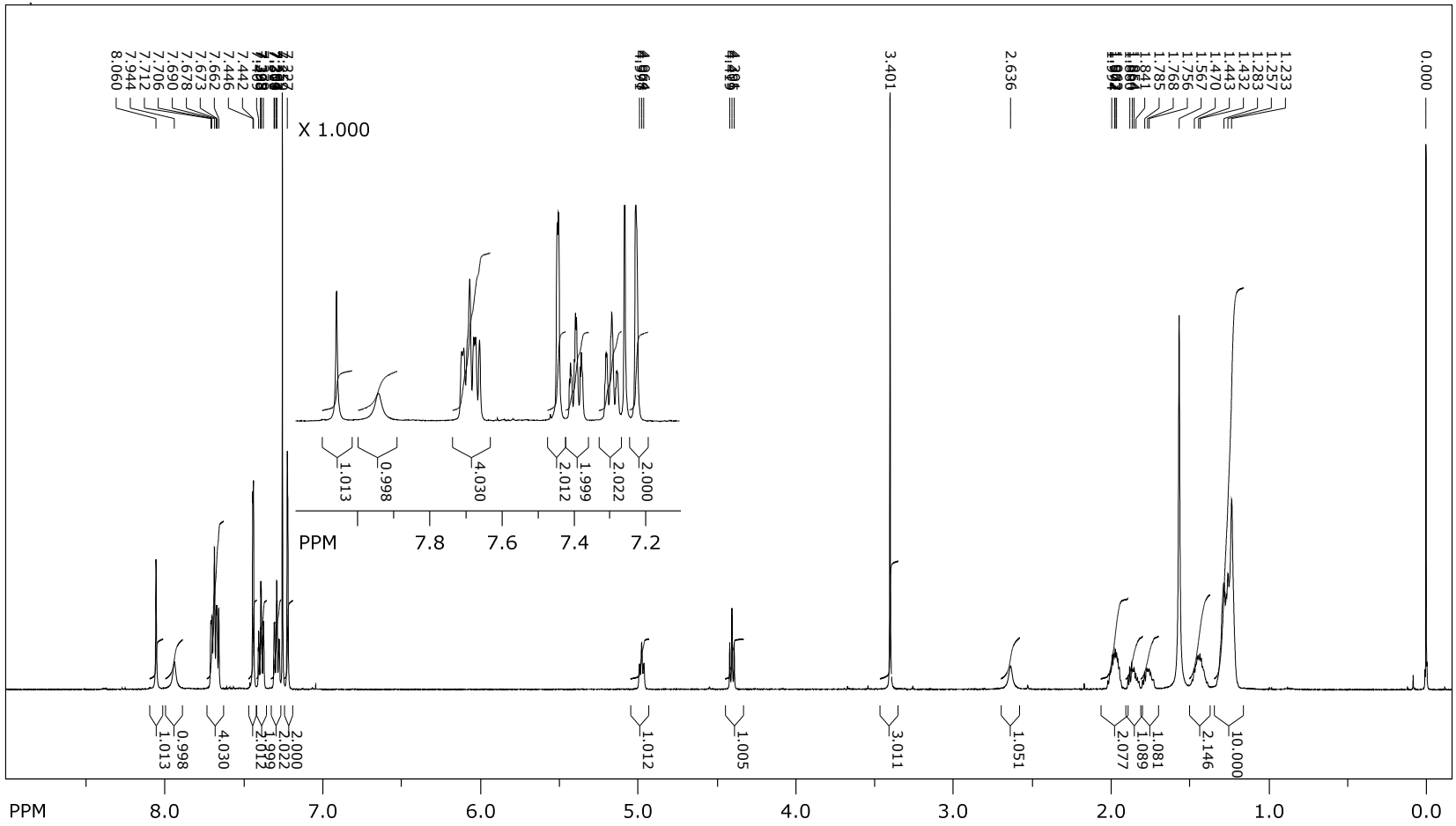

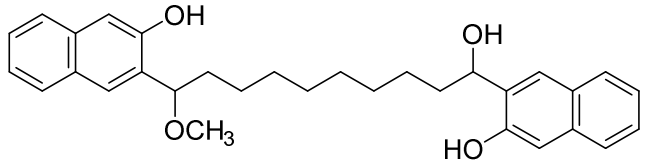

^{13}C NMR ($CDCl_3$, 125 MHz) of **10**

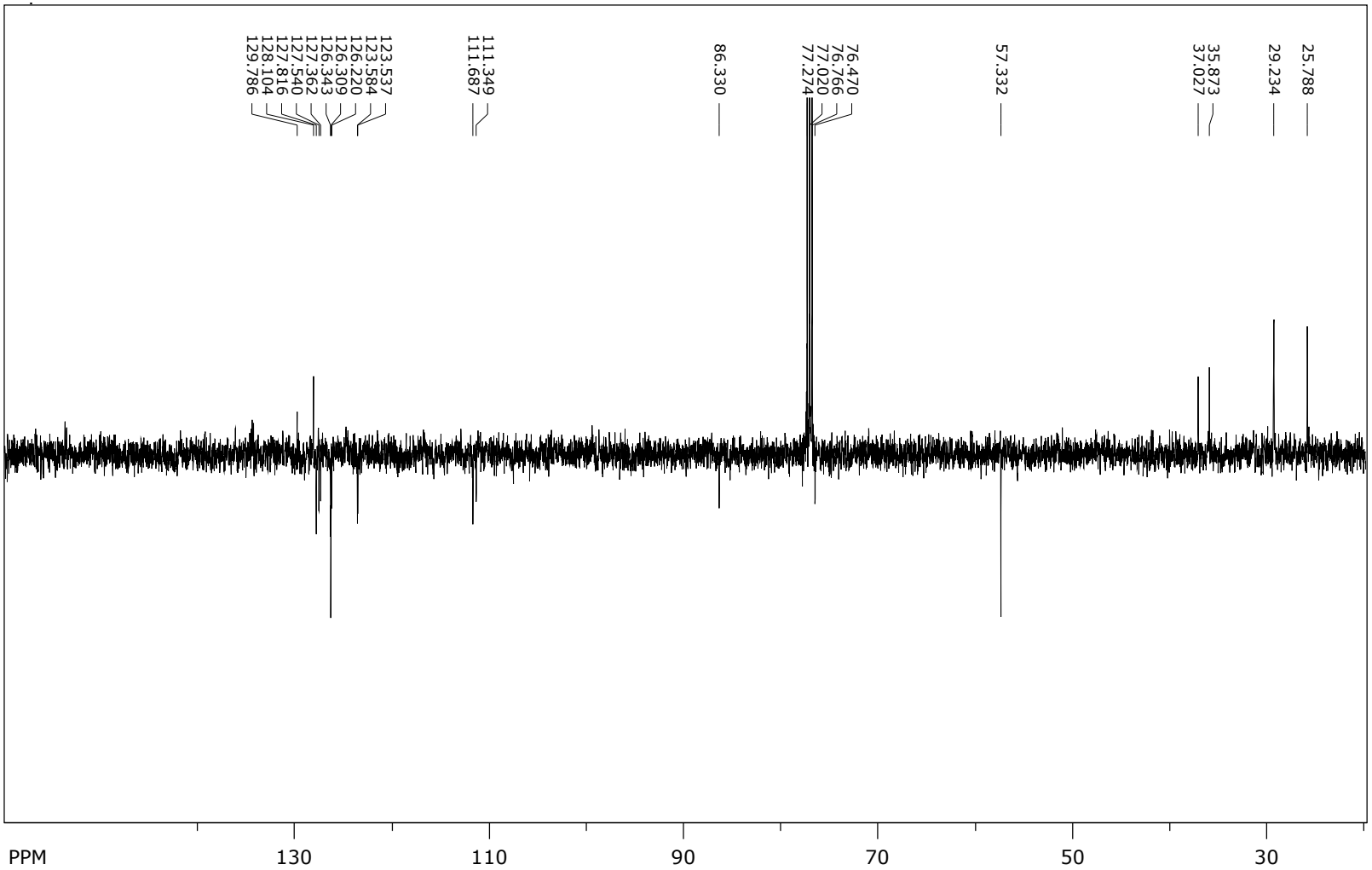

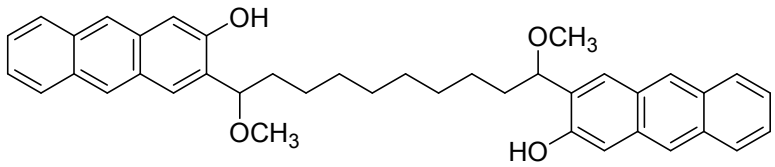

^{1}H NMR ($CDCl_3$, 600 MHz) of **13e**

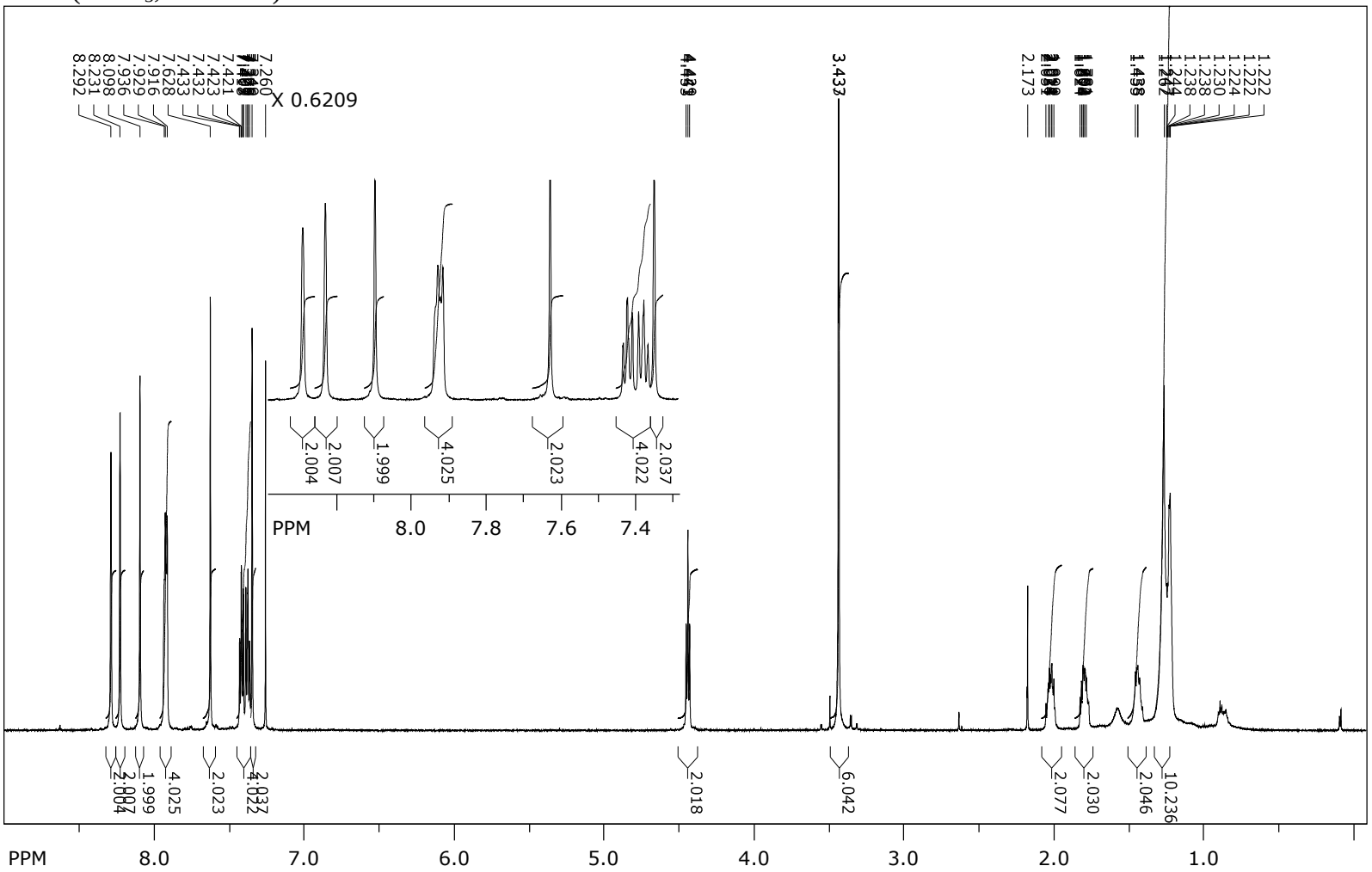

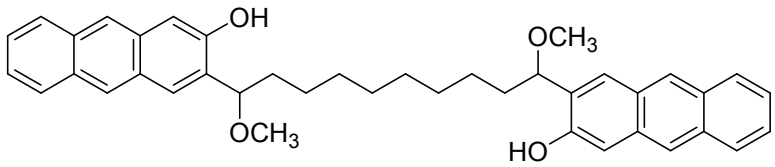

^{13}C NMR ($CDCl_3$, 150 MHz) of **13e**

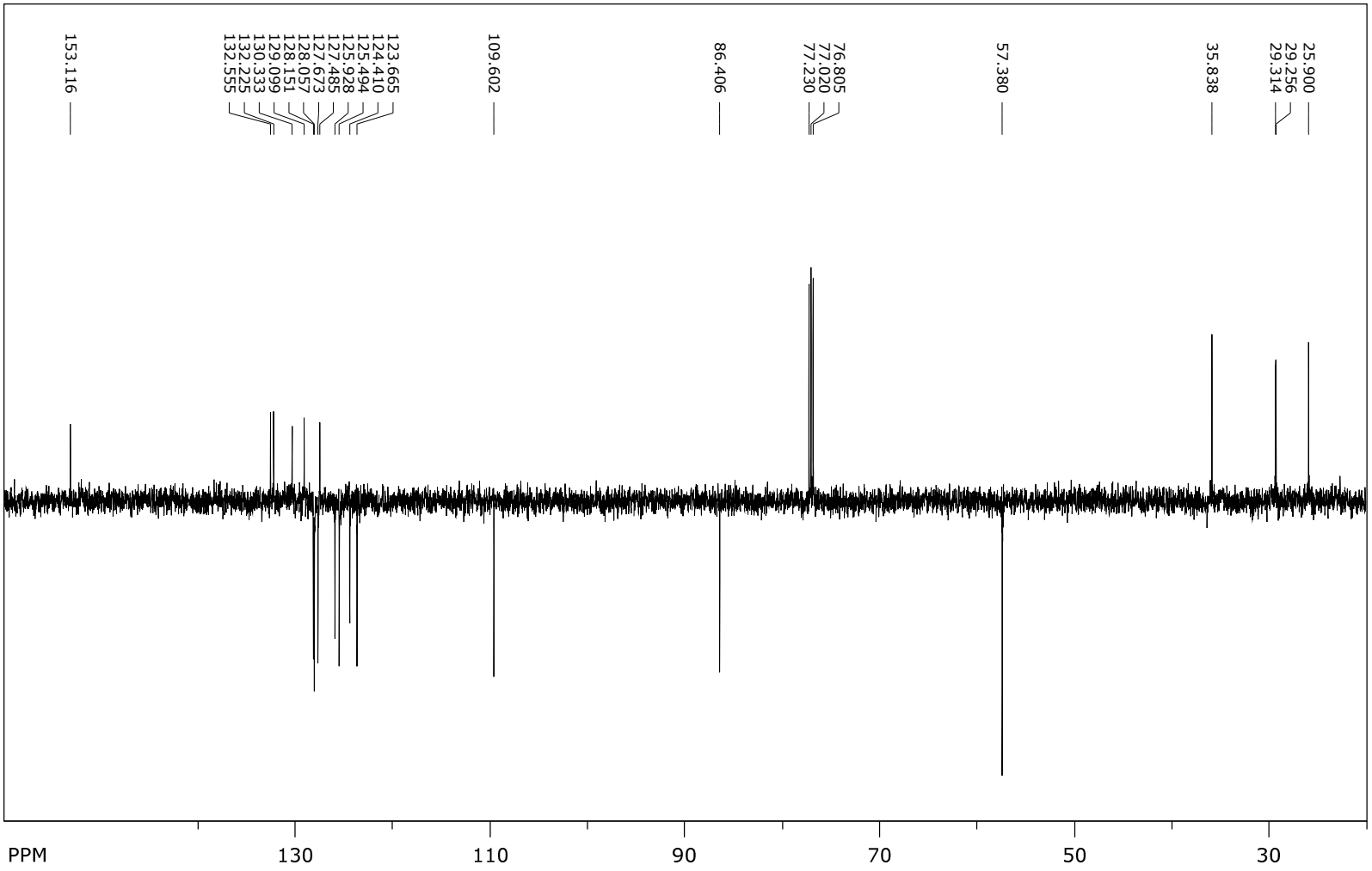

10. References

[1] K.-C. Wu, Y.-S. Lin, Y.-S. Yeh, C.-Y. Chen, M. O. Ahmed, P.-T. Chou, Y.-S. Hon, *Tetrahedron* 2004, **60**, 11861-11868

[2] Đ. Škalamera, J. Veljković, L. Ptiček, M. Sambol, K. Mlinarić-Majerski, N. Basarić, *Tetrahedron* 2017, **73**, 5892-5899.

[3] I. Ferrari, I. M. Hunsberg, H. S. Gutowski, *J. Org. Chem*. 1960, **25**, 485-486.

[4] S. Kobayashi, T. Semba, T. Takahashi, S. Yoshida, K. Dai, T. Otani, T. Saito, *Tetrahedron* 2009, **65**, 920-933.

[5] J. Olmsted, III, *J. Phys. Chem*. 1979, **83**, 2581-2584.

[6] N. Basarić, N. Cindro, D. Bobinac, L. Uzelac, K. Mlinarić-Majerski, M. Kralj, P. Wan, *Photochem. Photobiol. Sci*. 2012, **11**, 381-396.